

Geological setting, nature of mineralisation, and fluid characteristics of the Wang Yai prospects, central Thailand

John Vernon de Little

BSc



UNIVERSITY
OF TASMANIA

A Research Thesis submitted in partial fulfillment, of the requirements of
the Degree of Bachelor of Science with Honours



**School of Earth Sciences,
CODES Centre of Excellence
University of Tasmania**

November 2005

Declaration

This thesis contains no material which has been accepted for the award of any other degree or diploma in any tertiary institution, and to the best of my knowledge and belief, contains no material previously published or written by another person, except where due reference is made in the text of the thesis.

Signed

John Vernon de Little

November 2005

Abstract

The Wang Yai prospects are located along the Loei Foldbelt, central Thailand. They are a newly discovered resource and up until now have not been the subject of any scientific research. Eleven vein systems at Wang Yai were investigated in terms of vein textures, mineralogy, fluid inclusions and stable isotopes. The vein systems occur as either well-preserved outcrop or sparse sporadic float. The vein systems can be divided into two types. They include: (1.) mineralised veins which are characterised by quartz - chalcedony - calcite \pm adularia and (2.) poorly mineralised veins characterised by chalcedony and opaline quartz. The vein systems are hosted in volcanic and volcanosedimentary units intruded by andesite and diorite. LA-ICP-MS U-Pb zircon geochronological studies have revealed the age of host rocks as Late Permian to Early Triassic.

Volcanology studies of the host rocks indicate that the depositional environment was a submarine below wave base setting. Zr/Y vs Zr plot of least altered volcanic rocks have identified the andesitic sandstone and andesitic lithic breccia as having island arc affinities. The younger andesite and diorite intrusives were found to have continental arc affinities. These findings are consistent with interpretations of the volcanic setting at the nearby low-sulphidation Chatree deposit.

Vein texture, mineralogy, alteration and paragenesis studies have identified zonation between gold-bearing vein systems and barren vein systems. Gold-bearing systems yield crystalline quartz, lattice-bladed quartz, pseudo-acicular quartz and pseudomorphs after adularia. Ore mineralogy in these systems is hosted in ginguro bands which comprise of electrum \pm argentite \pm pyrite assemblages. Barren vein systems yield chalcedony and opaline quartz assemblages with associated recrystallisation textures. Based on quartz textural analysis and ore mineralogy assemblages the gold-bearing veins are interpreted to have formed at levels deeper in the system than the barren vein systems.

Fluid inclusion studies of quartz indicate salinities are between 1 to 5 wt % NaCl equiv. Fluid inclusion homogenisation data yields three different ranges. Crystalline gold-bearing quartz yields temperatures of 187 – 218 C°, comb quartz yields temperatures of 260 - 290 C°. and crustiform-colloform veins yield temperatures of 140 – 200 C°.

Stable sulphur isotope studies of pyrite range between +3.82 and -0.04 per mil. These values indicate a magmatic source. Stable oxygen isotope values of quartz range from +11 to +17.5 per mil. Low oxygen isotope values range from +11.0 to +13.0 per mil and are associated with crystalline quartz gold bearing systems. High oxygen isotope values (+15.0 to +17.5 per mil) are associated with barren quartz chalcedony dominated systems.

The volcanic setting, vein textures, mineralogy and alteration assemblages of the Wang Yai prospects are comparable with the nearby low-sulphidation epithermal Chatree deposit. The Wang Yai prospects appear to be at the top of the broader epithermal system and therefore potential for high grade mineralisation at depth exists.

Acknowledgements

I would firstly like to thank my supervisor, Dr Khin Zaw for granting me the opportunity to undertake this fun and interesting project. Khin Zaw's enthusiasm and great expertise in the area have been a motivating factor throughout the year. Khin has provided me with all the logistical support needed in order for things to run smoothly. I also owe a great deal of gratitude to my co-supervisors, Drs. Stuart Smith and Anthony Harris. Stuart played an invaluable role early in the year during my time of field mapping. His excellent introduction to the area and help during the first week in Thailand put me in good stead for the remaining 4 weeks. Anthony has provided me with many new ideas, and feedback. I would especially like to thank Anthony for his time and patience during the final two weeks of the year. A special thank you goes out to Sebastian Meffre who provided his expertise during field mapping, dating of host rocks at Wang Yai, and driving the microprobe.

Secondly I would like to thank the Thai Global Ventures Co., Ltd exploration team. Thank you Ian Cameron for making me feel welcome and supporting me during my time in Thailand. Henry Agupitan - thanks for your hospitality at Wan Hin and help with mapping and organisation of samples sent to me. Lek, Wittaya, Kittipong, C, Bank and Trent - thank you for taking me under your wing and making my time in Thailand enjoyable. I would also like to thank Pen for serving delicious Thai meals three times a day during 12 hour mapping excursions.

Many thanks also go out to the staff at University of Tasmania: Simon Stephens - thank you for supplying me with my constant need of more thin sections, Jim Hutton - your expertise with the microprobe instrument was invaluable, Keith Harris - thank you for undertaking sulphur isotope analysis at such late notice and Phil Robinson and Katie McGoldrick for XRF analysis.

Last but not least I would like to thank Laijing and my family and friends. Laijing has supplied me with support and motivation through very trying times and has put up with my crankiness. I would also like to thank her family for shipping strong Malaysian Ipo 'White elephant' coffee to me. Dad and Mum, thank you for your support and invitations to dinner during the final weeks of the year. To my fellow honours students McGeisha, Sekins (cAmeRa), Corzaaaa, Kit-Kenobi, Kingy (still has difficulty playing my spin bowling), Kat, Mel, and Kim thank you for your help, support and fun times during the year.

TABLE OF CONTENTS

List of Figures	<i>viii</i>
List of Tables	<i>xi</i>
CHAPTER 1: INTRODUCTION	1
1.1 PREAMBLE	1
1.2 LOCATION	1
1.3 ACCESS	3
1.4 TOPOGRAPHY	4
1.5 LAND USE	4
1.6 EXPOSURE	5
1.7 EXPLORATION HISTORY	7
1.8 AIMS	7
1.9 METHODOLOGY	8
CHAPTER 2: REGIONAL GEOLOGY	10
2.1 TECTONIC EVOLUTION	10
2.2 LOEI FOLDBELT	11
2.3 DISTRICT SCALE GEOLOGY AT WANG YAI	13
2.4 GEOCHRONOLOGY OF THE LOEI FOLDBELT	16
2.5 AGE OF HYDROTHERMAL ALTERATION	18
CHAPTER 3: LOCAL GEOLOGY	20
3.1 INTRODUCTION	20
3.2 STRATIGRAPHY OF WANG YAI	21
3.3 NON-VOLCANOGENIC SEDIMENTARY ROCKS	24
3.3.1 Fossiliferous limestone	24
3.3.2 Siltstone	25
3.4 VOLCANIC SUCCESSION	27
3.4.1 Andesitic volcanoclastic sandstone	27
3.4.2 Polymict andesitic lithic breccia	28
3.4.3 Polymictic massive volcanic conglomerate	30
3.4.4 Quartz polymictic breccia	33
3.5 COHERENT ROCKS	34
3.5.1 Quartz phyric rhyodacite	35
3.5.2 Feldspar phyric andesite	36

3.5.3 Feldspar phyric diorite	38
3.5.4 Quartz diorite	39
3.6 WHOLE ROCK GEOCHEMISTRY	41
3.7 GEOCHEMICAL CLASSIFICATION OF WANG YAI	42
3.8 SUMMARY	43
3.8.1 Environment of deposition	44
3.8.2 Sequence of events	44
3.9 COMPARISON OF WANG YAI AND CHATREE GEOLOGY	44
CHAPTER 4: GOLD-BEARING QUARTZ VEINS	51
4.1 INTRODUCTION	51
4.2 CONICAL HILL	49
4.2.1 Quartz vein textures	51
4.3.1 Conical Hill (West)	51
4.3.2 Ore mineralogy	54
4.4 CENTRAL RIDGE	58
4.4.1 Quartz vein textures	60
4.4.2 Ore mineralogy	61
4.5 T1 HILL	63
4.5.1 Quartz vein textures	65
4.5.2 Detailed vein and alteration assemblage	67
4.5.2.1 Silicic alteration assemblages	67
4.5.2.2 K-feldspar alteration assemblages	68
4.5.2.3 Argillic and phyllic alteration assemblages	69
4.5.2.4 Chloritic alteration assemblages	69
4.5.2.5 Propylitic alteration assemblages	70
4.5.3 Ore mineralogy	70
4.6 T4 HILL	72
4.7 GIFT PROSPECT	72
4.7.1 Quartz textures	74
4.7.2 Alteration	78
4.7.3 Ore mineralogy	78
4.8 MINERALOGY AND TEXTURAL ZONING	79
4.9 INTERPRETATION	83

CHAPTER 5: FLUID INCLUSIONS	91
5.1 OXYGEN ISOTOPES	91
5.1.1 Results	93
5.2 SULPHUR ISOTOPES	97
5.3 FLUID INCLUSION STUDIES	98
5.3.2 Homogenisation temperatures	99
5.3.2 Salinity	100
5.4 DISCUSSION	101
5.4.1 Oxygen isotopes	101
5.4.2 Sulphur isotopes	103
5.4.3 Fluid inclusions	104
CHAPTER 6: CONCLUSION	106
6.1 Geological setting	106
6.2 Nature of Mineralisation	106
6.3 Fluid characteristics	107
6.4 Significant findings and implications for exploration	108
REFERENCES	109
APPENDICES	
1. LITERATURE REVIEW	
2. MICROPROBE DATA	
3. XRF DATA	
4. STABLE ISOTOPE DATA	

LIST OF FIGURES

1.1 Map of showing the location of the Wang Yai prospects and the neighboring epithermal low-sulphidation Chatree deposit.	2
1.2 Map showing the location of the Wang Yai prospects, Chatree Mine, major provinces and districts.	3
1.3 (A-B) Photographs of land use at Wang Yai	5
1.4. Aerial photograph of the Wang Yai tenement with location of major hills, prospects, and the town of Wan Hin.	6
2.1. Distribution of continental terranes and sutures within and adjacent to Thailand.	12
2.2. Map showing the Pichit-Petchabun district scale geology and location of Wang Yai study area and Chatree gold mine.	14
2.3. Map showing the district scale geology of the Wang Yai district.	15
2.4. LA-ICP-MS U-Pb Concordia plot – Quartz phyric rhyolite.	17
2.5. LA-ICP-MS U-Pb Concordia plot – Quartz phyric sandstone/breccia	18
3.1. Geological map of south Wang Yai showing the location of lithological units and distribution of vein float, subcrop, and stockwork.	22
3.2. Geological map of the Gift Prospect showing the location of lithological units and distribution of vein float, subcrop, and stockwork.	23
3.3. (A-E) Photographs showing petrological and textural characteristics of fossiliferous limestone and siltstone.	26
3.4. (A-B) Photographs showing accretionary lapilli and textural characteristics of andesitic sandstone.	28
3.5. (A-D) Photographs showing petrological and textural characteristics of massive volcanic conglomerate.	32
3.6. (A-B) Photographs showing petrological and textural characteristics of quartz polymictic breccia.	34
3.7. (A-B) Photographs showing petrological and textural characteristics of quartz phyric rhyodacite.	36
3.8. (A-B) Photographs showing petrological and textural characteristics of feldspar phyric andesite.	37
3.9. (A-B) Photographs showing petrological and textural characteristics of fine grained perlitic breccia.	38

3.10. (A,B) Photographs showing petrological and textural characteristics of feldspar phyric diorite.	39
3.11. (A-B) Photographs showing petrological characteristics of quartz diorite.	40
3.12. Zr/TiO ₂ and Nb/Y rock discrimination diagram of andesitic sandstone, andesitic lithic breccia, rhyodacite, quartz diorite, and feldspar phyric andesite.	42
3.13. Zr/Y vs Zr discrimination diagram of andesitic sandstone, andesitic lithic breccia, quartz diorite, rhyodacite, and feldspar phyric andesite.	43
4.1. Aerial photo of the Wang Yai tenement showing the locations and names of vein systems.	48
4.2. Fact map of Conical Hill showing the location of subcrop for the main high grade vein system and location of vein float for the second system to the west.	50
4.3. (A-F) Photographs showing quartz textural characteristics of Conical Hill.	53
4.4. (A-F) Photomicrographs showing the ore mineralogy characteristics of Conical Hill.	56
4.5. Frequency histogram of gold fineness values for Conical Hill.	57
4.6. Photograph of Central Ridge.	58
4.7. Fact map of Central Ridge vein system.	59
4.8. (A-B) Photomicrographs of ore mineralogy at Central Ridge.	61
4.9 (A-F) Photographs showing the quartz textures at Central Ridge.	62
4.10. Photograph of T1 Hill.	63
4.11. Fact map showing the location of the main vein system at T1 Hill.	64
4.12. (A-F) Photographs showing the quartz textures at T1 Hill.	66
4.13. Photograph showing K-Feldspar alteration.	69
4.14. (A-B) Photomicrographs showing textures and characteristics of ore mineralogy at T1 Hill.	71
4.15. Fact map of Gift prospect showing the location of vein systems, vein float and surface alteration.	73
4.16. (A-B) Photographs showing the textural characteristics of vein system 'F' in the Gift prospect.	76
4.17. (A-F) Photographs showing the textural characteristics of A, B, C, D, E vein systems in the Gift prospect.	77
4.18. (A-B) Photomicrographs showing the characteristics of ore mineralogy at Gift prospect.	79

4.19. Epithermal model developed by Buchanan (1981) with the Wang Yai vein systems superimposed.	84
5.1. Aerial photo of Wang Yai show the raw ^{18}O SMOW values in per mil for each Gift prospect vein system.	94
5.2. Frequency histogram of calculated ^{18}O SMOW values of ore fluids at 180°C, 250°C, and 300°C.	96
5.3. Frequency histogram of ^{34}S values for wall rock and vein located pyrite.	97
5.4. Photomicrographs showing characteristics of Type I and II fluid inclusions.	99

List of Tables

2.1. Summary of the characteristics of magmatic events in the Loei Folbelt, Thailand.	16
4.1. Summary of microprobe analyses of argentite at Conical Hill.	55
4.2. Summary of microprobe analyses of electrum at Conical Hill.	57
4.3. Summary of primary, recrystallisation, and replacement quartz textures for Conical Hill, Central Ridge, T1 Hill, Gift prospect and T4 Hill.	81
5.1. Summary of ^{18}O SMOW values for quartz at Wang Yai.	92
5.2. Summary of isotopic compositions of ore fluids for calculated temperatures.	95
5.3. Summary of ^{34}S values for vein and wallrock located pyrite.	96
5.4. Summary of fluid inclusion data, Wang Yai.	101

Chapter 1 Introduction

1.1 Preamble

Epithermal gold mineralisation at the Wang Yai prospects, central Thailand is a resource which has been known for over 10 years and up until now no scientific research of the rocks have been undertaken. The Wang Yai district is being actively explored by Thai Global Ventures Co., Ltd. Exploration to-date includes soil and rock chip sampling combined with limited soil geochemistry, RAB, RC and diamond drilling. The results from this preliminary exploration have highlighted the need for further investigation. This thesis will build on the exploration data sets already available and provide new information from the field work undertaken in February 2005. Particular emphasis is given to the well preserved outcrops of epithermal veins in the district. Analytical techniques such as vein texture studies, petrography, stable oxygen and sulphur isotopes, and fluid inclusions were used to help better constrain the physiochemical character of fluids that were associated with the formation of the Wang Yai prospects.

1.2 Location

Wang Yai prospects are located in the Petchabun Province, central Thailand approximately 300km north of Bangkok and 15km NE of the Chatree gold mine (Figure 1.1). The small town of Wan Hin lies on the eastern border of the tenement and is the site of the Erawan Mining camp and accommodation for employees. Wan Hin is approximately 5km northwest of Wang Pong (Figure. 1.2). The Wang Yai tenement covers an area of 3 by 2km and consists of three different prospects. The prospects include Gift (in the north) , S.V (to the east), and the T4 Hill, T1 Hill, Central Ridge, and Conical Hill (in the south; Figure 1.4). In this study the Gift prospect and southern prospects (T4 Hill, T1 Hill, Central Ridge, and Conical Hill) will be the main focus.

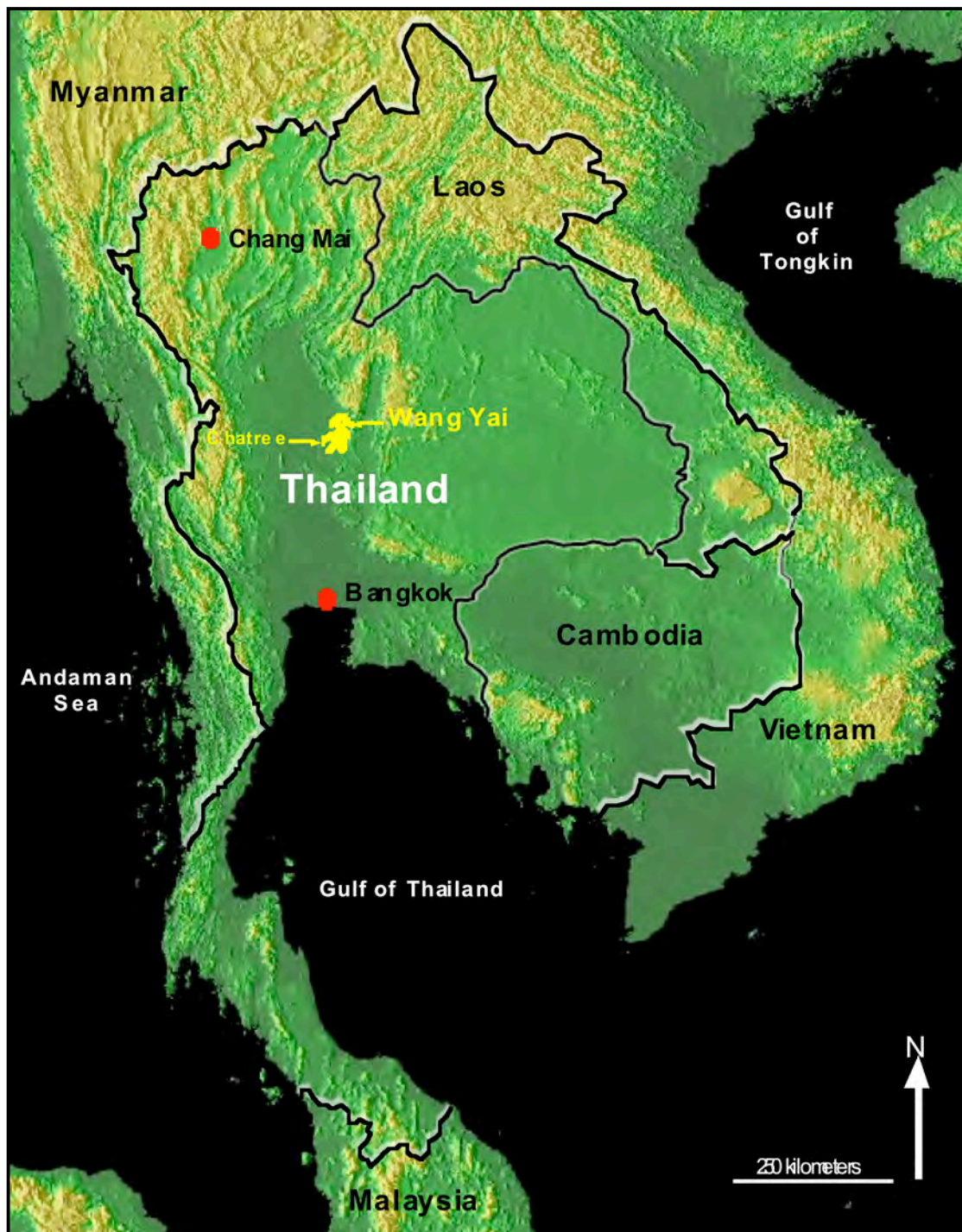


Figure 1.1 Map of Thailand showing the location of the Wang Yai prospect and the neighbouring epithermal low-sulphidation Chatree deposit to the south east

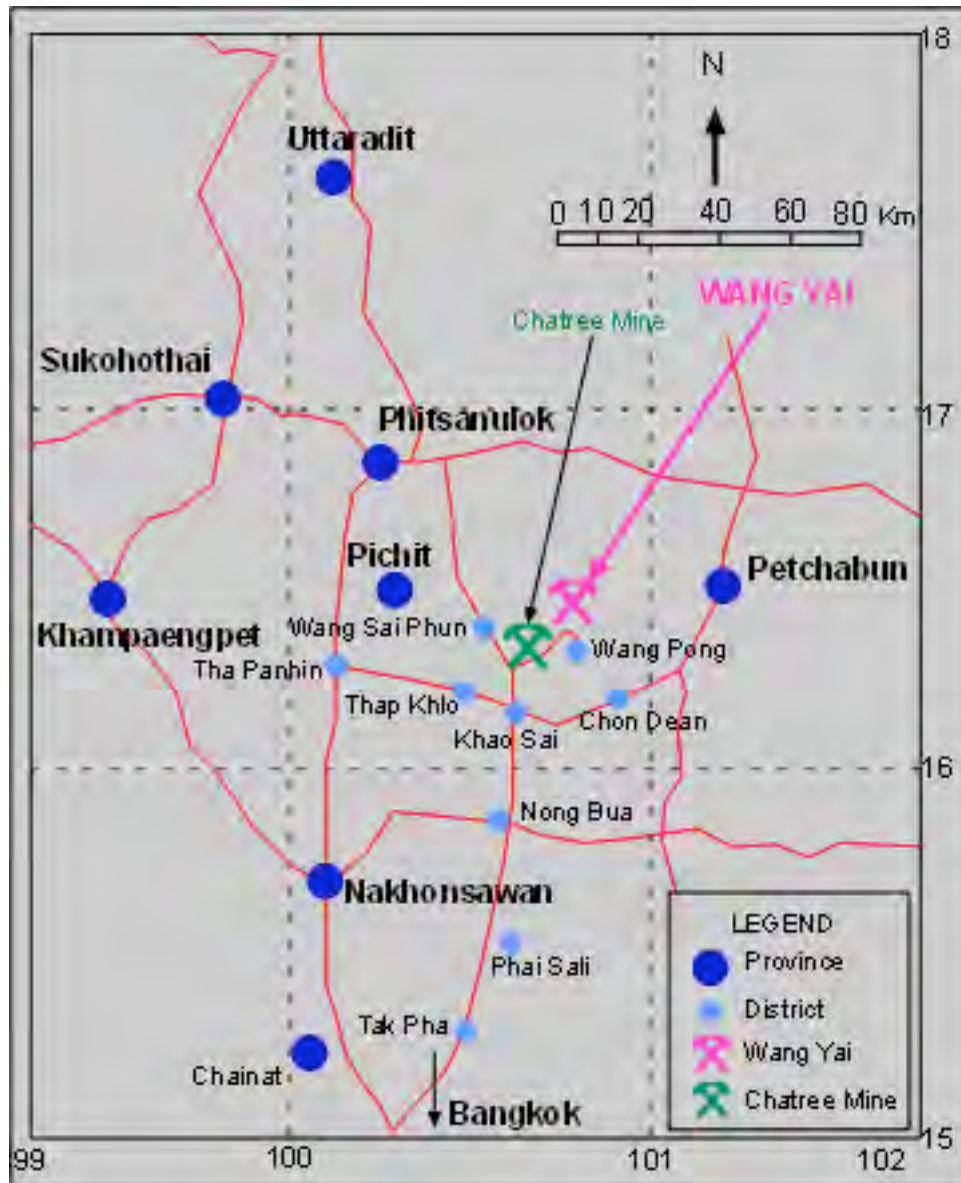


Figure 1.2 Map showing the location of the Wang Yai prospects, Chatree Mine, major provinces and districts (modified after Kromkhun, 2005).

1.3 Access

Access to the Wang Yai prospects is via a series of sealed bitumen roads linking the major provinces and towns. Within the tenement, gravel roads and tracks provide excellent access throughout the dry season to all parts of the prospects. During the wet season the roads become inaccessible to light vehicles and restricted to 4WD vehicles.

1.4 Topography

The topography of the area consists of relatively flat alluvial plains and a series of north south trending, low hills (up to 160m). In the south of the tenement, 60% of the land is dominated by 5 major hills and gently undulating topography. The remainder constitutes the top north western corner which is dominated by flat low lying alluvial deposits. The major hills and their corresponding heights in the Wang Yai prospect include Conical Hill (140m), Central Ridge (155m), T1 Hill (125m), and T4 Hill (135m). These hills are characterised by the occurrence of well preserved north south trending quartz vein float and silica hematite altered volcanogenic host rocks. Outcrop is sparse. Dividing the elevated land from the low lying land is the Khlong Namman River which meanders through the prospect in a south west direction. The associated alluvial deposits occur on the northern side of the river and extent up to 1km away from the river and into the south of Gift prospect. The alluvium covers outcrop. Land on the southern side of river is more elevated and as a result the lateral extent of alluvial deposition is less.

1.5 Land use

Land use in the area is dominated by agricultural practices (>80%) such as teak, tamarind and eucalyptus plantations, rice and corn farming. Farming practices, with the exception of rice, are generally located on the flanks of hills as soils are thinner and provide excellent drainage. Rice farming is restricted to fertile low-lying land which is subject to flooding during the wet season (Fig. 1.3A). As a result of the extensive agriculture most of the natural vegetation has been cleared. Minor pockets still exist in areas which are not suitable for farming such as some of the steep hill tops in the Gift prospect. The climate in the area consists of three seasons: summer (March to May), a rainy season (June to October), and winter (November to February).

1.6 Exposure

Exposure in the Wang Yai tenement is variable in and between the prospects. The elevated areas (Conical Hill, Central Ridge, and T1 Hill) of the Wang Yai tenement provide good outcrop of vein systems and the volcanic host rocks. Outcrop in the Gift prospect is less common and is mainly restricted to the hill tops, dam walls and irrigation trenches. Throughout the entire tenement exposure is increased during the dry season when farmers undergo routine burn offs. Burn offs were undertaken before and during the field work in February 2005 which resulted in excellent exposure of float and the accessibility needed to construct accurate geological maps despite the lack of outcrop.



Figure 1.3. A) Photo showing farming on flat low lying land and corn plantations on the hill flanks, taken from T1 Hill looking south east, (photo pers. Comm. Stuart Smith). B) Photo looking north west from Kham Hill in the Gift prospect showing the typical mapping terrain.

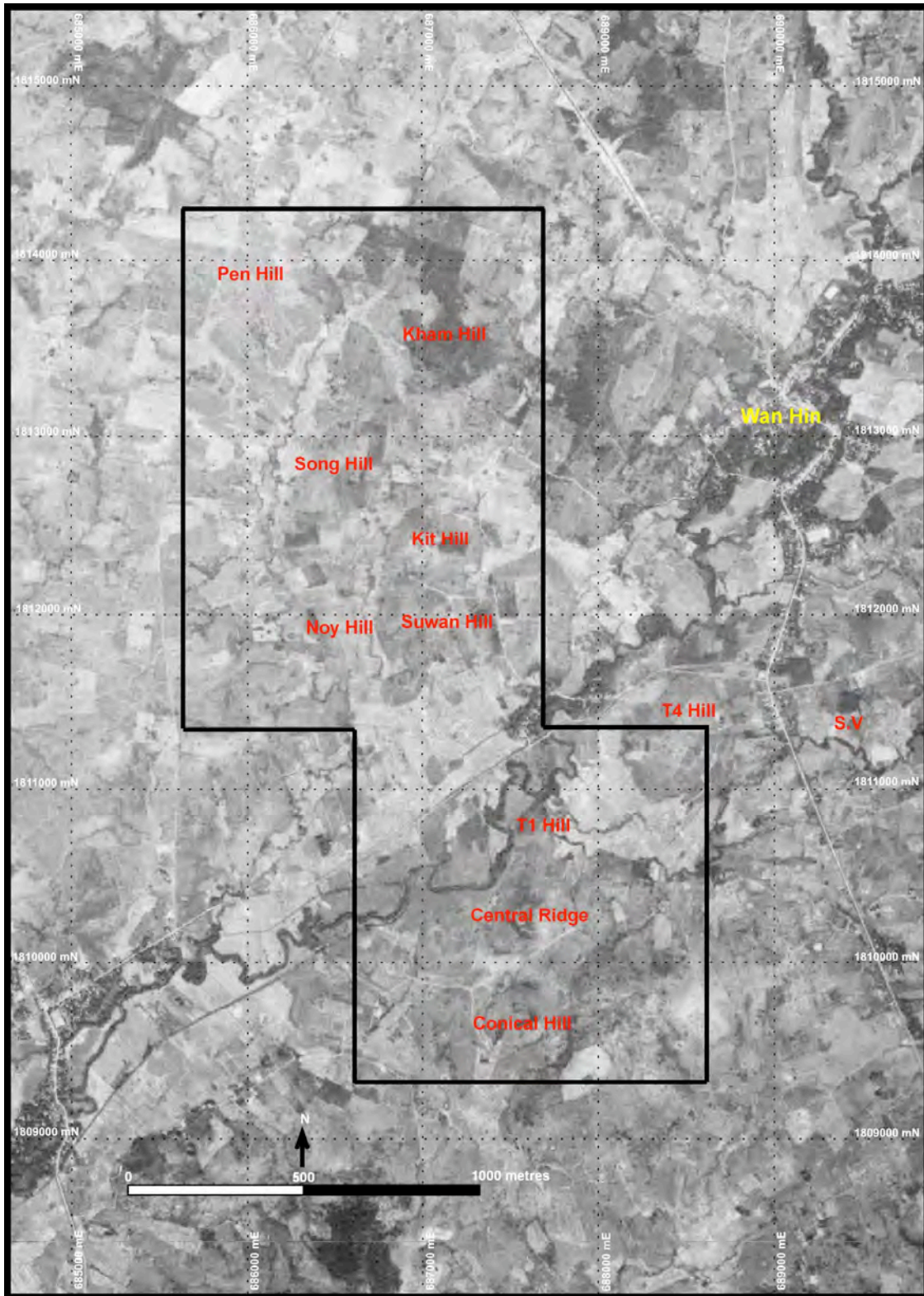


Figure 1.4. Aerial photograph of the Wang Yai tenement with location of major hills, prospects, and the small town of Wan Hin, central Thailand

1.7 Exploration History

In the 1990's the Special Prospecting Licenses for Wang Yai were granted to Phelps Dodge Ltd. Exploration in the area was undertaken by Erawan Mining Ltd which was in joint venture with Phelps Dodge at the time. Erawan Mining Ltd conducted magnetic surveys, radiometrics, AEM, RC drilling, trenching and diamond drilling at T1 Hill. In the year 2000 the exploration licences held by Phelps Dodge Ltd expired and were not renewed. Thai Global Ventures Co., Ltd (which is owned by Thai Goldfields NL, in joint venture with Oxiana Ltd) then applied for, and was granted new Special Prospecting Licenses for Wang Yai in the year 2000. Thai Global Ventures Co., Ltd has conducted work on the area from 2000 to present. This work has included rock chip collection, trenching, RC drilling and three additional diamond drill holes at T1 Hill. A further 2 diamond drill holes at Conical Hill are planned and this will commence once tenement licences are granted (pers.comm., Ian Cameron).

1.8 Aims

This study has several major aims, they include the following:

- To provide an understanding of the geological setting of the epithermal systems in the Wang Yai area.
- To describe and interpret the nature of mineralisation and alteration in the known prospect areas.
- To conduct a preliminary study of fluids responsible for the mineralisation in the area.
- To compare and contrast the Wang Yai systems with current models for epithermal systems with particular emphasis given to the nearby Chatree epithermal gold deposit.

1.9 Methodology

The methods used in this study include; geological mapping, logging of diamond drill core, transmitted and reflected light petrological examination, macroscopic and microscopic examination of quartz vein textures, stable isotope analyses, and fluid inclusions.

Geological mapping and logging of diamond drill was commenced at the Wang Yai district Thailand on 2nd February 2005. The aims of the geological mapping were to construct accurate 1:2500 base maps detailing the location of geology, alteration, and vein systems. The mapping was undertaken by foot with the aid of a 4WD for transportation to and from the prospect and also to areas that were difficult to access. A total of nine 1:2500 maps were constructed for the southern area of the Wang Yai prospects and 12 maps for the Gift prospect. During the mapping representative samples of the geology and veins were collected for detailed reflected and transmitted light examination. Nine diamond drill holes from T1 Hill were logged and five were used to construct a representative section. Field work was completed by 6th March 2005.

Detailed petrographic analysis and volcanologic analysis was conducted on each lithofacies to determine the depositional processes and environment, in order to compare rocks at Wang Yai with the stratigraphy at the Chatree gold mine. Geochemical characteristics of each lithofacies were determined by X-ray Fluorescence, (XRF) at the University of Tasmania (methods in Appendix 2).

Geochronology was undertaken using zircon LA ICPMS U-Pb on 5 samples. K-Ar was also used to constrain the timing of hydrothermal mineralisation (methods in Appendix 3).

A macroscopic and microscopic examination was used to describe the characteristics of vein textures. Microprobe analysis was conducted on sulphide grains to determine their composition, and highlight trace element variations.

Stable oxygen isotope analysis of 16 quartz vein samples was undertaken to infer the fluid source and/or important ore forming processes. Oxygen isotope data of vein quartz from each vein systems was used to establish a correlation between gold grade and oxygen isotope values (as to assess its usefulness as a vector to higher grade portions of the veins). Sulphur isotopes analysis of vein and wall rock pyrite were used to constrain the source of sulphur. Limited fluid inclusion microthermometry of vein quartz was used to determine the temperature and salinity of fluids and confirm inferences made for observed mineralogy and textures at Wang Yai.

Chapter 2 Regional Geology

2.1 Tectonic Evolution

Thailand comprises of two main tectonic terranes that include the Shan-Thai Terrane (west) and the Indochina Terrane (east). These two terranes are bound together along the north south trending Nan Suture zone (Figure 2.1). The Shan-Thai Terrane, lies on the western side of the Nan Suture, underlies the western and peninsular of Thailand, eastern Myanmar, southwestern Yunnan, and the western Malay peninsular (Metcalf, 1996). The geology comprises of Pre Cambrian basement rocks (gneiss, marble, calc-silicates, schists and quartz) overlain by Cambrian and Ordovician silicalastics, carbonates, and Permian shallow marine sequences (Charusiri et al., 2002). Paleogeographical reconstruction show that Shan-Thai Terrane was once connected to, the northwestern Australian Gondwanaland margin (Charusiri et al., 2002). During the Lower Palaeozoic, the Shan-Thai Terrane rifted off the Indian-Australian margin (Metcalf, 1996). This separation from Gondwanaland coincided with a marine transgression synchronous with the formation of Palaeotethys (Charusiri et al., 2002). The Shan-Thai Terrane migrated northwards towards the paleoequator and eventually collided with the Indochina Terrane block during the Permian-Triassic (Charusiri et al., 2002).

The Indochina Terrane flanks the eastern side of the Nan-Uttaradit-Sra Kao Suture (see Figure 2.1) and underlies northern Thailand, Cambodia, most of Lao PDR, Vietnam, and eastern Malaysia (Figure 2.1; Charusiri et al., 2002). The geology of the Indochina Terrane consists of Precambrian basement rocks overlain by Palaeozoic shallow marine sequences and Mesozoic continental deposits (Sashida and Igo, 1999). The Indochina Terrane was derived from the northern and north eastern margin of Gondwanaland (Burrett et al., 1990). It began to rifted away from Gondwanaland during the Devonian to Early Carboniferous (Metcalf, 1996). During the early Triassic the Indochina Terrane collided with Shan-Thai, which resulted in the closer of Palaeotethys. Closure and

sitching of these terranes occurred along the Nan Suture (Charusiri et al., 2002). Emplacement of I-type and S-type granites, development of NE and NW trending faults, uplift and erosion followed the collision of the two terranes.

2.2 Loei Foldbelt

The Loei Foldbelt is located in central Thailand on the western margin of the Indochina Terrane (Figure 2.1). Wang Yai is located in this foldbelt. The Loei Foldbelt trends north south and is bound with the Sukothai Foldbelt in the south by the Chao-Phraya strike slip fault (Sitthithaworn and Wasuwanich 1992). According to Sitthithaworn and Wasuwanich (1992), the depositional environment of the Loei Foldbelt represents a remanent island arc which occurred was the result of western-ward subduction of the leading edge of the Indochina Terrane.

The geology of the Loei Foldbelt comprises of units ranging in age from the Ordovician through to the Mesozoic (Intasopa, 1993). Geochemical evidence suggests that Precambrian crystalline basements rocks occur beneath the Loei Foldbelt, however they do not outcrop (Intasopa, 1993). Rocks of the Silurian-Devonian period consist of volcanic arc andesitic and rhyolitic suites and their volcanoclastic equivalents (Intasopa, 1993). Sedimentary units such as shale, siliceous carbonaceous shale, and chert also occur (Intasopa, 1993). The Carboniferous period represents the syn-tectonic deposition of chert, siliceous shale, tuffaceous sandstone, sandstone, conglomerate and limestone from an environment that changed from deep marine during the Early Carboniferous to a coastal swamp environment during the Late Carboniferous (Harris et al., 2004). This period is also marked by island arc backarc volcanism associated with the deposition of tholeiitic basalts (Intasopa, 1993).

During the Triassic period large granitoids together with rhyolitic volcanic and volcanoclastics were emplaced along the Loei Foldbelt (Harris et al., 2004). Associated

with this magmatism is significant Cu and Au mineralisation along the length of the Loei Foldbelt. This includes the multi million ounce Chatree Au-Ag epithermal deposit.

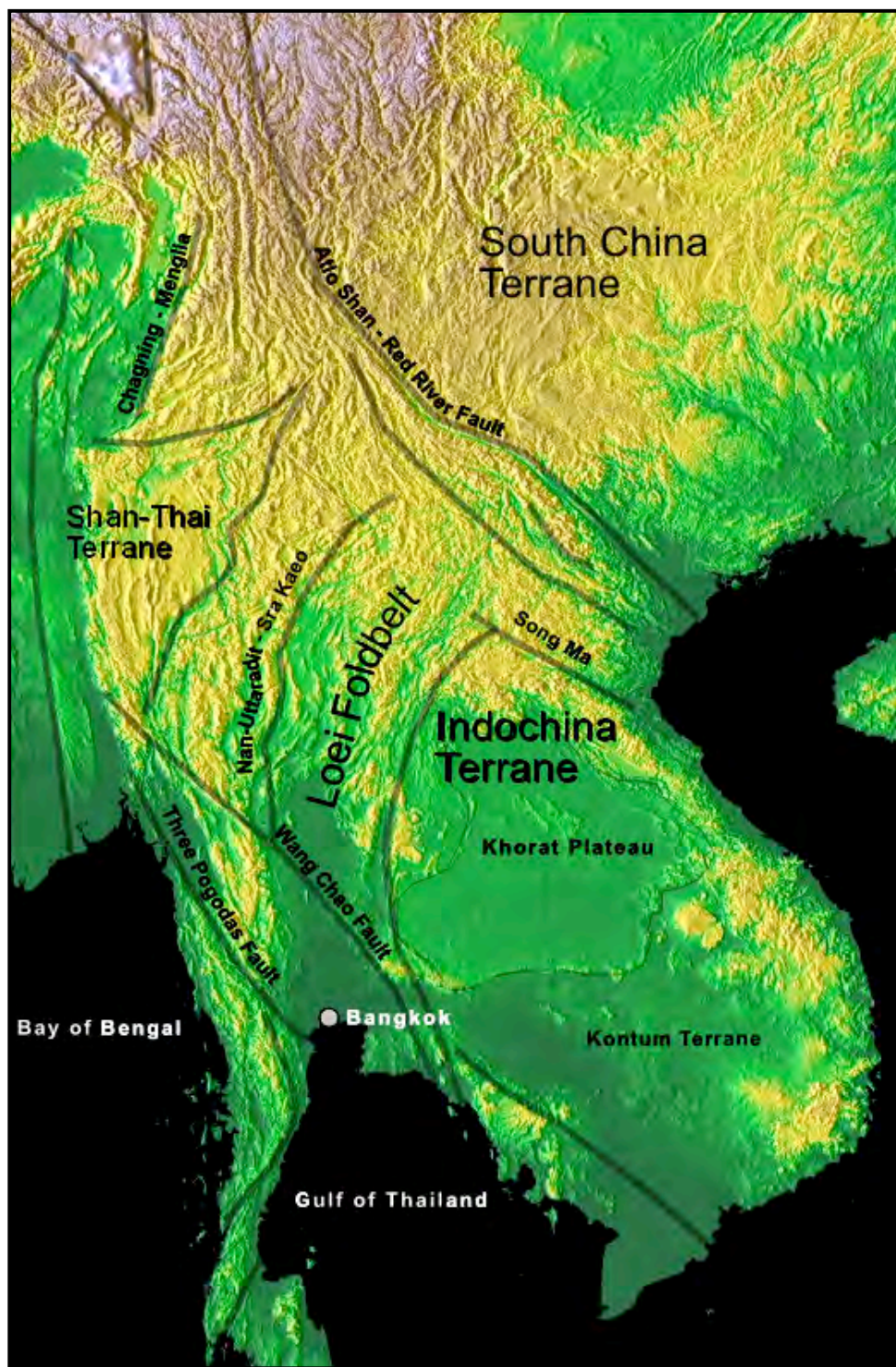


Figure 2.1 Distribution of continental terranes and sutures within and adjacent to Thailand (modified from Harris et al., 2004)

The Jurassic to Cretaceous period marks the uplifting event which subsequently resulted in the erosion and deposition of the continental red-bed sequences known as the Khorat Group (Charusiri et al., 2002).

2.3 District scale geology of Wang Yai

Wang Yai is located along the Loei Foldbelt in the Pitchit – Petchabun district. The district scale geology of Wang Yai comprises of Carboniferous, Permian – Triassic and Jurassic – Cretaceous Formations (Figure 2.2). Carboniferous rocks include the Huai Hin Lat and Dok Du Formations and consist of cherts, siliceous shale, tuffaceous sandstone, sandstone, conglomerate and limestone. Permo-Triassic rocks in the Wang Yai district include suites of rhyolite, dacite, andesite, basaltic andesite and their volcanoclastic equivalents (Figure 2.3; Diemar and Diemar 1999). Wang Yai quartz veins and the nearby Chatree gold deposit, are hosted in these Permo-Triassic rocks (Figure 2.3). Jurassic – Cretaceous continental red beds of the Khorat Group occur to the north of Wang Yai and form thick sequences of intra-continental derived sediments which unconformably overlie Permian – Triassic volcanics. Much of the district scale geology is covered by thick Quaternary slope wash, valley plain, and residual deposits. These deposits occur as a thick cover over the older volcanosedimentary Permian – Triassic successions (Figures 2.2 and 2.3).

Structure in the region comprises of regional north-south, northwest and northeast faulting which has been interpreted to have initiated from the Triassic orogenesis (Diemar and Diemar 1999).

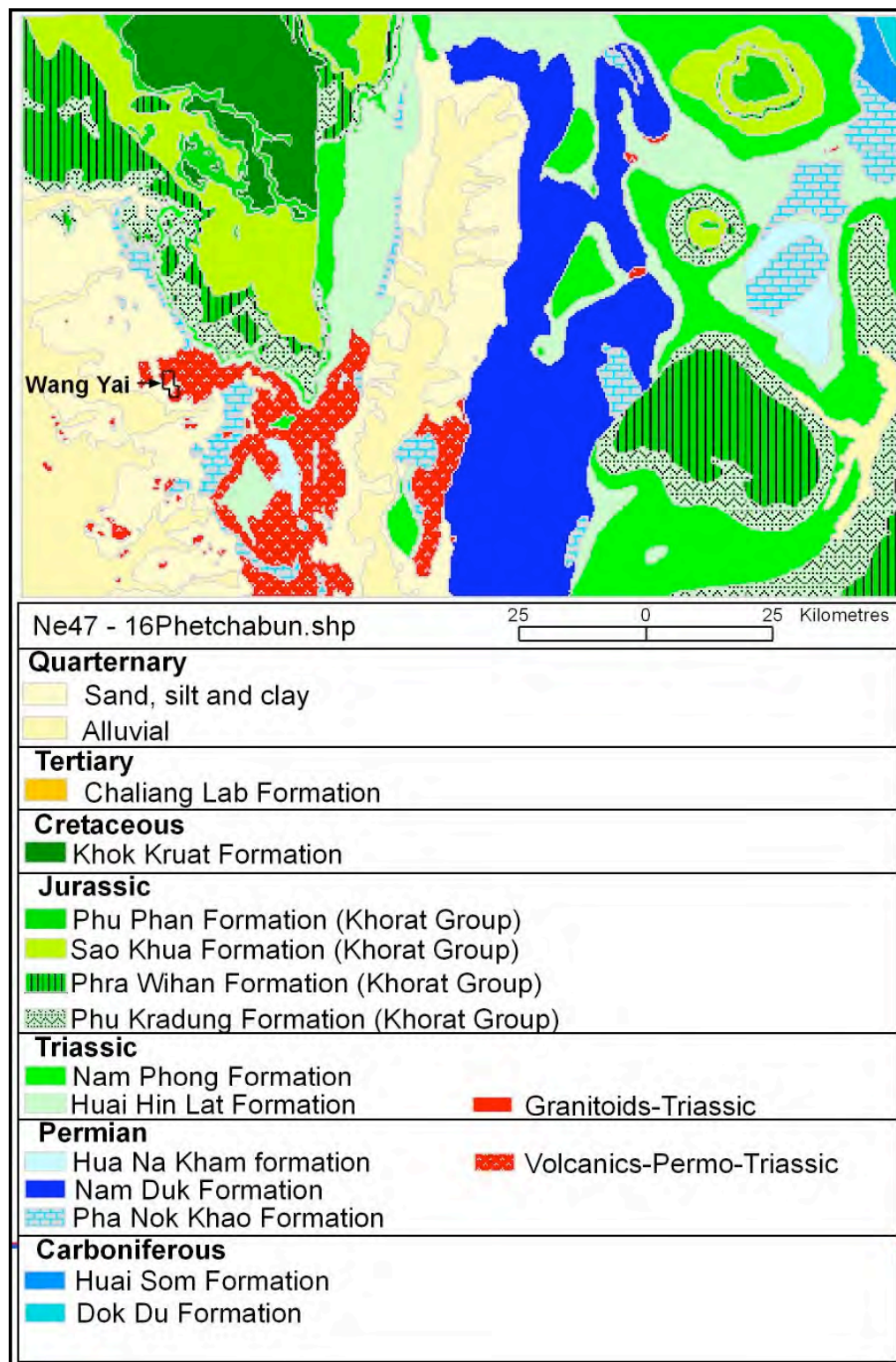


Figure 2.2. Map showing the Pichit – Petchabun district scale geology and location of Wang Yai study area and Chatree gold mine (modified after Khin Zaw, 2005).

2.4 Geochronology of the Loei Foldbelt

Geochronological studies of the Loei Foldbelt revealed five main events of magmatism occurred between the Ordovician and Triassic periods (Intasopa, 1993; Khin Zaw et al., 1999; Harris et al., 2004). They include Silurian (435-410 Ma), Devonian (400-350 Ma), Carboniferous (350 Ma), Early Permian (300-275 Ma), Triassic (245 – 210 Ma) and Tertiary events (Intasopa, 1993). The characteristics of magmatism events are shown in Table 2.1. Data from this table was obtained from Harris et al. (2004) ‘*epochs of magmatism*’ which includes a summary of previous literature together with new LA-ICP-MS U-Pb zircon and $^{40}\text{Ar}/^{39}\text{Ar}$ geochronology as part of the AMIRA P390A project.

Table 2.1 Summary of the characteristics of magmatic events in the Loei Foldbelt, Thailand

Event	Dating Method	Characteristics	Mineralisation	References
Silurian (435-410 Ma)	LA-ICP-MS U-Pb Zircon	Intermediate/felsic volcanics		(Harris et al., 2004)
Devonian (400-350 Ma)	Rb/Sr	Intermediate/felsic volcanics	Pb-Zn and Ag Carbonate hosted	(Harris et al., 2004)
Carboniferous (350 Ma)	LA-ICP-MS U-Pb Zircon, Rb/Sr	Basalt, rhyolite, and andesite	Pb - Zn	(Harris et al., 2004; Intasopa, 1993)
Permian (300-260 Ma)	LA-ICP-MS U-Pb Zircon	Intermediate/felsic volcanics with limestone horizons	Cu-Au porphyry, epithermal Au, Skarn style	(Harris et al., 2004)
Triassic (245-210 Ma)	$^{40}\text{Ar}/^{39}\text{Ar}$, LA-ICP-MS U-Pb Zircon, SHRIMP	Intermediate/felsic volcanics, large granitoids	Fe, Cu, Au porphyry, epithermal, and skarn	(Harris et al., 2004; Intasopa, 1993; Rak, 1999)

Geochronology of Wang Yai

As part of this study and collaboration with ARC Linkage Project ‘Geochronology, metallogenesis and deposit styles of the Loei Foldbelt in Thailand and Laos PDR’, five rocks from the Wang Yai tenement were dated using LA-ICP-MS U-Pb zircon. Dating was undertaken to confirm the Permian – Triassic age (Khin Zaw et al., 1999) of rocks at Wang Yai. Of the five samples dated, only two samples; rhyolite and quartz phyrlic

breccia/sandstone contained zircons. The rhyolite (ER017162) was found during field mapping outcropping in a dam wall at the Gift prospect and the quartz phyric breccia/sandstone outcrops on Central Ridge and on the hill east of Conical Hill.

LA-ICP-MS U-Pb zircon dating of the quartz phyric rhyolite yielded an age of 321 ± 5 Ma (Late Carboniferous; Figure 2.4). Previous to this study, Carboniferous rocks in the region were thought to consist of tholeiitic basalts and sedimentary packages such as chert, shale, sandstone, conglomerate, and limestone (Harris et al., 2004). The age of this rhyolite confirms that felsic magmatism occurred in the Loei Foldbelt. At Wang Yai Permian – Triassic host volcanic rocks overlie the rhyolite.

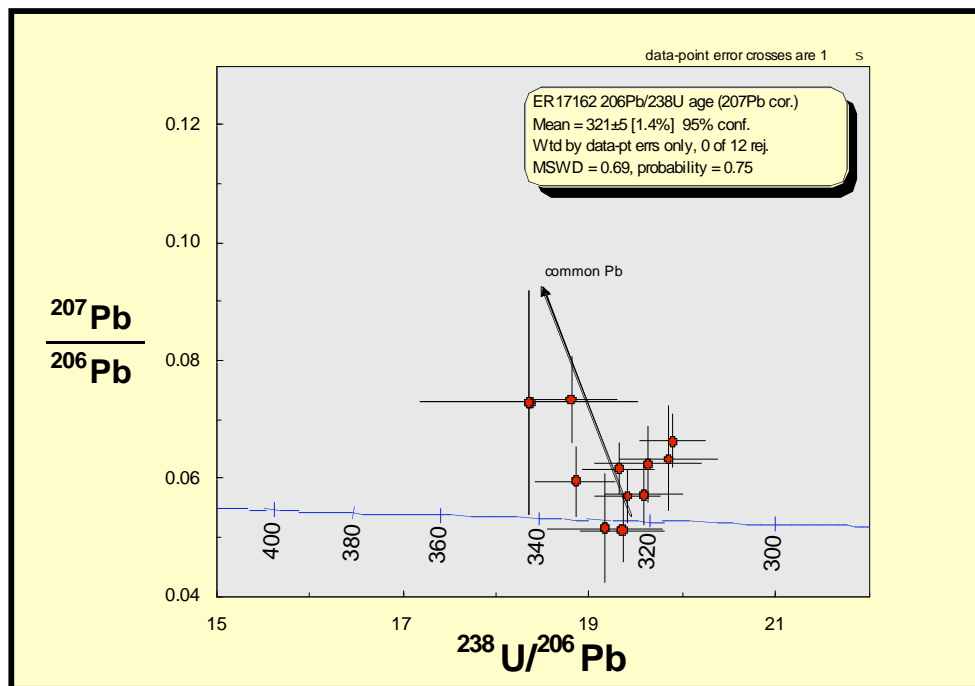


Figure 2.4 LA-ICP-MS U-Pb Concordia plot– Quartz phyric rhyolite, Wang Yai, central Thailand.

LA-ICP-MS U-Pb zircon dating of the quartz phyric sandstone/breccia host rock yielded an age of 247 ± 4 Ma (Lower Permian – Upper Triassic; Figure 2.5). This date is slightly younger than previous $^{40}\text{Ar}/^{39}\text{Ar}$ dating of andesitic sandstone which gave an Early

Permian age of 293.8 ± 0.6 Ma (Khin Zaw et al., 1999). The 247 ± 4 Ma age for the sandstone is however, consistent with LA-ICP-MS U-Pb zircon ages obtained for the host volcanic stratigraphy (250 ± 6 Ma) at the Chatree gold mine (Meffre et al., 2005).

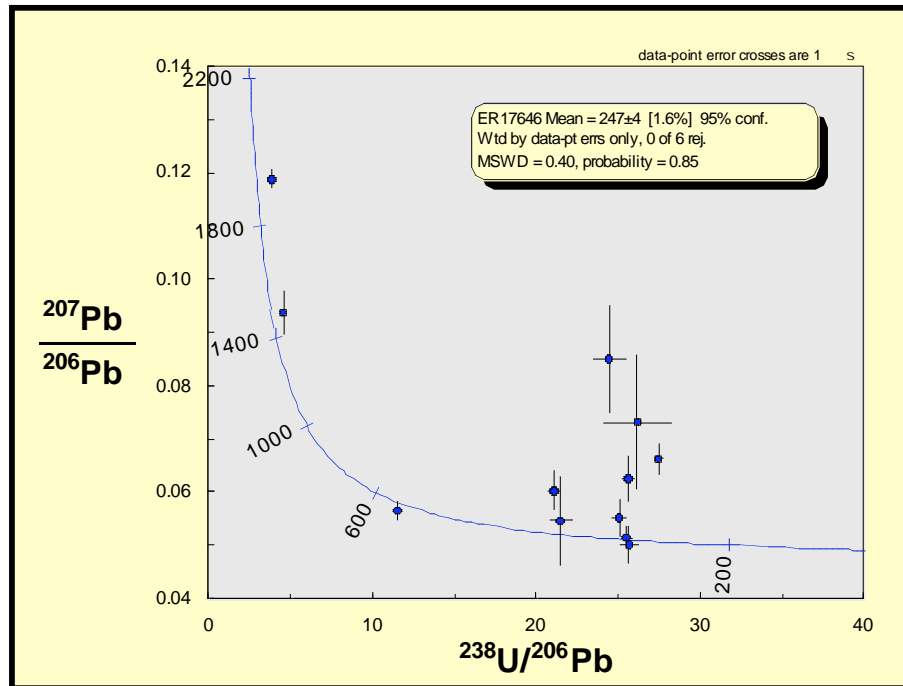


Figure 2.5 LA-ICP-MS U-Pb Concordia plot– Quartz phyric sandstone/breccia, Wang Yai, central Thailand.

2.5 Age of hydrothermal alteration

Constraining the age of hydrothermal alteration at Wang Yai has important implications in terms of determining its relationship with the nearby Chatree deposit and potential for further exploration in the district. The hydrothermal alteration at Chatree deposit has been bracketed between 256 Ma and 232 Ma (pers.comm., Harris 2005). This age range is based on previous laser ablation $^{40}\text{Ar}/^{39}\text{Ar}$ dating of fine-grained adularia (as part of the AMIRA project P390A) and LA-ICP-MS U-Pb zircon age of 238 ± 6 Ma for crosscutting dykes (Meffre et al., 2005).

Hydrothermal alteration assemblages at Wang Yai have been previously dated. Khin Zaw et al. (1999) undertook laser ablation $^{40}\text{Ar}/^{39}\text{Ar}$ dating of fine-grained adularia of intensely altered host rock at Wang Yai. The samples yielded ages of; 206.1 ± 0.3 Ma, 228.5 ± 0.2 Ma, 234.5 ± 0.3 Ma (Khin Zaw et al., 1999). As part of this project a further 2 whole rock samples, comprising of near total rock replacement of fine grained adularia, were submitted for K-Ar dating (University of Queensland). The samples yielded ages of 123.8 ± 5.3 Ma and $111.4 \pm$ Ma. This younger age is inferred to be due to thermal resetting. K-feldspar is particularly susceptible to resetting by overprinting thermal events such as deformation (faulting and metamorphism) and/or magmatism and associated fluid flow.

Chapter 4 Gold-bearing quartz veins

4.1 Introduction

At Wang Yai, gold is hosted in a series of outcropping quartz-chalcedony vein systems trending roughly north south. These quartz veins are best exposed as a line of discontinuous, bulbous hills. In the southern part of the tenement, Erawan Mining has individually named vein systems; these prospects include Conical Hill, Central Ridge, T1 Hill, and T4 Hill (Figure 4.1). Preliminary exploration in this area has included 5 diamond drill holes along a 190m long east-west transect at T1 Hill and two additional holes on the north and south side of the transect. These holes have intercepted sporadic stringer and stockwork quartz veins with minor gold mineralization. Gold is typically hosted in comb quartz-carbonate-chlorite-illite \pm adularia (hematite) veins. The northern part of the tenement is characterized by vein systems collectively referred to as Gift. A total of six vein arrays occur in the Gift portion of Wang Yai; of these five follow a north-south trend, and one trends to the northeast. Exploratory trenches have been dug across the veins, but as yet no diamond drilling has taken place.

This chapter describes the location and size of quartz veins and mineralised zones at Wang Yai. Vein textures will be classified using the classification scheme of epithermal quartz textures developed by Dong et al. (1995). A description of surface alteration assemblages will be given for host rocks proximal to vein systems and a more detailed description of primary hydrothermal alteration from T1 Hill drill core. Where present, vein paragenesis and ore mineralogy will also be described. Discussions presented here focus on the mineralogical and textural zoning in Wang Yai.

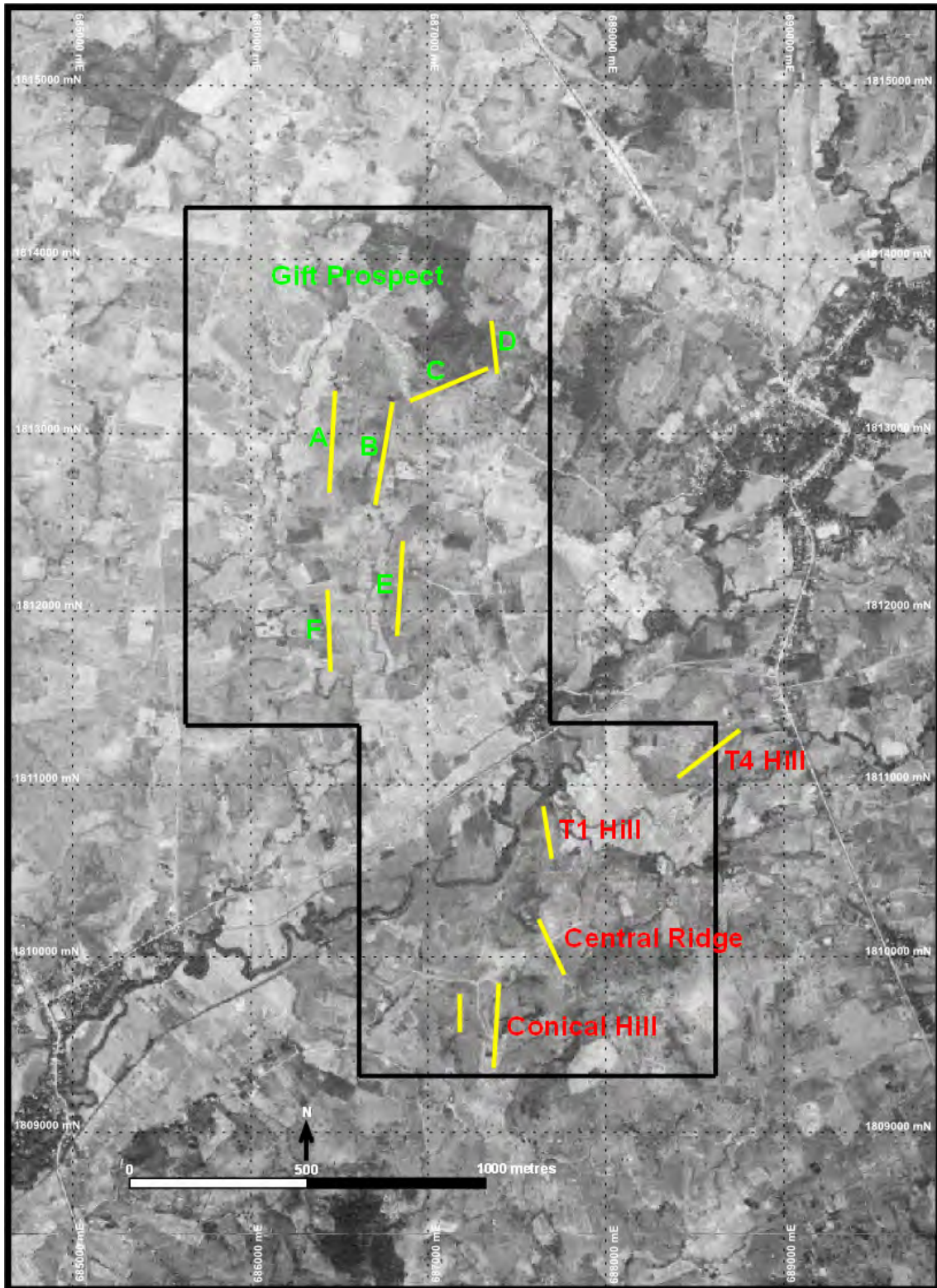


Figure 4.1 Aerial photograph of the Wang Yai tenement showing the locations and names of vein system, Central Thailand.

4.2 Conical Hill

Location: Conical Hill occurs at the southern end of the Wang Yai tenement. The hill on which the centre vein outcrop occurs rises approximately 140m. Vein exposures include massive crystalline quartz veins, quartz-chalcedony stockwork and sporadic host rock outcrops.

The Conical Hill area comprises of two vein systems (see Figure 4.2). The main system is a single *in situ* quartz vein (with anomalous Ag-Au values) outcropping on the western slope of the hill (GR-1809600mN, 688615mE). Massive quartz-chalcedony outcrop covers an area of 100m in strike (350°N) and approximately 35m wide. The vein zone narrows to several metres in the north and terminates at (GR1809625mN, 688615mE). Large boulders (up to 1m) of quartz-chalcedony float are scattered on the slopes flanking this outcrop and give the false impression of a considerably wider vein. Vein float surrounding the main vein zone suggests that the vein zone pinches northward (terminates at GR1809725mN, 6885785mE), while to the south the vein appears to swell to a maximum width of 75metres (terminates at GR1809475mN, 688600mE). In part, the quartz vein float includes host rock sandstone and breccia that is cut by quartz-chalcedony stockwork. Based on the vein float distribution, it appears that the stockwork zone covers an area approximately 100m wide and 325m long, and occurs immediately to the east of the main massive quartz-chalcedony vein zone. Associated with this stockwork zone is silicified, hematite-stained volcanogenic sandstone and breccia.

Two isolated outcrops of massive quartz and chalcedony also occur at Conical Hill. These are considered here as off shoots of the main vein, described above. The first vein outcrops in the northern and southern parts of a small dam wall (grid reference 1809475mN, 688615mE), approximately 20m south of the main vein zone. This vein exhibits a massive sugary quartz texture, is 1 to 2m wide, strikes ~170° and dips 85°E. It was not found outcropping to the north or south of this location. The second vein was

found during excavation of a drill pad (GR1809620mN, 688645mE) and this vein is approximately 12m long, 70cm wide and trends $\sim 345^\circ/85^\circ\text{E}$.

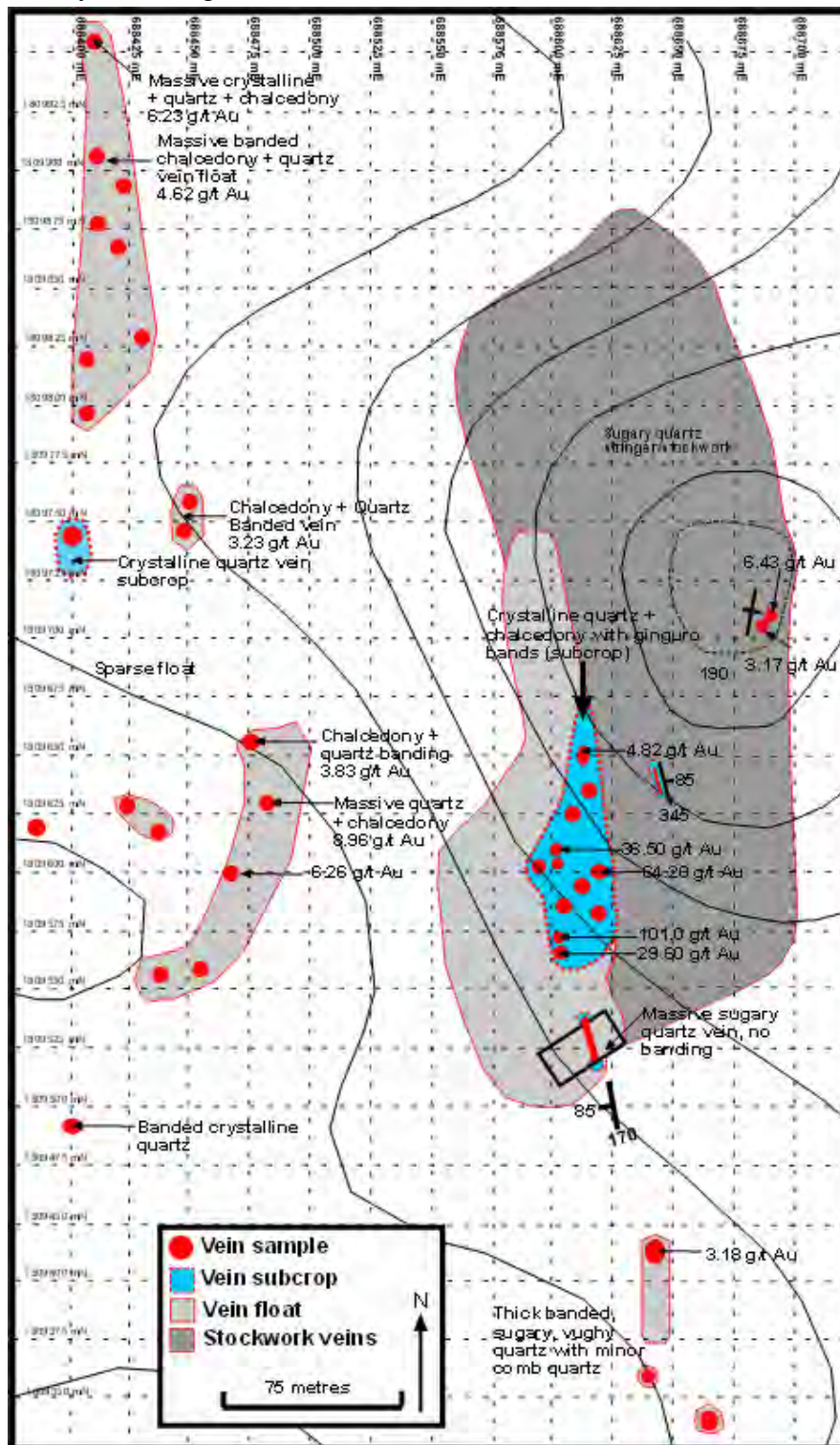


Figure 4.2 Fact map of Conical Hill showing the location of subcrop for main high grade vein system and the location of vein float for the second system to the west.

4.3 Quartz vein textures

Based on paragenetic and textural relationships, quartz veins in the main vein zone at Conical Hill have been grouped into four distinct categories;

A-type veins are characterized by milky white, crustiform and colloform quartz and chalcedony. They are typically associated with ‘ginguro’ (very fine disseminated sulfide) ore. Where seen this ginguro ore is associated with the micro-crystalline quartz bands. Thin adularia needles (now pseudomorphed by quartz) occur on the margins of chalcedony bands. These ‘A-type’ veins also display bladed quartz, silicified pseudomorphs of bladed calcite, and sericite alteration. Well-developed pseudo-acicular textures after calcite (plus adularia) also occur (see figure 4.3C).

B-type veins are characterized by brecciated vein with crystalline quartz cement and clasts of chalcedony, limestone and sandstone. In the quartz cement moss and ghost sphere textures usually occur. Typically, B-type veins do not host any mineralisation.

C-type veins are characterized by massive sugary or saccharoidal quartz with occasional moss and ghost sphere textures. C-type veins, like A-type at Conical Hill are host to ginguro ore and disseminated pyrite (Figure 4.3A).

D-type veins cut all vein stages and are characterized by banded chalcedony and minor clear often mineralised crystalline quartz which displays well developed moss textures (Figure 4.3E).

4.3.1 Conical Hill (West)

Location: This vein is located approximately 175 metres immediately west of the main Conical Hill vein. Although the vein does not outcrop, a line of scattered vein float implies its occurrence. Mapping was made difficult by vegetation cover plus disruption

of the vein float by farming equipment. The distribution of vein float suggests a north-south trend and a vein wide comparable to other vein systems in the area. The trend of surface vein float is north south and has a strike length of approximately 475metres. Float first occurs in the north at GR1809950mN, 688404mE and extends to GR1809475mN, 688400mE in the south. The width of float can be up to 50m wide in parts but is more commonly 25-30m. The vein is hosted in fine-grained clay + silica altered volcanoclastic sandstone and breccia. Due to poor outcrop and access there is potential for the vein to be more laterally extensive than what is interpreted here.

Quartz vein textures

The best gold grades are found in massive and banded sugary quartz and chalcedony veins with minor comb quartz. Relict pits containing goethite, jarosite, and limonite after sulphides occur. The highest gold assays (8.96g/t Au, 6.26g/t Au) occur in weathered volcanoclastic host rock with recrystallised chalcedony 5-7cm wide stockwork. These high assays may be a result of supergene enrichment rather than true gold grade, but grades up to 4.38g/t Au have been found in relatively fresh, massive recrystallised chalcedony.

Massive recrystallised chalcedony vein float exhibits cavities infilled with euhedral growth zoned faceted quartz grains. Chalcedonic zones display well-developed moss textures. Samples with these textures (including ER017417 and ER017522) have representative assays of 1.27g/t Au and 4.38g/t Au, respectively. Zones of clear translucent chalcedony tend to be preferred hosts of disseminated pyrite whereas white milky chalcedony is barren.

Crustiform colloform vein float consists of an outer milky white chalcedony layer with disseminated sulphide bands followed by alternating thin <4mm euhedral comb quartz and 8mm chalcedony bands. The vein material in the centre has been completely weathered but may have been late calcite infill.

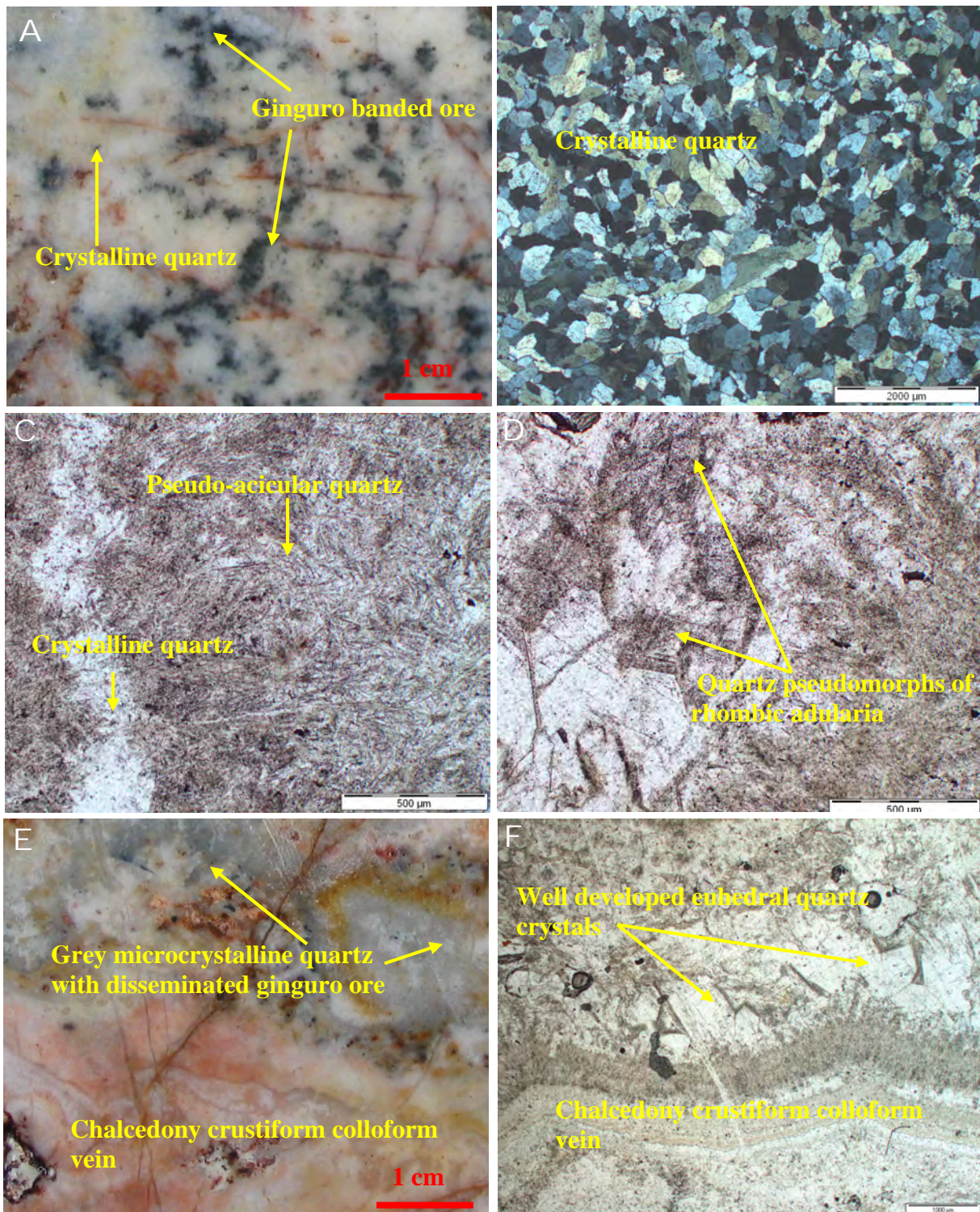


Figure 4.3 A) - Massive crystalline quartz showing banded and disseminated ginguro ore (ER017427). B) - Photomicrograph of crystalline quartz in xpl (ER017427). C) - Pseudo-acicular texture with thin preserved quartz vein (ER017960). D) - Silica pseudomorphs of former rhombic adularia (ER017960). E) - Pink chalcedony crustiform colloform vein cutting grey crystalline quartz vein with disseminated and banded ginguro ore (ER017422). F) - Photomicrograph of crustiform colloform vein with moss textures and euhedral quartz (ER017960).

4.3.2 Ore Mineralogy

Three sulphides have been identified in vein samples hosting ginguro ore at Conical Hill; they include electrum, argentite, and pyrite. Argentite is the most abundant and constitutes 90% of all sulphides. The sulphides are largely hypogene in origin. Electrum, argentite and pyrite occur in dark grey to black 'ginguro' bands. These metallic ginguro bands are typically associated with crystalline quartz, flamboydial quartz, lattice bladed quartz, and tabular adularia pseudomorphs. Supergene electrum also occurs as inclusions in hematite and goethite lined cracks.

Argentite: Argentite (AgS) occurs as small less than 1mm aggregates that most commonly occurs in thin >0.05mm bands, or on the edges of quartz grains (Figure 4.4A). Banded aggregates occur in the hinges of colloform chalcedony and in association with lattice bladed quartz pseudomorphs the resemble lattice bladed calcite. Argentite is intimately associated with electrum grains and where seen, it commonly occurs immediately adjacent to electrum. The presence of argentite is clearly visible in hand specimen and occupies up to 95% ginguro ore mineralogy. Microprobe analysis (see Table 4.1) detected trace amounts of Se (0.2 – 2.0 wt.%) and Te (0.1 wt.%). Anomalous Cu was detected in one grain (14 wt.%), whereas all other argentite grains have Cu values below the detection limit.

Electrum: In high grade samples (101g/t Au, 63g/t Au) individual electrum grains are visible in ginguro bands. In thin section they occur as large (>0.5 mm) free grains on the margins of quartz or within quartz. Electrum and argentite preferentially occur in fine-grained quartz horizons, colloform chalcedony and lattice bladed quartz. Electrum also occurs as smaller (<5 mm) blebs within, or on the margins of argentite grains. Electrum has also been seen in small cracks within argentite grains. Less commonly small electrum blebs are found as free grains in or along the margins of single quartz crystals.

Supergene electrum also occurs in weathered samples cut by cracks filled with hematite and goethite. Electrum occurs as small rounded intergrowths within hematite bands.

Relict sulphides display colloform weathering textures after hematite replacement. It is these secondary colloform hematite grains that commonly host small blebs of electrum.

To determine the composition of electrum, microprobe analysis was conducted on nine different electrum grains from three different vein samples (see Table 5.1). Microprobe analysis along transects of single electrum grains has revealed a gradation from a silver rich rim to a gold rich core. This was reflected in the large variation (from 28 to 61%) of Ag in electrum. However, this large variation may reflect errors in positioning the electron beam rather than a true gradation of silver to gold. Trace amounts of Cu (4.2 wt%) were detected in one grain which also contained detectable S (0.1 wt%), Se (0.1wt%), and Te (0.1 wt%). Tellurium was present as trace amounts (0.1 wt%) in all grains, whereas S and Se were restricted to grains with appreciable Cu. Gold fineness values for the electrum grains were calculated using the equation $(\text{Au}/\text{Au}+\text{Ag}\times 1000)$. Values ranged from 610 to 490 and are consistent with values from other low sulphidation deposits such as Chatree (see Figure 5.3; Dedenczuk, 1998; Kromkhun, 2005).

Table 4.1 Summary of microprobe analyses of argentite at Wang Yai, central Thailand.

Sample no.	Au (wt%)	Ag (wt%)	Cu (wt%)	S (wt%)	Se (wt%)	Te (wt%)	Total (wt%)
ER017957	-0.1	83.3	0.0	14.0	1.9	0.1	99.4
ER017957	0.0	82.8	0.0	11.6	0.7	0.1	95.4
ER017426	1.1	70.1	14.5	13.2	0.0	0.1	99.1
ER017426	-0.1	84.3	0.0	17.0	0.7	0.1	102.2
ER017426	0.2	82.4	0.0	11.8	3.3	0.1	98.1
ER017426	-0.2	83.9	0.0	13.3	2.0	0.1	99.4

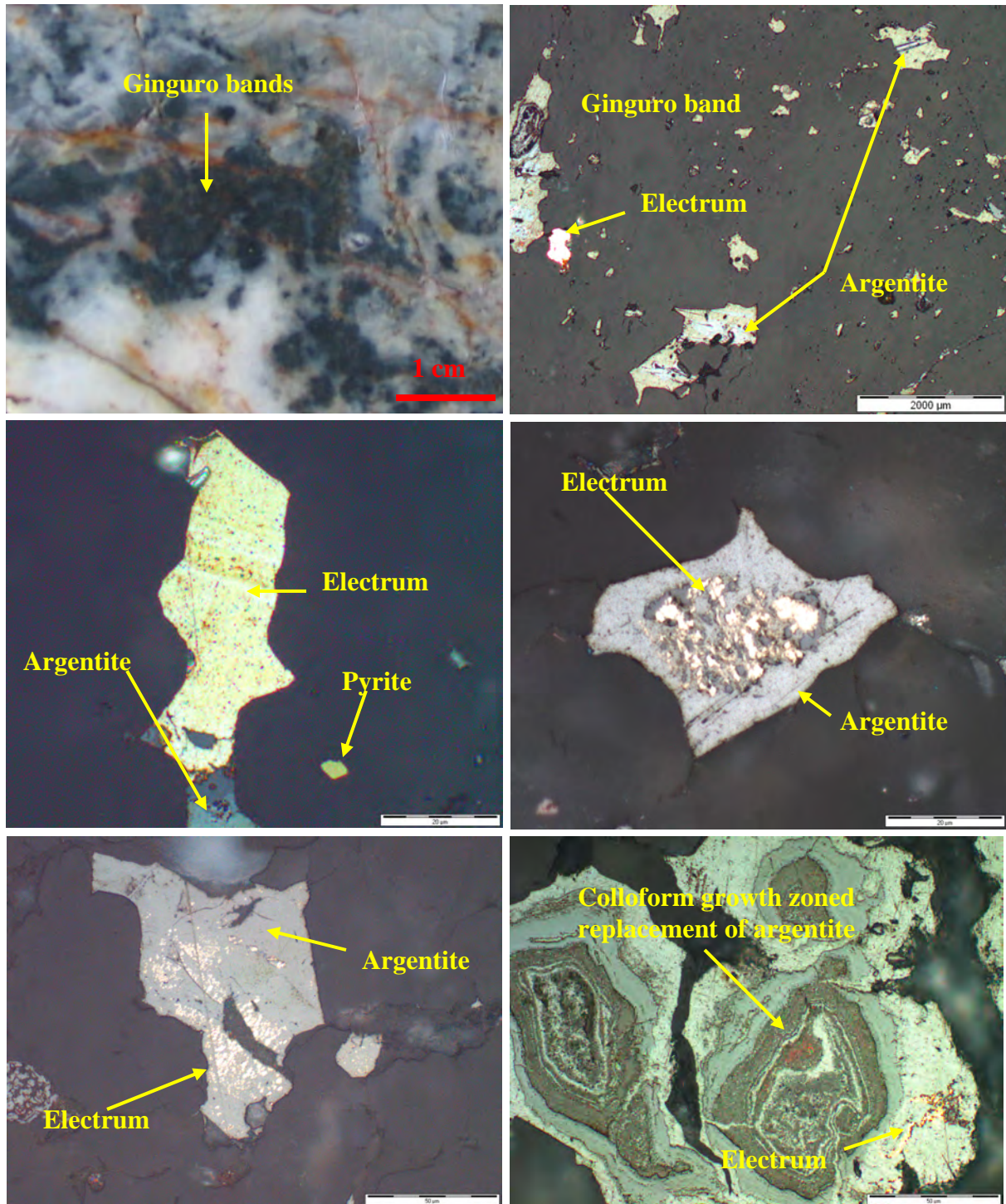


Figure 4.4. A) – Ginguro banded ore in crystalline quartz vein (ER017957). B) Photomicrograph in reflected light showing a electrum grain associated with argentite dominated ginguro ore (ER017690). C) – Photomicrograph of an angular electrum grain joined to argentite (ER017690). D) – Photomicrograph of electrum occurring within cracks of argentite (ER017957). E) – Photomicrograph of electrum occurring as small inclusions within large argentite grain (ER017957). F) – Supergene replacement of argentite by hematite forming radial colloform growths (ER017960).

Table 4.2 Summary of microprobe analyses of electrum at Conical Hill, Wang Yai, central Thailand

Mineral							
Sample no.	Au (wt%)	Ag (wt%)	Cu (wt%)	S (wt%)	Se (wt%)	Te (wt%)	Total (wt%)
ER017957	60.8	40.0	0.0	0.0	0.0	0.1	101.2
ER017957	40.6	42.1	4.2	0.1	0.1	0.1	89.2
ER017960	61.5	40.3	0.0	0.0	0.0	0.1	102.1
ER017960	53.6	46.5	0.0	0.0	0.0	0.1	100.4
ER017426	33.5	31.1	0.0	0.0	0.0	0.1	64.8
ER017426	59.5	40.6	0.0	0.0	0.0	0.0	100.4
ER017426	59.4	41.8	0.0	0.0	0.0	0.1	101.5
ER017426	45.0	42.0	0.0	0.0	0.0	0.1	87.3
ER017426	59.5	40.6	0.0	0.0	0.0	0.0	100.4

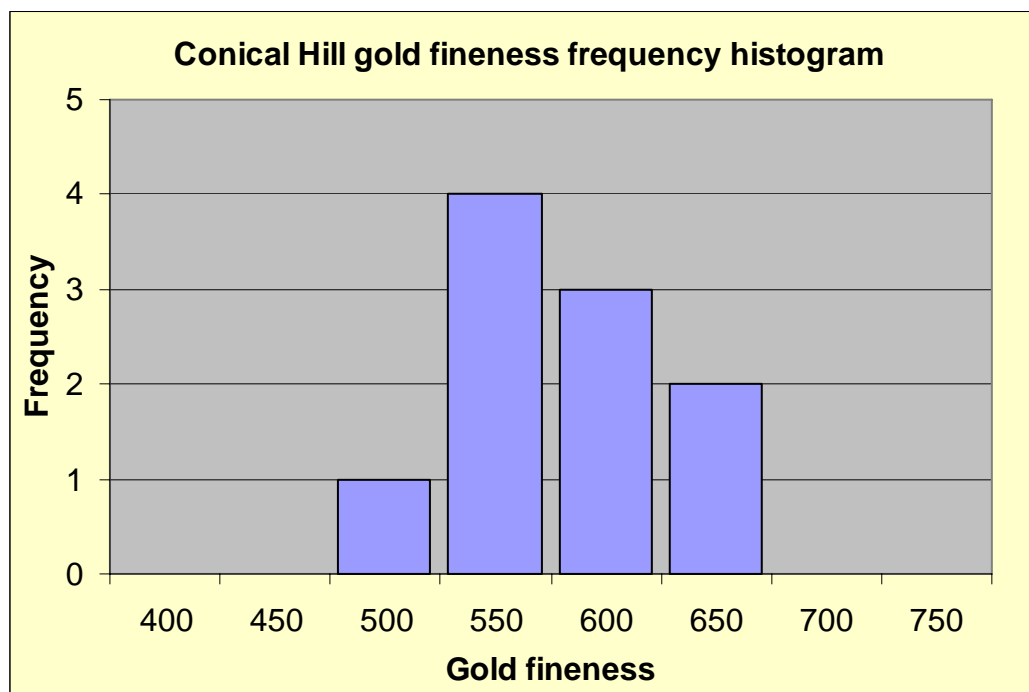


Figure 4.5 Frequency histogram of gold fineness values for Conical Hill, Wang Yai, central Thailand.

Chalcopyrite and Pyrite: Chalcopyrite and pyrite are very minor stages and their occurrence is relatively rare. One chalcopyrite grain was observed on the edge of a quartz grain in sample ER017426. Cubic pyrite grains are relatively more common but have largely weathered to hematite, so the correct identification as pyrite is difficult except for the distinct rhombic shape.

4.4 Central Ridge

Location: Central Ridge is a prominent hill up to 155 m high and is found approximately 750m north of Conical Hill and 500m south of T1 Hill. Vein exposures include massive opaline silica to chalcedony, chalcedony quartz crustiform colloform and sporadic host rock outcrops.

The Central Ridge vein system outcrops at ‘monument’ (GR1809750mN,688825mE) and continues as subcrop and float train along a ~170 strike for approximately 580m and eventually terminates at the pinnacle of Central Ridge (GR1810275mN, 688700mE; Figure 4.7). The vein pinches at the northern and southern ends and swells in the middle section, but this observed relationship may be due to float in the steeper middle sections moving down slope. The inferred maximum vein width (up to 50m wide) occurs approximately 250m from ‘monument’ (GR1810025mN, 688750mE). Here the vein system is hosted in volcanogenic breccia and sandstone and grades upslope to a silicified mudstone, limestone, and a quartz phyrlic breccia at the pinnacle.



Figure 4.6 Looking south from T1 Hill towards Central Ridge, Wang Yai, central Thailand (photo pers.comm Stuart Smith)

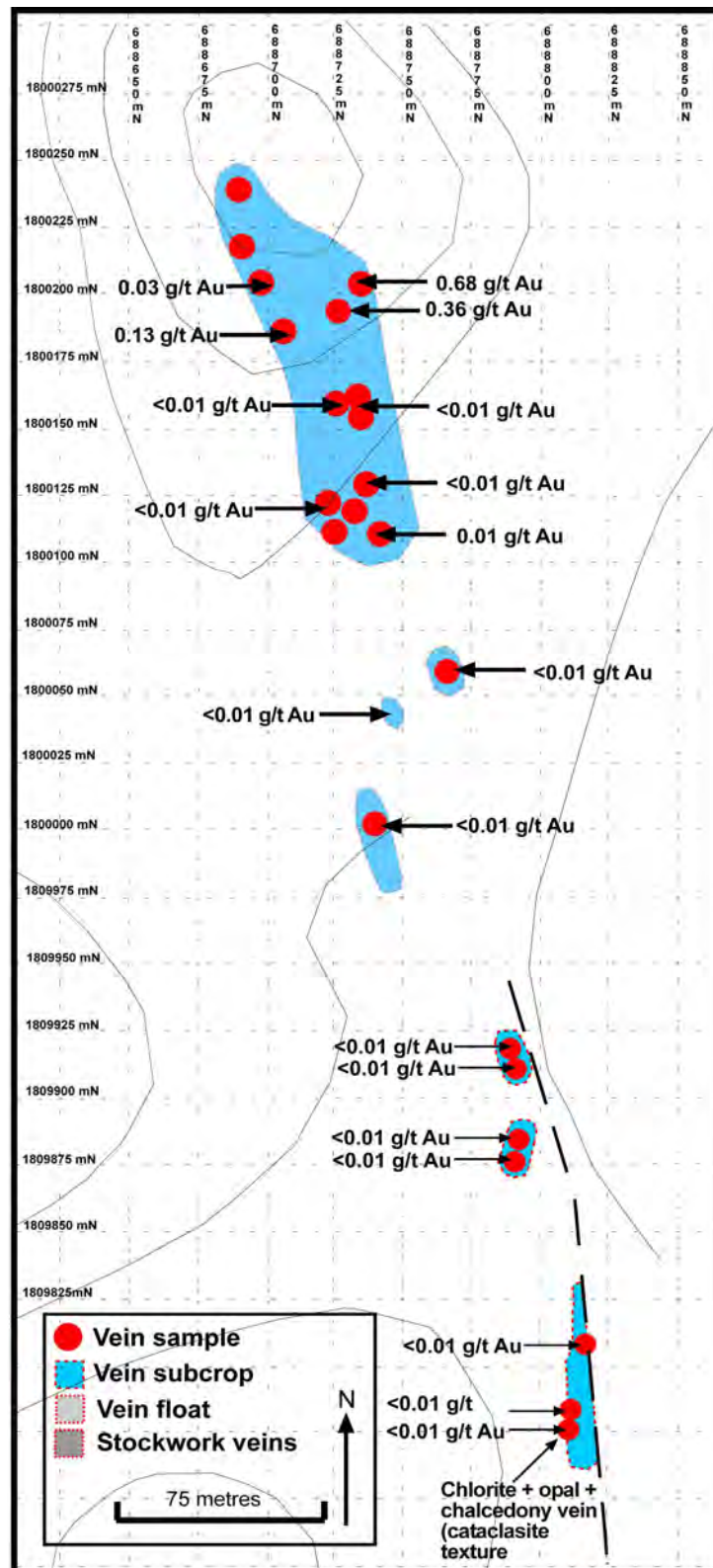


Figure 4.7 Fact map of Central Ridge showing distribution of vein float and subcrop, Wang Yai, central Thailand.

4.4.1 Quartz vein textures

Along the entire strike of the Central Ridge vein, gold assays are low and most samples have gold values below the detection limit. The only significant gold grade (0.68g/tAu, 0.36gt/Au, 0.26gt/Au) occurs in the northern most 200m of the vein (Figure 4.7). South of this area, vein quartz are all below detection limit values. Quartz textures along strike of this vein display a zonation which correlates with increase in gold grade towards the northern end. For example opaline silica and chalcedony (<0.01g/t Au) dominate in the south of the system, whereas in the north, chalcedony, crustiform colloform veins (0.36gt/Au, 0.26gt/Au) dominate. The boundaries between quartz textures are gradational and textures belonging to both zones occur in transition. At Central Ridge the veins have been subdivided into three types; A and B-type quartz veins occur at the southern end of the ‘monument’ vein, whereas C-type quartz is found in the north.

A-type veins are characterized by well-developed crustiform banding of alternating chlorite (1-3 mm) and chalcedony/opal bands (2-5 mm). Cockade and comb quartz textures are marginal to banded chalcedony and opal (Figure 4.9 A and B). Chlorite occurs as bands (with hematite dusting) or sphere like shapes closely associated with chalcedony. Approximately 200 m north of the ‘monument’ vein, A-type veins are much thinner (1 cm) and occur as isolated vein adjacent to the main vein zone (effectively as a vein selvage).

B-type veins are predominant in the southern end of this vein and are interpreted to be a late stage chalcedony flooding event (Figure 4.9 C). They cut A-type veins at high angles and consist of massive dark yellow-brown chalcedony 20-30 cm wide veins which contain occasional lithic clasts and zones of hydrothermal breccia. Cavities within the chalcedony are in-filled with euhedral growth zoned faceted quartz grains. Chalcedonic zones display well developed moss textures and are unmineralised.

C-type The inside margin of A-type veins have C-type chalcedony veins with well developed crustiform colloform banding and cockade and comb quartz textures (Figure 4.9 D, E and F). The margins of comb quartz bands are host to pyrite mineralization (Figure 4.8 A). Pyrite mineralisation is interpreted to be the host of gold mineralisation although electrum is not visible in hand specimen. Assays for C-type vein samples include 0.68gt/Au, 0.36gt/Au, and 0.13gt/Au. C-type veins are followed by breccia stage (D) with chalcedony cement and clasts of crustiform colloform banding.

4.4.2 Ore Mineralogy

Only two samples from Central Ridge display sulphides. These include ER016933 (0.68gt/Au) and ER016955 (0.26gt/Au). In both samples the sulphides have been replaced by colloform secondary hematite. The euhedral shape of sulphides is still preserved and based on this together with microprobe data they are interpreted to be chalcopryite and pyrite. Chalcopryite and pyrite occur in the fine grained crystalline quartz horizons of crustiform colloform chalcedony (Figure 4.8, A). Electrum was also thought to occur but microprobe analysis confirmed these grains as unaltered chalcopryite. Relatively pristine grains of chalcopryite forming on the margins of quartz crystals were observed in sample ER016955 (Figure 4.8, B).

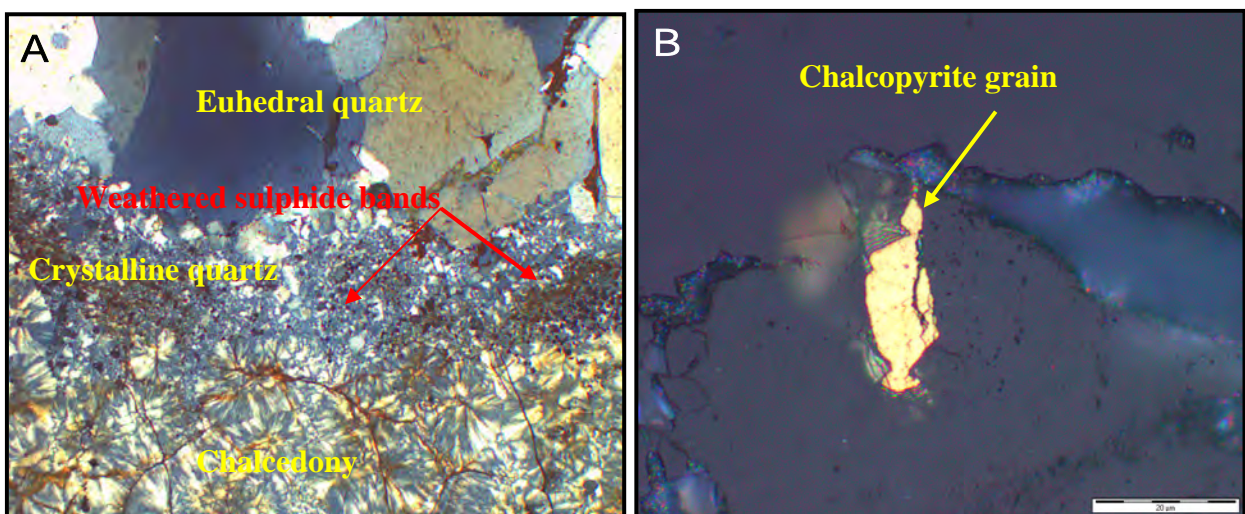


Figure 4.8 A) Photomicrograph of a cross section through a typical chalcedony quartz crustiform colloform band. Weathered sulphide bands occur within the crystalline quartz bands (sample ER016933). B) Photomicrograph of a rare isolated chalcopryite grain occurring in a quartz grain (sample ER016955).

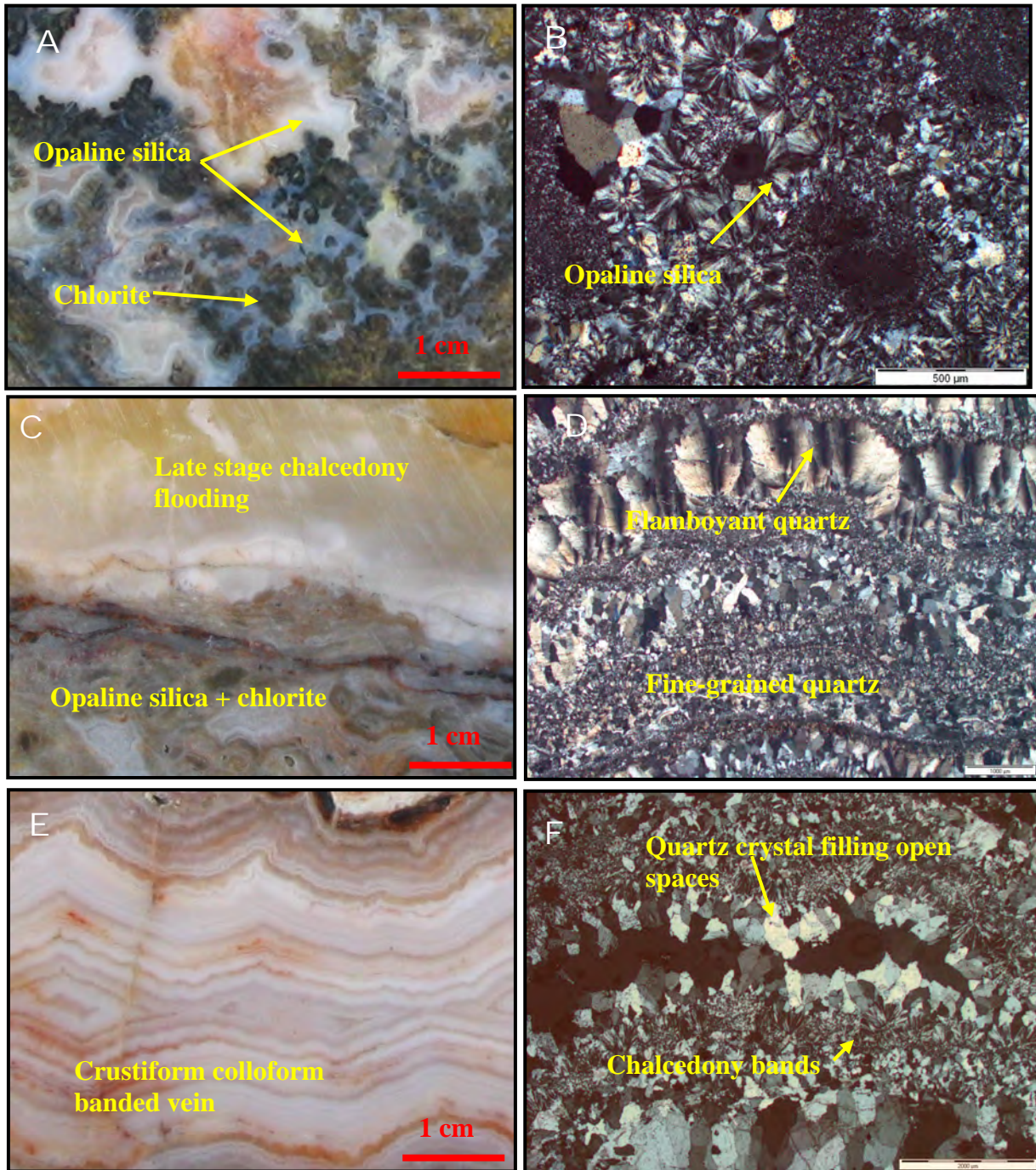


Figure 4.9 A) – Opaline silica chlorite vein at the southern end of the Central Ridge vein system (sample ER017246). B) – Photomicrograph of opaline silica vein (sample ER017246). C) - Late stage yellow chalcedony flooding, cross cutting opaline silica chlorite vein (sample ER017249). D) – Photomicrograph of thin alternating, crustiform colloform bands with quartz and chalcedony. Quartz displays flamboyant textures. E) – Chalcedony crustiform colloform bands (sample ER017422). F) – Photomicrograph of alternating chalcedony and quartz crustiform bands. Euhedral quartz crystals infill open spaces (sample ER016955).

4.5 T1 Hill

The T1 Hill prospect is located approximately 425 immediately north from the top of Central Ridge. T1 Hill is the only prospect in the Wang Yai tenement that has been drilled (three diamond drill holes by Phelps Dodge Ltd. and an additional four holes drilled by Thai Global Ventures Co., Ltd.). Vein exposures include massive crystalline quartz veins, quartz-chalcedony stockwork and sporadic host rock outcrops.

At the top of T1 Hill quartz vein subcrop starts at (GR1810675mN, 688750mE), trends north, and curves around to the northwest terminating at (GR1810800mN, 688650mE). The strike length of vein float from south to the northwestern end is approximately 150m and has a width of 25 metres (Figure 4.11). Vein dimensions are inferred from the distribution of vein float so the actual vein size is probably much smaller. Stockwork veining in *in situ* volcanoclastic breccia and sandstone host rock occurs on the northern, eastern, southern, and western sides of the vein.

In addition to the descriptions of surface quartz textures and ore mineralogy, more detailed descriptions of the vein textures, alteration assemblages, and ore mineralogy will be presented for T1 Hill. Observations presented here focuses on a single drill hole (i.e., WYRD016), which was given the most attention during the logging exercise.



Figure 4.10 Looking north from Central Ridge towards T1 Hill, Wang Yai, central Thailand.

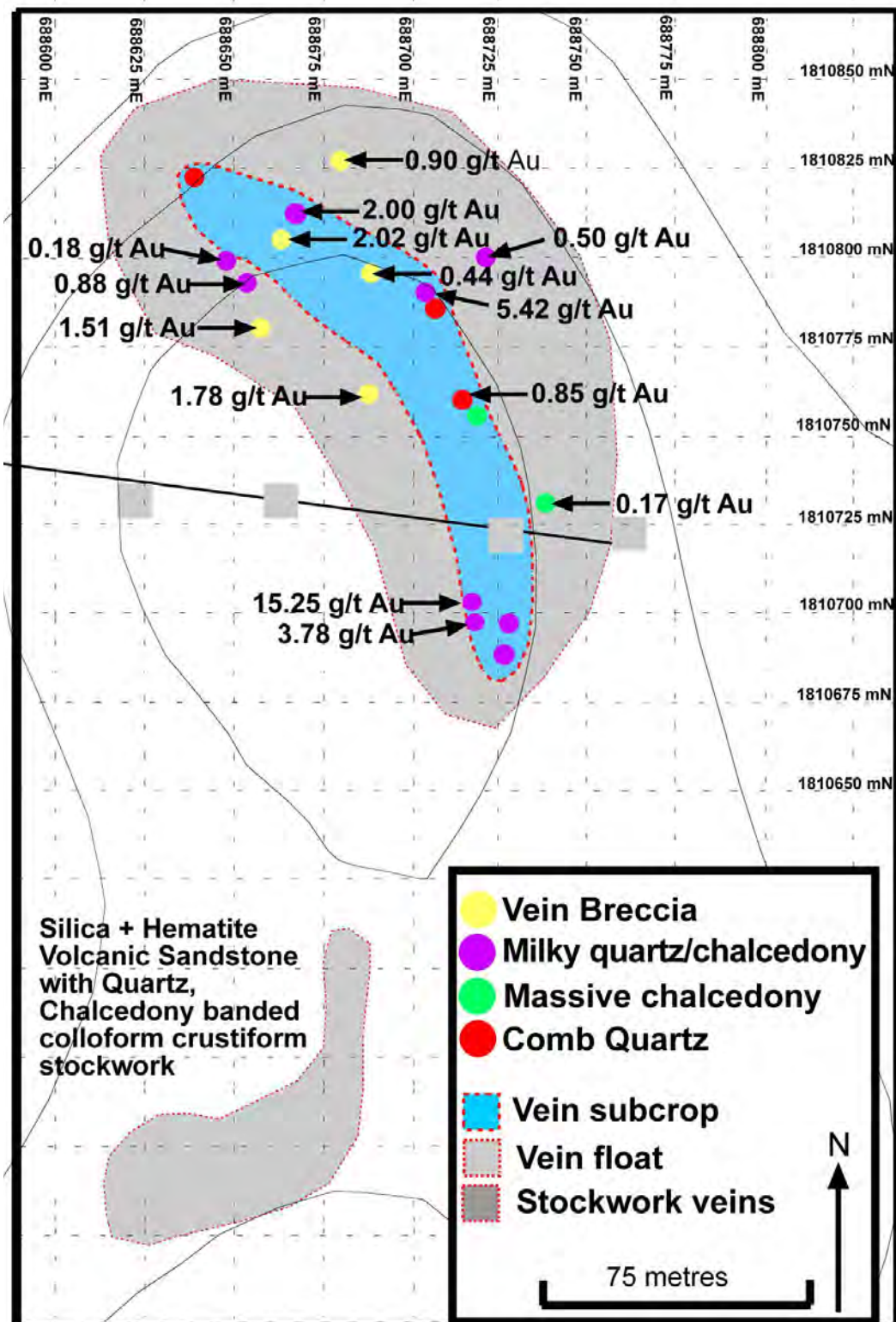


Figure 4.11 Map of T1 Hill showing location of the main vein system and associated quartz vein textures, Wang Yai, central Thailand

4.5.1 Quartz vein textures

Four types of quartz veins occur on the surface of T1 Hill.

A-type veins are characterized by 2-3cm milky white chalcedony bands and darker coarse grained quartz exhibiting pseudoacicular textures after calcite. Thin bands of sulphides occur in between the chalcedony and quartz bands. The sulphides seem to be associated with quartz bands rather than chalcedony (Figure 4.12, A).

B- type veins consist of an breccia stage that comprises of angular lithic silicified sand and siltstone clasts in a clear dark grey crystalline quartz matrix. Angular fragments of unmineralised chalcedonic, crustiform colloform vein also occur (Figure 4.12, B).

The grey crystalline quartz matrix displays ghost sphere textures, zoned quartz, lattice bladed quartz and disseminated sulphides. Lattice bladed quartz after calcite seems to be associated with fine grained ore bearing bands.

Some samples exhibit weathered hematite bands which may have been ginguero ore. Sulphides are generally restricted to fine quartz and lattice bladed quartz zones. Most B-type veins exhibit gold assays >1.0 g/t Au but these high values may be attributed to supergene enrichment rather than true values as most of the samples are intensely weathered.

C-type veins consist of massive milky white recrystallised chalcedony with abundant cockade structures that have centres composed of euhedral quartz grains. Moss textures are also present. No mineralisation is visible (Figure 4.12, C).

D-type veins cross cut all other vein stages and consist of 1-2cm comb quartz with euhedral growth zoned.

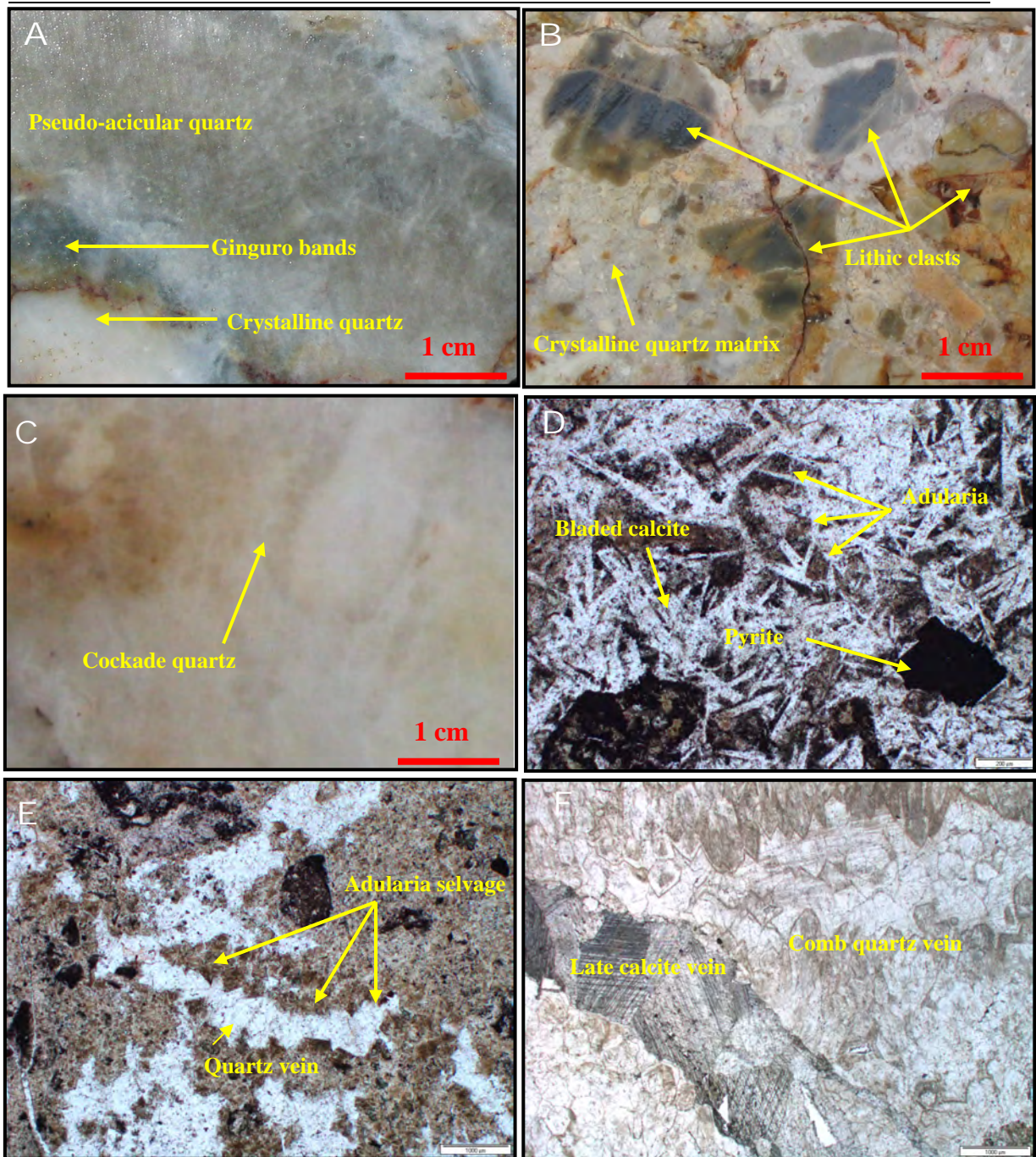


Figure 4.12 A) - Grey pseudo-acicular quartz band with sulphide and white crystalline quartz selvages (ER016901). B) - Hydrothermal breccia vein with silicified lithic clasts. Matrix is comprised of crystalline quartz and disseminated sulphides (ER016907). C) - Massive aggregates of comb and crystalline quartz (ER016902). D) - Photomicrograph of lattice bladed calcite band with rhombic adularia and rhombic pyrite (WYRD016@243.7 metres). E) - Photomicrograph of adularia occurring on a comb quartz vein selvage (WYRD016@243.7 metres). F) - Photomicrograph of late stage unmineralised calcite vein cutting comb quartz carbonate vein (WYRD016@243.7 metres).

4.5.2 Detailed vein and alteration assemblage

Four different alteration assemblages and associated vein types have been observed during core logging at T1 Hill. They include silicic, K-feldspar, chloritic, argillic and phyllic alteration assemblages.

4.5.2.1 Silicic alteration assemblages

The earliest alteration stage consists of pervasive silica flooding of andesitic host rock and rare chalcedony horizons (up to 2 m thick). These pervasive alteration zones are associated with, and cut by quartz veinlets (4 to 30 mm). Chalcedony horizons are dark brown/ grey chalcedony with chlorite hematite, pyrite selvages and singular anhedral quartz crystals.

The second stage of silicic alteration assemblages is variable in both mineralogy and textures. Veins in this stage do not contain all the phases listed below but generally have at least two of the characteristics. This stage is characterized by dark/light grey 1-4 cm comb quartz with chlorite, hematite, calcite and 1-2 cm sericite haloes (Figure 4.12, F). Calcite usually occurs as infill in the thicker veins >4 cm whereas the smaller veins calcite occurs along the vein selvage. Fine grained crystalline quartz, chlorite and hematite form bands along vein selvages. Crystalline zones of chalcedony occur in conjunction with euhedral quartz and often form on the upper margins of euhedral quartz grains. Some phases exhibit thick rhombic adularia selvages and zones of very well developed lattice bladed silica pseudomorphs after calcite (Figure 4.12, D and E). Lattice bladed textures tend to preferentially occur with fine grained saccharoidal quartz and adularia rhombs. Pyrite content is mostly confined to the banded 'smoky green' chlorite/quartz rich phases. Wall rock located pyrite also increases around the presence of smoky green vein phases.

Fine grained quartz crystals that flood wall rock adjacent to veins infill vesicles after K-feldspar and pervasively alter the host rock groundmass. Grain size is variable with

larger growth zoned quartz occurring in amygdales and finer grained quartz occurring in thin veinlets and the host rock groundmass.

The textures and abundance of chalcedony and quartz are significantly different across the vertical interval of T1 Hill. Quartz veins from the surface are dominated by crystalline quartz and chalcedony and minor comb quartz. In contrast, drill core veins are dominated by comb quartz with well developed growth zoned euhedral crystals and very little chalcedony. According to Morrison et al., (1991) quartz textures can be used to determine the approximate level in an epithermal system and this will be discussed further in the interpretation section.

4.5.2.2 K-feldspar alteration assemblages

K-feldspar alteration assemblages are wide spread at T1 Hill and are closely associated with pervasive silicic alteration. This alteration zone is characterised by low temperature K-feldspar, adularia.

K-feldspar alteration occurs as thin pink bands (>1 mm) within quartz carbonate veins but more commonly along vein selvages as rhombic adularia (>0.5 mm) aggregates. Bands of adularia within quartz carbonate veins are generally associated with silica pseudomorphs of lattice bladed calcite. K-feldspar alteration also occurs as thin selvages around amygdales in andesitic host rock and also replaces large euhedral plagioclase phenocrysts and small plagioclase laths in the groundmass.

K-feldspar staining was undertaken at the University of Tasmania using hydrofluoric acid on 20 samples from drill hole WYRD016. K-feldspar staining was conducted to determine the distribution of K-feldspar alteration assemblages relative to the gold-bearing quartz veins. Samples used for chemical staining were selected at intervals of 5m from 135 m to 248 m down hole. Samples included those immediately adjacent to the veins and altered host rock upto 50 metres away from the vein. Results from staining

showed a clear increase in K-feldspar alteration down hole towards the quartz-chlorite-carbonate vein zones (Figure 4.13).

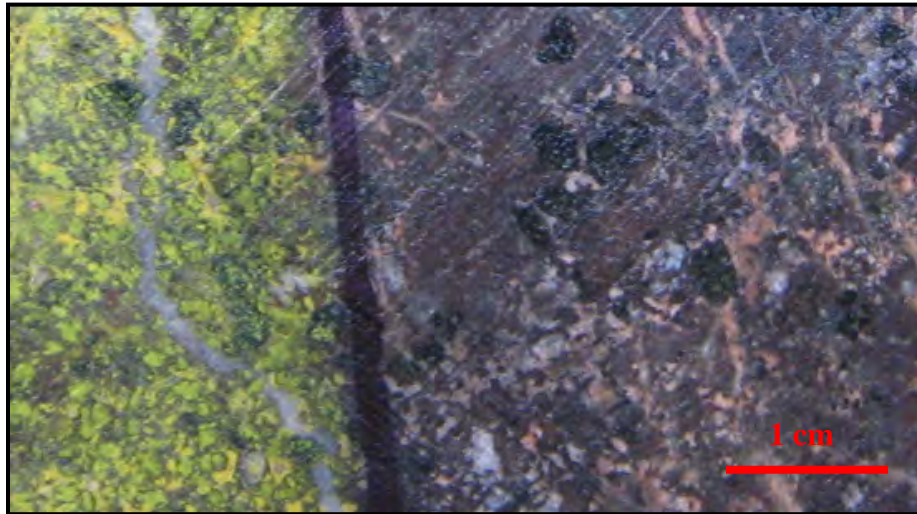


Figure 4.13 K-feldspar stained andesitic host rock (sample WYRD016@280 metres).

4.5.2.3 Argillic and phyllic alteration assemblages

At T1 Hill clay alteration haloes around veins have been identified in hand specimen and also under the microscope. In hand specimen sericite alteration forms conspicuous pale yellow/green 4-8 cm haloes around quartz carbonate veins. In thin section clays selectively replace adularia, plagioclase and pyroxene phenocrysts, and vein calcite. Sericite also occasionally pervasively replaces the groundmass in andesitic clasts. In order to identify the type of phyllosilicate assemblages PIMA analysis was applied to zones exhibiting argillic alteration. However, the analysis failed to identify the presence of any clays although they are clearly visible in hand specimen and thin section. This may have been due to the host rock being intensely silicified and containing abundant disseminated pyrite.

4.5.2.4 Chloritic alteration assemblages

Pervasive and selective chloritic alteration assemblages are common at T1 Hill. Selective alteration of glass, plagioclase, pyroxene, and amygdales occurs in coherent andesite

facies, sandstone facies, and breccia facies. Pervasive chloritic alteration is best developed around the hydrothermal zone where chlorite replaces the entire groundmass and phenocryst assemblages. Chlorite also occurs along vein selvages in conjunction with hematite, epidote and sericite and is not necessarily associated with hydrothermal zones.

4.5.2.5 Propylitic alteration assemblages

In epithermal systems propylitic alteration is considered by Buchanan (1981) to be a wide spread assemblage commonly forming halos of hundreds of metres around vein zones and is usually considered to be post-ore. Similarly at T1 Hill it has been interpreted from overprinting relationships of K-feldspar, and phyllic assemblage that propylitic alteration occurred later or post ore.

Propylitic alteration assemblages are well developed away from the hydrothermal zone. They include the following assemblages; chlorite, epidote, sericite, quartz, albite, carbonate, pyrite and hematite. PIMA analysis conducted on drill core distal from the hydrothermal zone shows that chlorite, epidote and phrenite are the dominant phyllosilicates. Chlorite and epidote selectively replace K-feldspar, hornblende and plagioclase andesite phenocrysts. Where feldspars are not replaced by chlorite and epidote they exhibit albite replacement with a sericite dusting. Epidote occurs along vein selvages in association with sericite, chlorite and pyrite. Hematite and silica pervasively alter the groundmass in all lithofacies. Pyrite is usually associated with these assemblages.

4.5.3 Ore Mineralogy

In surface vein float samples ore is hosted in grey/black disseminated sulphide bands. Pyrite, chalcopyrite, and minor electrum are the dominant sulphides. Pyrite grains assume subhedral to euhedral shapes with an average size of 50 μm . 15 % pyrite grains exhibit sizes up to 350 μm . Pyrite typically occurs in the vein matrix and within clasts of

the breccia. Crustiform colloform banded veins do not exhibit any sulphides. Most of the pyrites are weathered especially within the hematite altered zones. In these zones it loses its colour changing to a light blue to brown and exhibits growth zoned colloform texture. Only one 70 μm chalcopyrite grain was observed and this was partially replaced by secondary covellite. Sulphides are generally restricted to small bands along the boundaries between saccharoidal and mosaic quartz although they also occur as disseminations on the edges of quartz. Supergene sub-rounded electrum (25 μm) was observed within a hematite weathered crack.

In drill core, pyrite and chalcopyrite are the dominant sulphides. Large euhedral 200-300 μm pyrite grains preferentially occur within the wallrock rather than quartz carbonate veins. Occasional small grains <50 μm occur in the centre and along the selvages of quartz carbonate veins. Chalcopyrite occurs as very minor <50 μm grains and is restricted to quartz carbonate veins. Chalcopyrite can occur as free grains or as inclusions within pyrite (Figure 4.14).

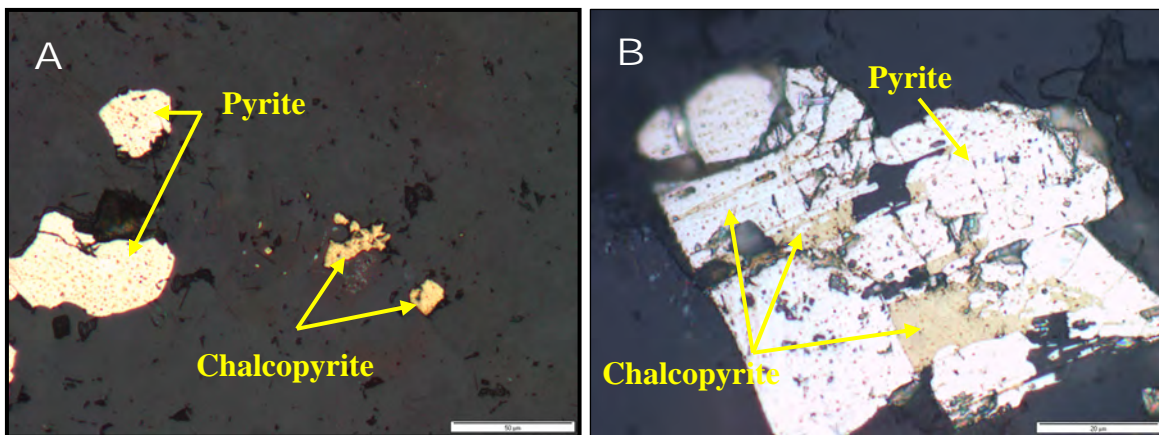


Figure 4.14 A) Photomicrograph showing two pyrite grains occurring with two chalcopyrite grains (sample WYRD016@234 metres). B) Photomicrograph of a large pyrite grain with chalcopyrite grains occurring in cracks of pyrite (sample WYRD016@234 metres).

4.6 T4 Hill

Location: T4 Hill occurs at the northeast corner in the southern portion of the Wang Yai tenement. The hill on which the vein system is located rises approximately 135 m. The vein system trends northeast and occurs as scattered float flanking the base of the southeast side of the Hill. Intensely weathered vein float starts at (GR1811050 mN, 689600 mE) and extends for 200 metres terminating at the edge of rice paddies (GR1811175 mN, 680700 mE).

Quartz textures: Quartz textural analysis is limited for T4 Hill due to the sample set consisting of 3 vein samples, the remainder are silicified wall rock. The highest assays to date include 3.20 g/t Au, and 0.69 g/t and these values are likely to reflect supergene enrichment rather than hypogene as they occur in brecciated and highly weathered samples.

The vein samples are characterized tabular aggregates of coarse grained barite crystals which infill vugs within micro crystalline quartz dominated groundmass. Very thin quartz lattice bladed textures occur and have barite crystals growing perpendicular from the blade direction.

4.7 Gift Prospect

The Gift prospect is located in the northern part of the tenement and comprises of 6 different vein systems. They will be referred to as A, B, C, D, E and F (Figure 4.15).

Location:

Vein system A: occurs in the northern end of the Gift prospect flanking the western side of Song Hill (Figure 4.15). Vein float occurs in alluvium at the base of Song Hill and in eucalyptus plantations on the flanks of Song Hill. The vein starts at (GR1812800 mN, 687525 mE) in the south and extends approximately 300m due north and terminates at (GR1813025 mN, 687525 mE). The approximate width of vein float ranges from 25-

30m and is hosted in silica \pm pyrite \pm hematite \pm clay altered volcanic breccia and sandstone.

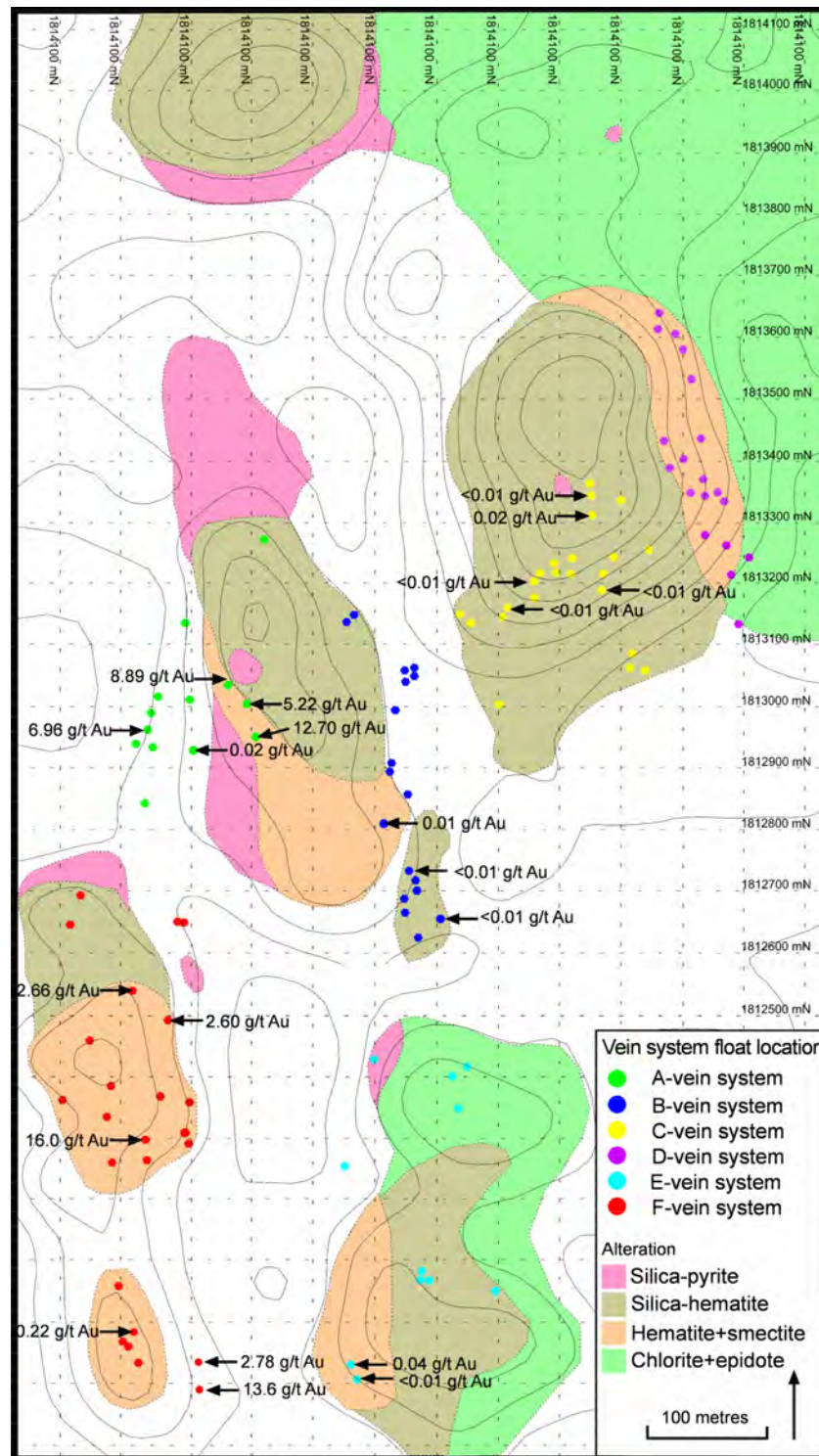


Figure 4.15 Location of vein systems, vein float and surface alteration in Gift prospect, Wang Yai, central Thailand.

Vein system B: occurs as float on the eastern side of Song Hill along the same latitude as vein system A (Figure 4.15). In the south, vein system B starts at (GR1812650 mN, 687975 mE) and extends approximately 500m immediately north terminating at (GR1813150 mN, 687975 mE).

Vein system C starts at the northern end of B and trends north east towards the top of Kham Hill. Vein float occurs along this trend for approximately 500m (Figure 4.15).

Vein system D occurs at the northeastern end of C and trends north south from the southwestern base of Kham Hill (Figure 4.15). Vein float is conspicuous with an average width of up to 50 metres. It is hosted in intensely silicified hematite volcanic breccia to the west and epidote-chlorite massive volcanic conglomerate to the east (Figure 4.15)

Vein system E is located directly south of system B and extends to the southern end of Suwan Hill. This vein system is characterized by very sparse scattered vein float. The trend of the vein is difficult to determine as barite quartz veins in patchy outcrop strike east west and the trend of float is north south.

Vein system F could potentially be a southern extension of 'A'-system to the north but will be considered here as a separate system.

4.7.1 Quartz textures:

Vein System A: This vein system exhibits the highest gold grade in the Gift prospect. Quartz vein textures in system A are dominated by massive white crystalline quartz (Figure 4.17 C). Massive white crystalline quartz veins consist of randomly oriented quartz grains with variable sizes. Primary textures are the dominant quartz texture and include massive, moss, cockade, comb quartz textures. Recrystallisation textures include ghost bladed and saccharoidal quartz, tabular aggregates of former barite, calcite or adularia also occur (Figures 4.17D, A, B). Former adularia rhombs now replaced by silica form thin bands associated with lattice bladed and ghost bladed textures.

Mineralisation preferentially occurs in zones where ghost bladed, tabular aggregates and pseudomorphs of adularia occur.

Vein system B: Vein system B exhibits the lowest gold grade in the Gift prospect.

Most samples are below detection limits with only two samples exhibiting grade >0.01 g/t Au. Three main vein stages occur in this system; chalcedony crustiform, massive chalcedony quartz and a later breccia stage consisting of chalcedony vein clasts.

Chalcedony crustiform vein exhibits well-developed thin chalcedony bands with occasional thin discontinuous sulphide bands. The vein centre consists of bladed pseudomorphs after either calcite or barite. The late breccia stage consists of angular (5-10 mm) brown-yellow chalcedonic vein fragments which display cockade and crustiform colloform textures. The matrix is typically fine-grained quartz with small >1 mm vein and wall rock fragments.

Vein system C and D

Similarly to system B, system C exhibits a very low gold grade with the highest assay being 0.02 g/t Au. Quartz vein textures in this system also share similarities with B in that they exhibit well-developed chalcedony dominated crustiform colloform banded veins (Figure 4.17 E and F). Primary quartz textures include crustiform, colloform, moss, comb and zonal quartz. Recrystallisation textures are less common and include minor flamboyant and ghost sphere textures.

Vein system E

Vein system E is interpreted to be a southern extension of system B and similarly to B it is characterized by very low gold grade. Only 4 samples from this system have been collected so it is difficult to get a true representation of the dominant quartz textures. There is one sample that exhibits well developed bands of former adularia and bladed calcite. This sample (ER017494) has a gold grade of <0.01 g/t Au which contradicts

what has been observed in other vein systems in that gold grade is associated with adularia and bladed calcite.

Vein system F

The main vein phase in this system consists of vuggy hydrothermal quartz breccia with angular quartz chalcedony vein clasts and host rock clasts. Vein clasts range in size from 3 cm to 2 mm and commonly display pseudo-acicular recrystallisation textures. Matrix quartz exhibits a white or grey texture and is composed of variable sized euhedral quartz grains (1-2mm) which occasionally display zonal, cockade, flamboyant, moss textures and fine-grained microcrystalline white quartz. In fresh samples pyrite is abundant (25%) and occurs as euhedral disseminations throughout the vein (Figure 4.16A). It preferentially occurs in the matrix rather than vein clasts. There is evidence to suggest weathered samples also contained up to 25% disseminated pyrite as sulphide pits now replaced by goethite and limonite are common. Quartz textures associated with gold grade tend to include grey and white microcrystalline quartz (Figure 4.16, A and B). The distribution of pyrite also seems to be associated with gold grade as samples with either fresh disseminated pyrite or weathered sulphide pits yield the highest assays.

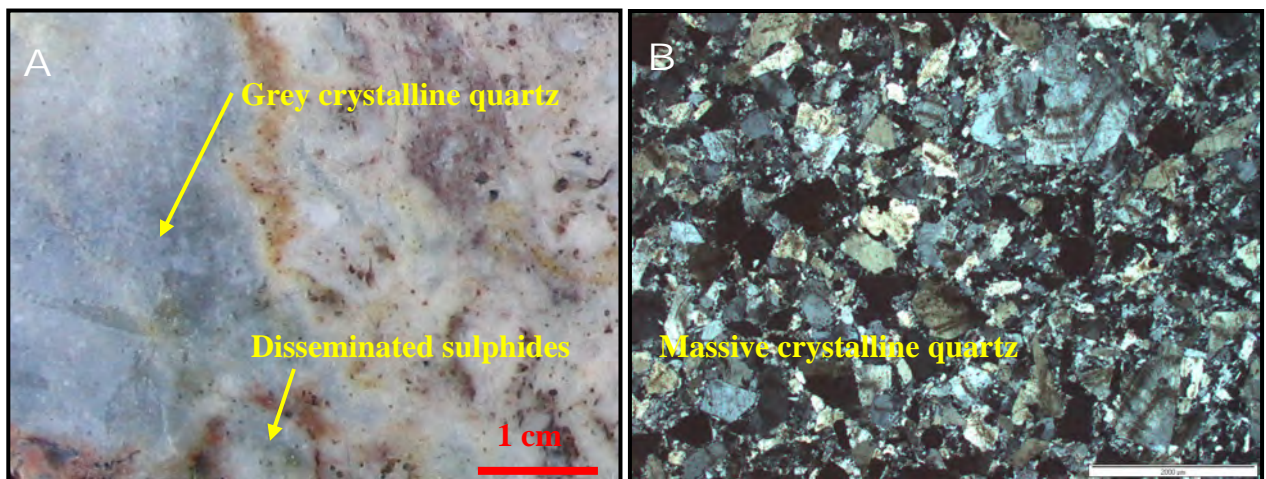
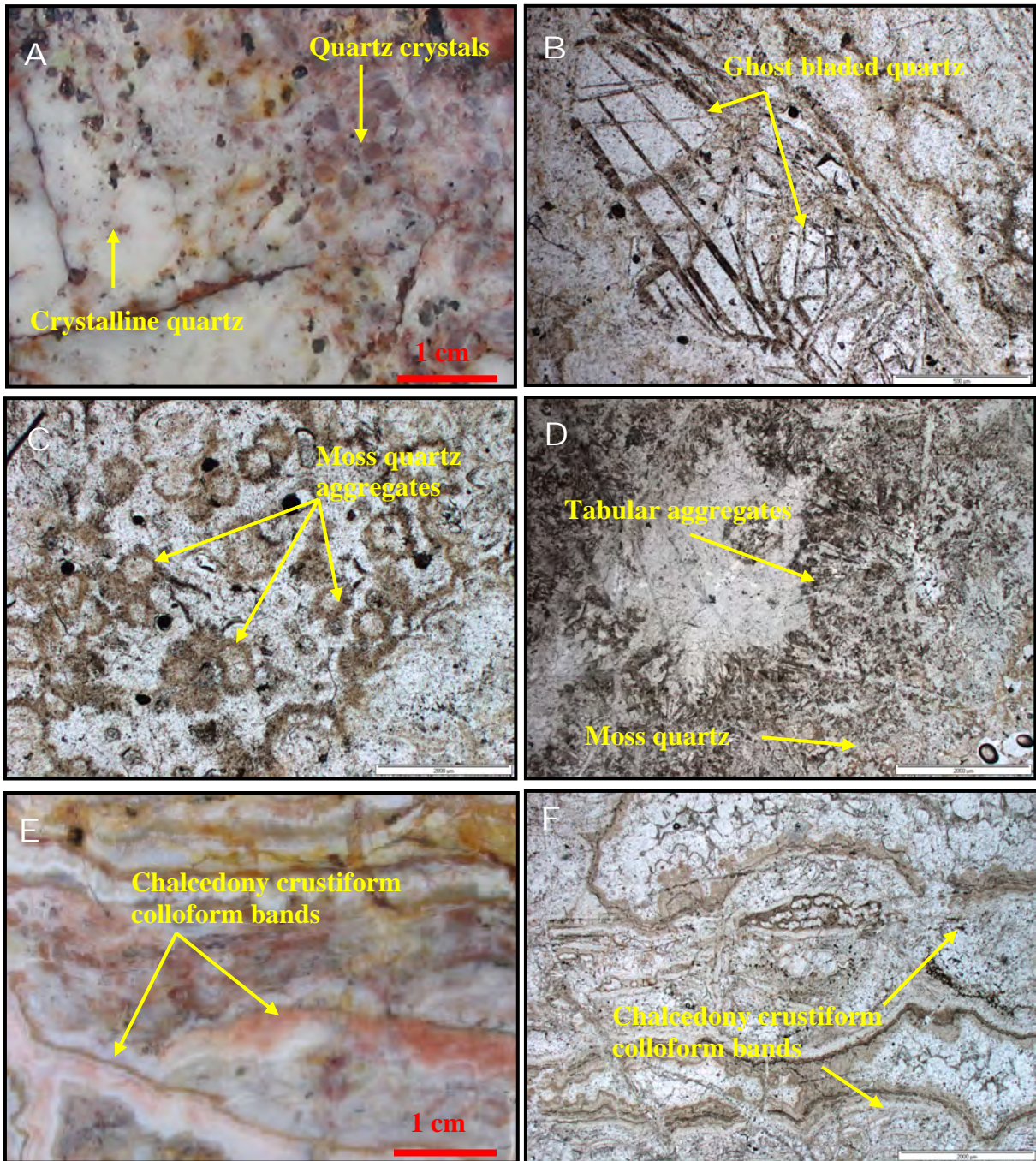


Figure 4.16 A) Hand specimen from 'F' system showing grey crystalline quartz with disseminated pyrite and chalcopyrite (sample ER017479). B) Photo micrograph from 'F' system showing randomly orientated and variable sized massive crystalline quartz (sample ER017479).



4.17 A) Hand specimen from 'A' system showing crystalline milky quartz and well-developed euhedral aggregates of quartz (sample ER017470). B) Photomicrograph from 'A' system show ghost bladed quartz after calcite (sample ER017474). C) Photomicrograph showing typical quartz moss textures in 'A' zone (sample ER017474). D) Photomicrograph showing moss, and tabular aggregates of either barite, adularia, quartz or calcite in 'A' zone (sample ER017474). E) Hand specimen sample of typical chalcedony and opaline silica crustiform colloform banded veins in 'C' zone (sample ER017509). F) Photomicrograph of chalcedony crustiform colloform banded vein from 'C' zone (sample ER017509).

4.7.2 Alteration

Surface alteration in Gift prospect (see Figure 4.15) comprises of four assemblages. They include silica + hematite, silica + pyrite, hematite + clay, and epidote + chlorite. The distribution of each assemblage is shown in Figure 4.15. Silica + hematite alteration is the most extensive and is characterized by pervasive silicification and weathering of mafic minerals to hematite. This alteration forms conspicuous red, silicified outcrops on hill tops and is usually proximal to vein zones. The degree of silicification increases with proximity to the vein and stockwork systems. Hematite + clay alteration usually forms along the fringes of silica hematite alteration distal from intense silicification associated with vein and stockwork zones. Silica + pyrite alteration occurs in association with the high grade vein zones (A, E). It is characterized by intense pervasive alteration of host rock forming very hard subcrop zones containing up to 25% disseminated pyrite. Chlorite + epidote alteration is similar to a typical propylitic style assemblage and occurs to the north east in volcanic conglomerate.

4.7.3 Ore Mineralogy

Sulphides observed in the Gift prospect were from high grade vein systems (i.e, A and E) Low grade systems were completely barren of sulphides although evidence of hematite weathering bands and sulphide pits indicates that veins may have been host to mineralisation. Sulphides in vein systems A and E include pyrite, chalcopyrite, electrum and secondary covellite. Pyrite is the most abundant sulphide and occurs in discrete bands or disseminations associated with chalcopyrite. Pyrite grains range in size from 50 to 110 μm and occasionally contain inclusions of chalcopyrite. Chalcopyrite occurs (20 to 100 μm) as isolated grains on the edge of quartz crystals or with pyrite aggregates. Covellite occasionally replaces the entire chalcopyrite grain but more commonly replaces only the rims (Figure 4.18A). Electrum occurs very rarely and was observed once in thin section (sample ER017474). The electrum is approximately 10 to 15 μm (Figure 4.18B) and forms along the edges of intersecting quartz grains. Microprobe analysis of this grain

showed trace amounts of Fe (0.12wt %), Bi (0.12wt %). Tellurium was below detection limits and gold, silver content was 72 wt % and 26 wt % respectively. Gold fineness value for the electrum grain was 720.

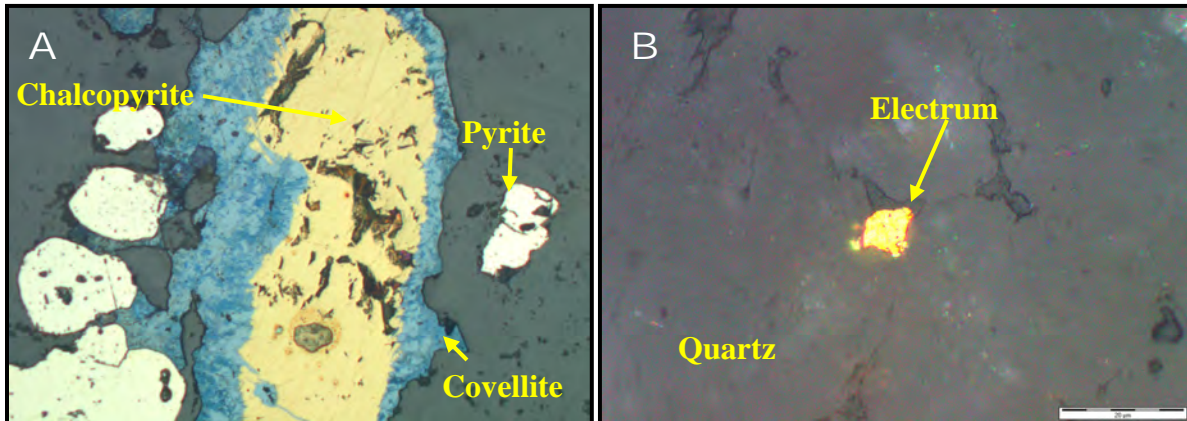


Figure 4.18 A). Covellite, pyrite and chalcopyrite, covellite is replacing the chalcopyrite rim (sample ER017479). B) Isolated electrum grain occurring on the edge of intersecting euhedral quartz crystals (sample ER017474).

4.8 Mineralogical and textural zoning

One of the major aims of this project is to determine what level the surface vein systems at Wang Yai are at with reference to current quartz textural, gangue mineralogy and ore mineralogy zonation in current epithermal models. Constraining the approximate level of formation can implicate whether there is potential for mineralisation at depth or the system has been eroded away. In the above section, vein systems have been described in terms of dominant primary, recrystallisation, and replacement quartz textures. Using the descriptions of quartz vein textures this discussion will focus on the lateral zonation between the different vein systems and then lead into interpretation of why and how quartz textures and gold grade differ between each vein system.

Quartz textures

A summary of quartz textures for each vein system in Wang Yai is shown in Table 4.3. At Conical Hill primary massive, moss, and crustiform textures predominate. Massive and moss textures are likely to have formed from precipitation of a silica gel (Dong et al., 1995). Recrystallisation mosaic textures are common and are a result of recrystallisation of massive chalcedony or amorphous silica (Lovering, 1972). Replacement textures such as saccharoidal, pseudo-acicular and lattice-bladed quartz are associated with ginguero bands and are a likely product of recrystallisation from either calcite, adularia, or barite phases (Dong et al., 1995).

Quartz vein textures at Central Ridge differ significantly from Conical Hill. At Central Ridge, primary and recrystallisation textures in chalcedony vein phases predominate and replacement textures are absent. Primary quartz textures such as crustiform colloform banding are likely to have formed from episodic pressure release (Buchanan, 1981) and precipitation from a silica gel precursor (Adams, 1920). Recrystallisation textures such as mosaic, feathery, and ghost-sphere are indicative of recrystallisation of amorphous silica or chalcedony (Dong et al., 1995).

At T1 Hill quartz vein textures share many similarities with Conical Hill in that they exhibit well developed replacement textures such as saccharoidal, pseudo-acicular, ghost-bladed and lattice-bladed quartz. The presence of these textures and their close association with sulphides suggests that ore bearing phases precipitated adularia, calcite and quartz gangue. Quartz vein textures at T4 Hill are dominated by primary and recrystallisation textures. Quartz forms the dominant phase with minor chalcedony. Lattice-bladed quartz is closely associated with sulphides thus suggesting ore-bearing fluids precipitated either barite or calcite.

Quartz vein textures in the Gift prospect vary significantly between mineralised and unmineralised veins. Unmineralised veins share many similarities with the veins at Central Ridge such as the predominance of chalcedony crustiform colloform banded

veins and the absence of sulphides. Mineralised veins exhibit primary and replacement similar to Conical Hill and T1 Hill.

Table 4.3 Summary of primary recrystallisation and replacement quartz textures for Conical Hill, Central Ridge, T1 Hill, Gift prospect, and T4 Hill, Wang Yai, central Thailand.

Texture Type	Conical Hill	Central Ridge	T1 Hill	Gift Prospect	T4 Hill
Primary					
Massive	***		**	**	
Crustiform	*	***		*	**
Colloform	*	***	*	**	
Cockade	**	**	*	*	
Moss	***		**	*	
Comb	**	*	*	***	**
Zonal	*	**		*	
Recrystallisation					
Mosaic	**	**	*	*	**
Feathery		**			
Flamboyant		**	*	**	
Ghost-sphere		**	*	**	
Replacement					
Lattice-bladed	*		***	**	*
Ghost-bladed			**	*	
Parallel-bladed					
Pseudo-acicular			***		
Saccharoidal	**		*	**	

*rare **common ***dominant

Gangue Mineralogy

Each vein system at Wang Yai has its own gangue mineralogy assemblage. Due to intense weathering and silica replacement of original gangue mineralogy most gangue assemblages have been determined from the texture, and morphology of silica replacement textures.

Quartz is the major gangue mineral at Wang Yai and occurs in all vein systems. Pervasive silica replacement textures indicating a calcite, adularia, or barite precursor are present in only some vein systems. These systems include Conical Hill, T1 Hill, T4 Hill and mineralised veins in the Gift prospect. The replacement textures are indicative of calcite and adularia precursors and are generally associated with mineralisation. Barite pseudomorphs occur only in the Gift prospect although barite was found in host rock replacing plagioclase phenocrysts proximal to the Central Ridge vein. Replacement textures are absent or less extensive for the chalcedony dominated veins of Central Ridge and Gift (B, C, D, and E veins) but chlorite is sometimes preserved with opaline silica bands.

The association of calcite and adularia with mineralisation is quite significant in terms of constraining the mechanism of ore deposition. This has further implications with regard to exploration in that the identification of replacement textures in vein systems can assist in determining barren veins from mineralised veins.

Mineralisation

Precious metal mineralisation is best developed at Conical Hill, where grains of electrum occur within ginguero ore bands dominated by argentite usually associated with fine grained quartz, silica pseudomorphs of adularia, and replacement textures. At T1 Hill ginguero ore bands also occur in conjunction with microcrystalline quartz and replacement textures. Sulphides assemblages at T1 Hill differ from Conical Hill in that rather than argentite and electrum assemblages, pyrite and chalcopyrite form the dominant assemblages. Similarly at Gift prospect mineralised zones exhibit pyrite and chalcopyrite and not argentite.

Mineralisation at Wang Yai is characterized by the paucity of base metals. Considering that current epithermal models (e.g Buchanan, 1981) show a vertical zonation of precious metals occurring above base metals, it is likely that the current surface at Wang Yai represents the upper part of a larger hydrothermal system.

4.9 Interpretation

There are many descriptive zonation models for epithermal low-sulphidation deposits. This study will reference the model proposed by Buchanan (1981) which is a summary of 60 epithermal deposits hosted in volcanics in western USA. This model illustrates the ore, gangue, and alteration zones in epithermal veins and is widely used in the current literature. More recently Morrison et al. (1990) has developed a zoning model of quartz textures in epithermal deposits. For this study the model developed by Morrison et al. (1990) will be superimposed on the model by Buchanan (1981) (See Figure 4.19).

The aim of this interpretation is to use the observations of quartz textures, gangue mineralogy, and ore mineralogy of the Wang Yai prospects to determine the relative depth of formation for each system.

Conical Hill

In the main vein at Conical Hill, four vein types have been recognised and of these A-type (milky white quartz chalcedony crustiform colloform) and C-type (massive sugary and saccharoidal quartz) veins that host ‘ginguro’ sulfide-rich mineralization assemblages. Quartz textures are predominantly primary and replacement. Mineralisation preferentially occurs adjacent to replacement textures such as adularia pseudomorphs, bladed-calcite, microcrystalline quartz, saccharoidal quartz, and pseudo-acicular textures. Ore minerals occur in ginguro bands and comprise of electrum and argentite. Electrum can occur as free grains or within cracks of argentite. Minor pyrite and chalcopyrite also occur.

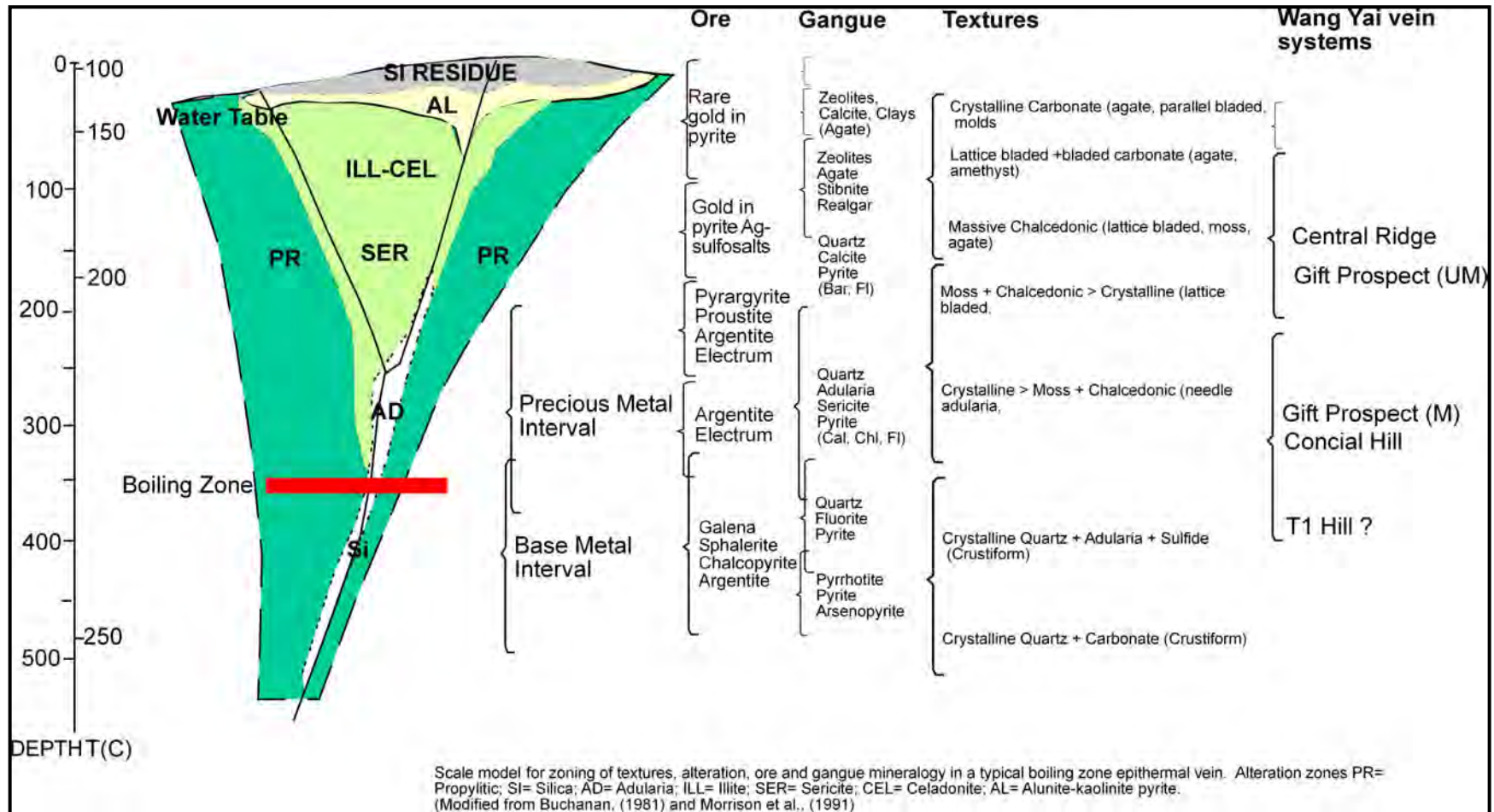


Figure 4.19 Epithermal model developed by Buchanan, (1981) showing the zonation of ore and gangue mineralogy as a function of depth and temperature. Morrison et al., (1991) quartz textural classification scheme and interpreted positions of Wang Yai vein systems are superimposed the Buchanan, (1981) model.

Based on mineralisation styles, gangue, ore mineralogy and quartz textures Conical Hill is interpreted to have formed at the precious metal interval slightly above or at the zone of boiling. This zone is located approximately 200 m-300 m below the palaeo-surface and is the position whereby precious metal deposition occurs in response to boiling (Buchanan, 1981). Conical Hill exhibits many of factors that are consistent with this level of formation. This interpretation is based on the evidence below.

- The predominance of primary quartz textures such as massive, moss, crustiform and crystalline quartz is consistent with the lower part of the crustiform colloform zone (Morrison et al., 1991).
- The predominance of argentite and electrum and absence of base metal sulphides is consistent with formation at the precious metal ore interval (Buchanan, 1981).
- The presence of vein adularia and bladed calcite strongly suggests a boiling event (Simmons et al., 2000) and this is consistent with the precious metal ore interval (Buchanan, 1981).
- Upon initiation of boiling, hydrothermal fluid becomes alkaline which allows for the precipitation of adularia, and CO₂ loss occurs allowing for the precipitation of calcite (Dong et al., 1995). Adularia and calcite both occur at Conical Hill.
- The presence of rhombic adularia suggests that formation was formed under rapid crystallisation conditions such as boiling of hydrothermal fluids (Dong and Morrison, 1995).

Central Ridge

Three dominant vein types occur at Central Ridge. All vein types are characterized by poor gold grade and the predominance of chalcedony rather than quartz in well developed crustiform colloform vein stages. In contrast to Conical Hill, Central Ridge quartz textures are dominated by primary and recrystallisation textures rather than replacement

textures. Calcite and adularia pseudomorphs are absent and the only sulphides observed were very minor weathered pyrite and chalcopyrite grains preferentially occurring within fine grained crystalline quartz horizons of crustiform colloform veins.

Based on the observations of quartz textures, gangue mineralogy and ore mineralogy Central Ridge is interpreted to have formed at a lower temperature than Conical Hill. A shallower level of formation than Conical Hill, possibly within the upper 100-150 m of the vertical interval is proposed for Central Ridge. However it is possible that they formed at the same level but at different temperatures. The evidence to suggest lower temperature hydrothermal fluids or shallow level of formation are based on quartz, gangue and ore mineralogy assemblages and include the following;

- Primary chalcedony and opal and their associated recrystallisation textures at Central Ridge are possibly inherited from an amorphous silica gel precursor (Dong and Morrison, 1995). Henley and Ellis (1983) state that amorphous silica is predominant at high elevations in epithermal fields and indicates a temperature of up to 150°C.
- To precipitate amorphous silica the fluids should be slightly saturated with silica and temperatures between 100°C and 190°C (Fournier, 1985; Henley and Ellis, 1983).
- Gold grade is characteristically low and only occurs in samples which exhibit pyrite grains which suggests that either electrum was not present in cut thin sections of forms as inclusions within pyrite grains. Electrum occurring as inclusions in pyrite is consistent with the upper 100 metres of the model proposed by Buchanan (1981).

T1 Hill

The availability of drill core at T1 Hill allows the assessment of quartz textures, gangue mineralogy and ore mineralogy over a vertical interval of up to 250m. Four main vein stages can be identified from surface samples at T1 Hill. Mineralised stages are characterized by primary quartz textures such as milky white chalcedony crustiform bands, 'smoky' grey crystalline quartz and moss textures. Replacement textures after calcite and/or adularia are common and include lattice bladed and pseudoacicular quartz. Sulphides are associated with micro crystalline quartz horizons and replacement textures. In drill core mineralisation is also associated with replacement textures in 'smoky' green chlorite quartz veins. Ore mineralogy is dominated by pyrite and chalcopyrite grains occurring within the wall rock and to a lesser extent in veins. In surface samples pyrite and chalcopyrite preferentially occur together in thin bands. Pyrite and chalcopyrite in drill core are more abundant than in surface samples. Most pyrite preferentially occurs in wall rock and chalcopyrite in quartz carbonate veins.

It is interpreted that like Conical Hill the level of formation is deeper than that of Central Ridge and could potentially be deeper than Conical Hill. Similar to Conical Hill boiling is thought to be closely associated with ore bearing phases.

- Zonation of increasing quartz and decreasing chalcedony with depth is observed at T1 Hill. This zonation is a typical feature of epithermal deposits and has been documented at Pajinjo (Bobis et al., 1995), McLaughlin (Sherlock et al., 1995), Cracow (Dong and Zhou, 1996), Comstock (Hudson, 2003), and Guanajuato (Buchanan, 1981).
- In drill core, vein textures are dominated by comb quartz carbonate chlorite veins. The presence of comb quartz indicates that the fluids were slightly saturated with respect to quartz which requires slow cooling at temperatures between about 200°C and 340°C (Fournier, 1985). This temperature is much higher than the interpreted temperature between 100°C and 180°C for Central Ridge.

- Crystalline quartz and chalcedony in surface samples represent temperatures of between 150°C and 200°C and an amorphous silica precursor (Dong et al., 1995). This is lower than temperatures inferred to occur in drill hole located veins. Late stage comb quartz veins resembling veins at depth cross-cut quartz and chalcedony surface samples. This comb quartz stage is inferred to be a high temperature stage.
- Replacement textures, adularia rhombs, and bladed calcite associated with sulphides suggests that boiling occurred during ore deposition.
- The breccia stage in surface vein float suggests that episodic hydraulic fracturing occurred which is probably a result of quartz and/or calcite precipitation sealing fluid channel conduits (De Ronde and Blattner, 1988; Fournier, 1985). Episodic fracturing caused by imbalances of confining pressures may create conditions that are conducive to the precipitation of precious metals (Fournier, 1985). These conditions include increase in permeability, decrease in pressure, partitioning of H₂S and CO₂ into a steam phase (steam = ↑ ph; Fournier, 1985).

Gift Prospect

The Gift prospect comprises of 5 vein systems that differ in terms of mineralogy, quartz textures and gold grade. Quartz textures associated with high grade A and F systems include primary massive, crystalline, moss, cockade and comb quartz. Replacement textures including ghost bladed, lattice bladed, saccharoidal and quartz pseudomorphs after adularia are also common. Low grade systems (ie B, C, D, E) exhibit primary quartz textures dominated by chalcedony crustiform colloform banded veins. Breccia veins also occur and comprise of unmineralised chalcedony crustiform colloform vein clasts in a chalcedony dominated matrix.

Based on gold grade, vein systems at Gift can be divided into barren and mineralised veins. Mineralised veins (A and F) share similar quartz textures, gangue mineralogy, and

ore mineralogy and are interpreted to have formed at around the same vertical interval or from similar fluids and temperatures. This interval is interpreted to be at or slightly above the zone of precious metal deposition (200-250 metres). This classification is largely based on quartz textural analysis and gangue mineralogy as most sulphide assemblages have weathered to limonite and goethite. In contrast to mineralised systems, barren systems are characterized by the predominance of chalcedony + quartz \pm barite crustiform colloform banded veins which, display textural similarities to Central Ridge veins. It is interpreted that these veins form at shallow levels or at lower temperatures than the mineralised veins.

Evidence suggesting formation at or slightly above the precious metal zone for mineralised veins includes:

- Quartz textures are dominated by crystalline quartz and only minor chalcedony phases. This is consistent with the quartz textural zonation model of Morrison et al. (1990) at the precious metal interval. Ore mineralogy including pyrite, chalcopyrite, and rare electrum are typical assemblages of the precious metal ore interval (Buchanan, 1981).
- Gangue mineralogy such as crystalline quartz, calcite, and adularia is indicative of formation just above the precious metal zone (200-250 metres; Buchanan, 1981).
- Replacement textures generally associated with ore mineralogy such as bladed quartz and pseudoacicular quartz indicates that during ore deposition boiling provided favourable conditions for the precipitation of adularia and calcite.
- Absence of precious metals and predominance of pyrite and minor chalcopyrite suggest that formation occurred above the precious metal interval.

Evidence to suggest barren veins formed at shallower levels (100 – 200 metres) than mineralised veins includes.

- Predominance of chalcedony in vein stages suggest that fluids were saturated in respect to quartz and were at temperatures of 180°C or below (Fournier, 1985). According to Buchanan (1981) and Hedenquist (2000) temperatures of around 180°C are likely to occur at shallow levels between 180 and 90 metres.
- Gangue mineralogy assemblages including chalcedony, calcite, and barite are consistent with formation at 200 – 100 metres below the surface (Buchanan, 1981).

Chapter 5 Fluid Characteristics

Stable isotopes (oxygen and sulphur) and fluid inclusions have been used to help better constrain the fluid characteristics responsible for mineralisation at Wang Yai. This chapter will present a description of results followed by a discussion for the implications of the results.

5.1 Oxygen Isotopes

$\delta^{18}\text{O}$ values of vein quartz can be used in epithermal systems to characterize the hydrothermal fluids, identify the source of water in the system, and to estimate the degree of meteoric water-rock exchange (John et al., 2003). Studies such as these may also provide important insights into ore forming processes. In this study an isotopic study of vein quartz was undertaken in an attempt to understand the source of fluids and the relationship between oxygen isotope, gold grade and vein textures at Wang Yai. The broad aim of this research was to establish a useful exploration tool that could vector towards high grade parts of the system.

Methods

A total of 16 vein samples were selected from vein systems at Wang Yai. The silica polymorphs in samples ranged from crystalline quartz to chalcedony to opaline quartz. All samples displayed a variation in gold grade (from 0.00 to 36.5 g/t Au). The samples selected include two from Conical Hill, four from Central Ridge, three from T1 Hill, one from T4 Hill, five from the Gift prospect (see Table 5.1).

The quartz selected for $\delta^{18}\text{O}$ analyses was analysed using conventional techniques and a Micromass 602E mass spectrometer. $\delta^{18}\text{O}$ values are given in per mil relative to Vienna Standard Mean Ocean Water (SMOW). Analytical precision is ± 0.2 per mil (one standard deviation). Measured isotopic values were normalised against an international standard through the repeat analysis of NSB 28 ($+9.6\text{‰ } \delta^{18}\text{O}$).

Table 5.1 Summary of $\delta^{18}\text{O}$ (SMOW) values for quartz at Wang Yai, Central, Thailand

Sample no.	Material analysed	Occurrence	$\delta^{18}\text{O}$ (SMOW)	Location	Description	Assay g/t Au
ER017966	Crystalline quartz	Massive vein	13.5	Conical Hill	Milky white, crystalline quartz vein	6.3
ER017427	Crystalline quartz	Massive vein	13.0	Conical Hill	Crystalline quartz with ginguro ore	36.5
ER017439	Opaline silica	Banded vein	17.5	Central Ridge	Banded opaline silica + chlorite vein	0.00
ER017244	Opaline silica	Vein	16.5	Central Ridge	Opaline silica-chlorite banded vein	0.00
ER017244	Opaline silica	Vein	16.2	Central Ridge	Opaline silica-chlorite banded vein	0.00
ER016951	Chalcedony, opal	Vein	14.0	Central Ridge	Crustiform colloform banded	0.00
ER016934	Chalcedony, opal	Vein	14.5	Central Ridge	Crustiform colloform banded	0.4
ER016905	Crystalline quartz	Vein	12.2	T1 Hill	Crystalline quartz with cockade textures	2.0
ER016925	Quartz, chalcedony	Vein breccia	12.4	T1 Hill	Massive crystalline quartz + chalcedony	0.7
ER016926	Quartz, chalcedony	Vein breccia	13.3	T1 Hill	Grey crystalline quartz + chalcedony clasts	3.8
ER017453	Crystalline quartz	Vein	13.3	T4 Hill	Poorly developed crustiform colloform bands	0.1
ER017511	Crystalline quartz	Vein breccia	11.0	S.V Prospect	Brecciated crystalline quartz vein	0.1
ER017507	Chalcedony	Banded vein	14.6	Gift Prospect	Pink recrystallised chalcedony	0.0
ER017509	Chalcedony	Banded vein	14.8	Gift Prospect	Pink chalcedony crustiform colloform bands	0.0
ER017499	Chalcedony, quartz	Banded vein	15.5	Gift Prospect	Banded chalcedony vein with comb quartz	0.0
ER017464	Quartz	Massive vein	12.5	Gift Prospect	Massive grey milky quartz vein	2.8

5.1.1 Results

The data of $\delta^{18}\text{O}$ values are spatially shown in Figure 5.1. $\delta^{18}\text{O}$ values show a range from +11 to +17.5 per mil. $\delta^{18}\text{O}$ values broadly correlate with variation of gold grade and vein textures. For example, low $\delta^{18}\text{O}$ values are associated with high gold grade and textures dominated by crystalline quartz. These vein systems (Conical Hill, T1 Hill, T4 Hill and 'D' Zone at Gift) have average $\delta^{18}\text{O}$ values of between +12 and +13.5 per mil. The S.V prospect which is distant from the main vein zones at Wang Yai has a value of +11 per mil. High $\delta^{18}\text{O}$ values correlate with low or no gold grade and opaline silica-chalcedony dominated quartz textures. For example Central Ridge and B, C, D and E vein systems at Gift show high (+14.6 – +17.5 per mil) oxygen isotope values. These systems are characterised by unmineralised chalcedony \pm opaline quartz veins. At Central Ridge $\delta^{18}\text{O}$ values show an excellent relationship of zoning with vein textures and gold grade. This zonation is characterised by high $\delta^{18}\text{O}$ values (+17.5, +16.5, +16.2 per mil) occurring at the southern end of the system where opaline quartz phases predominant and gold grade is negligible. At the northern end of the vein $\delta^{18}\text{O}$ values are lower (+14.0 , +14.5 per mil) corresponding with an increase in gold grade.

Quartz vein $\delta^{18}\text{O}$ values for vein systems in the Gift prospect also correlate with vein textures and mineralogy. Vein systems B, C, D and E which are dominated by chalcedony crustiform colloform banded veins and negligible gold grade (i.e; <0.01 g/t Au) exhibit values of 14.6 and 14.8 per mil. In contrast, vein system D which is dominated by crystalline quartz and average gold grade >2.0g/t Au shows values of 12.5 per mil.

Calculated oxygen isotope compositions of ore fluids

Oxygen isotope compositions of ore fluids were calculated using quartz-water fractionation data from Zheng (1993) (Equation 5.1). Calculated isotopic compositions of ore fluids for 180°C, 250°C, and 300°C are summarised in Table 5.2.

$$1000 \ln \alpha = D \frac{(10^6)}{T^2} + E \frac{(10^3)}{T} + F$$

Equation 5.1. Quartz-water fractionation equation (Zheng 1993)
D: 4.480; E: -4.77; F: 171 (from <http://www.ggl.ulaval.ca/cgi-bin/isotope/isotope4alpha.cgi>)

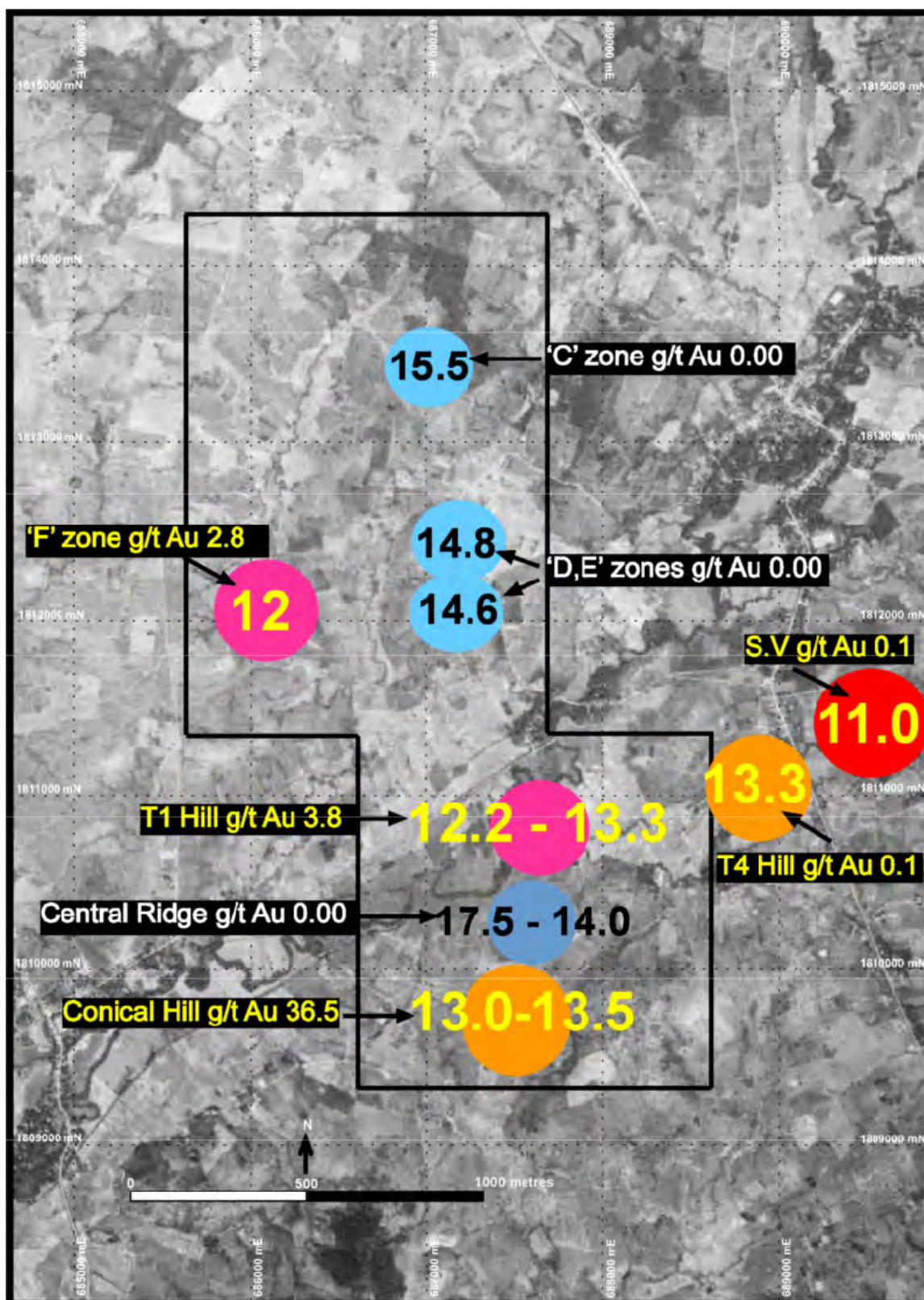


Figure 5.1 Aerial photo of Wang Yai showing the raw $\delta^{18}\text{O}$ SMOW values in per mil from each vein system (in yellow and black). Bright colours (red, orange, pink) represent low $\delta^{18}\text{O}$ SMOW values and dark colours represent (blue) high oxygen isotope values. Corresponding gold grade is labelled for each $\delta^{18}\text{O}$ value. Yellow represents gold grade and white no gold grade.

Table 5.2 Summary of isotopic compositions of ore fluids for 180°C, 250°C, and 300°C calculated from quartz-water fractionation Zheng (1993)

Location/ Sample no	Assay g/t Au	$\delta^{18}\text{O}$ (SMOW)	$\delta^{18}\text{O}_{180^\circ\text{C}}$	$\delta^{18}\text{O}_{250^\circ\text{C}}$	$\delta^{18}\text{O}_{300^\circ\text{C}}$	Vein Descriptions
Conical Hill						
ER017966	6.3	13.5	0.5	4.5	6.5	Milky white, crystalline quartz vein
ER017427	36.5	13	0	4	6	Crystalline quartz with ginguero
Central Ridge						
ER017439	0	17.5	4	8.8	10.5	Banded opaline silica + chlorite
ER017244	0	16.5	3	7.5	9.5	Opaline silica-chlorite banded vein
ER017244	0	16.2	3.2	7.2	9.2	Opaline silica-chlorite banded vein
ER016951	0	14	1	5	7	Crustiform colloform banded
ER016934	0.4	14.5	1.5	5.5	7.5	Crustiform colloform banded
T1 Hill						
ER016905	2	12.2	-0.8	3.2	5.2	Crystalline quartz with cockade textures
ER016925	0.7	12.4	-0.6	3.4	5.4	Massive crystalline quartz + chalcedony
ER016926	3.8	13.3	0.3	4.3	6.3	Grey crystalline quartz + chalcedony clasts
T4 Hill						
ER017453	0.1	13.3	0.3	4.3	6.3	Poorly developed crustiform colloform bands
S.V						
ER017511	0.1	11	-0.2	2	4	Brecciated crystalline quartz vein
Gift Prospect						
ER017507	0	14.6	1.6	5.6	7.6	Pink recrystallised chalcedony
ER017509	0	14.8	1.8	5.8	7.8	Pink chalcedony crustiform colloform bands
ER017499	0	15.5	2.5	6.5	8.5	Banded chalcedony vein with comb quartz
ER017464	2.8	12.5	-0.5	3.5	5.5	Massive grey milky quartz vein

Table 5.2 shows that calculated oxygen isotope compositions for 180°C yielded values between 1.0 and 4.0 per mil for poorly mineralised chalcedony dominated veins (i.e; Central Ridge, B, C, D, and E Gift) and -0.8 to 0.5 per mil for well mineralised, crystalline quartz veins. Oxygen isotope compositions at 250°C yielded values between 8.0 and 5.0 per mil for poorly mineralised veins and between 2.0 and 4.5 per mil for well mineralised veins. At 300°C, oxygen isotope compositions yielded values between 7 and 10.5 per mil for poorly mineralised veins and between 2 and 4.5 per mil for well mineralised veins. Figure 5.2 shows a histogram of the calculated oxygen isotopic compositions of ore fluids.

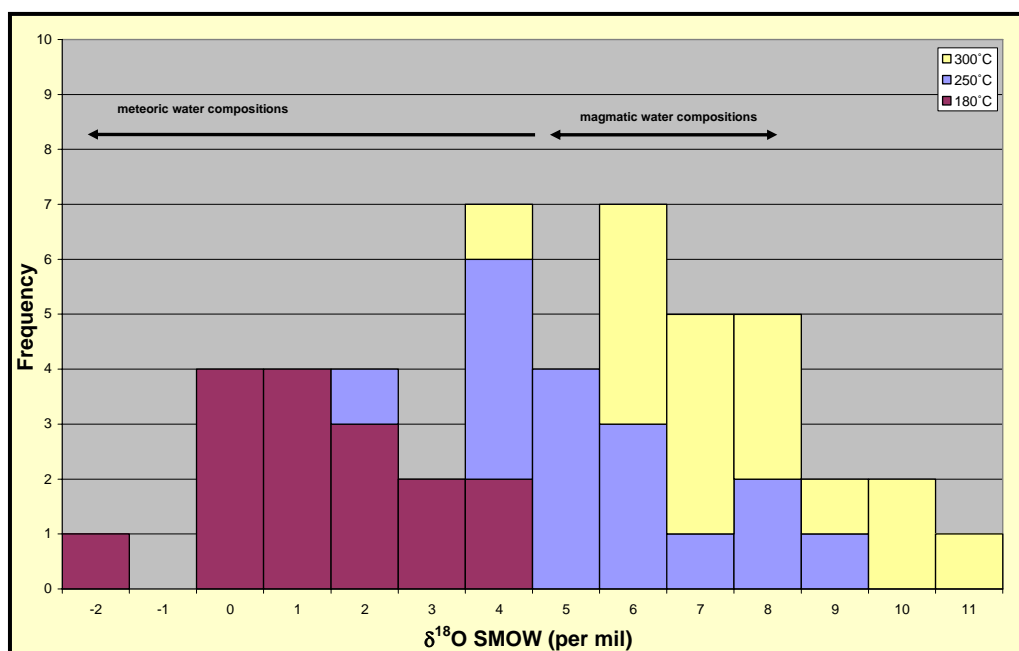


Figure 5.2 Frequency histogram of calculated $\delta^{18}\text{O}$ SMOW of ore fluids at 180°C, 250°C, and 300°C using quartz fractionation data from Zheng (1993). Note the compositions of magmatic water and meteoric water in black (Rollinson, 1993.).

The isotopic compositions show a shift towards depleted compositions with declining model temperatures. This shift corresponds/overlaps with typical meteoric fluid composition. At higher model temperatures (300°C), $\delta^{18}\text{O}$ compositions are more magmatic. This may be attributed to four factors including; water rock interaction, fluid mixing, finite reservoir effects, and boiling. Each of these factors is discussed in more detail at the end of the chapter.

5.2 Sulphur isotopes

Stable δS^{34} isotope analyses of wallrock and vein located pyrite were undertaken to determine the source of sulphur at Wang Yai. For this study three samples with vein or wallrock disseminated pyrite were selected for laser ablation at the Central Science Laboratory, University of Tasmania. One sample (ER017459) was selected from the Gift prospect and two were from T1 hill drill hole WYRD016.

The results from laser ablation of pyrite (summarised in Table 5.3) show that vein located pyrite yields $\delta^{34}S$ per mil values between +1.59 and -0.09 per mil. Wallrock located pyrite yields $\delta^{34}S$ values between +3.82 and -0.04 per mil. There is a broad trend of wall rock pyrite assuming heavier $\delta^{34}S$ values.

Table 5.3 Summary of $\delta^{34}S$ values for vein and wallrock located pyrite, Wang Yai, central Thailand

Sample no	Location	Number spots ablated	$\delta^{34}S$ ‰
ER017459 (Gift)	Vein	2	+1.56
ER017459 (Gift)	Vein	1	+0.46
WYRD016@240m	Vein	1	+1.59
WYRD016@240m	Vein	2	-0.09
WYRD016@240m	Wallrock	2	-0.04
WYRD016@240m	Wallrock	2	+2.39
WYRD016@243.7m	Wallrock	3	+3.82
WYRD016@243.7m	Wallrock	4	+0.58
WYRD016@243.7m	Vein	1	+0.03

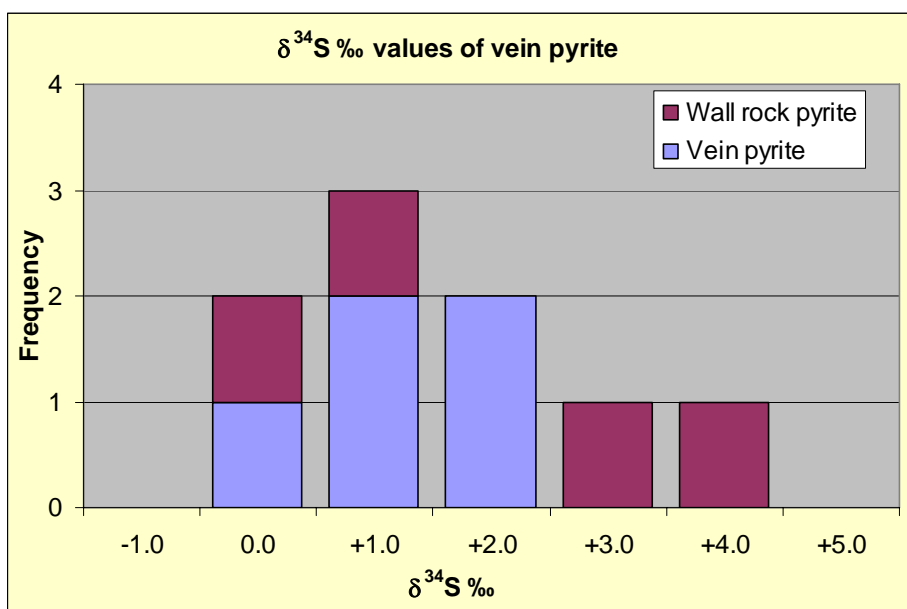


Figure 5.3. Histogram of $\delta^{34}S$ values for wall rock and vein located pyrite.

5.3 Fluid inclusion studies

Fluid inclusion studies was carried out to understand the thermal aspect of ore deposition and to constrain the variation of oxygen isotopic composition. Linkam TH600 heating/freezing stage was used in this study. The general method and procedure for heating/freezing experiments are reported elsewhere (Roedder, 1984). The precision of the temperature measurements is better than $\pm 1^{\circ}\text{C}$ for heating and $\pm 0.3^{\circ}\text{C}$ for freezing. Accuracy of the measurements was insured by calibration against synthetic fluid inclusions and the observed triple point of CO_2 (-56.6°C), the freezing point of water (0.0°C), and the critical point of water (374.1°C). Fluid inclusions were classified in a temporal sense as primary, secondary and pseudosecondary relative to the time of trapping as defined by Roedder (1984). The fluid inclusion characteristics of the Wang Yai prospects are shown in Figure 5.4

Fluid inclusions from the Wang Yai prospect can be classified into two major types based on phases observed in the inclusions at room temperature. They include:

Type I: Two-phase, liquid and vapor inclusions. Type I inclusions are isolated, and occur away from healed microfractures. They are primary inclusions as their formation can be related to the growth zones of the host quartz (Figure 5.4A). In this study, only primary Type I inclusions are studied.

Type II: Two-phase, liquid-rich inclusions with a variable liquid and vapor ratio. Their irregular shape with variable liquid and vapor ratio indicates a secondary origin. The randomly distributed array of these secondary Type II inclusions and their textural features possibly suggest post-deformational shearing during their emplacement.

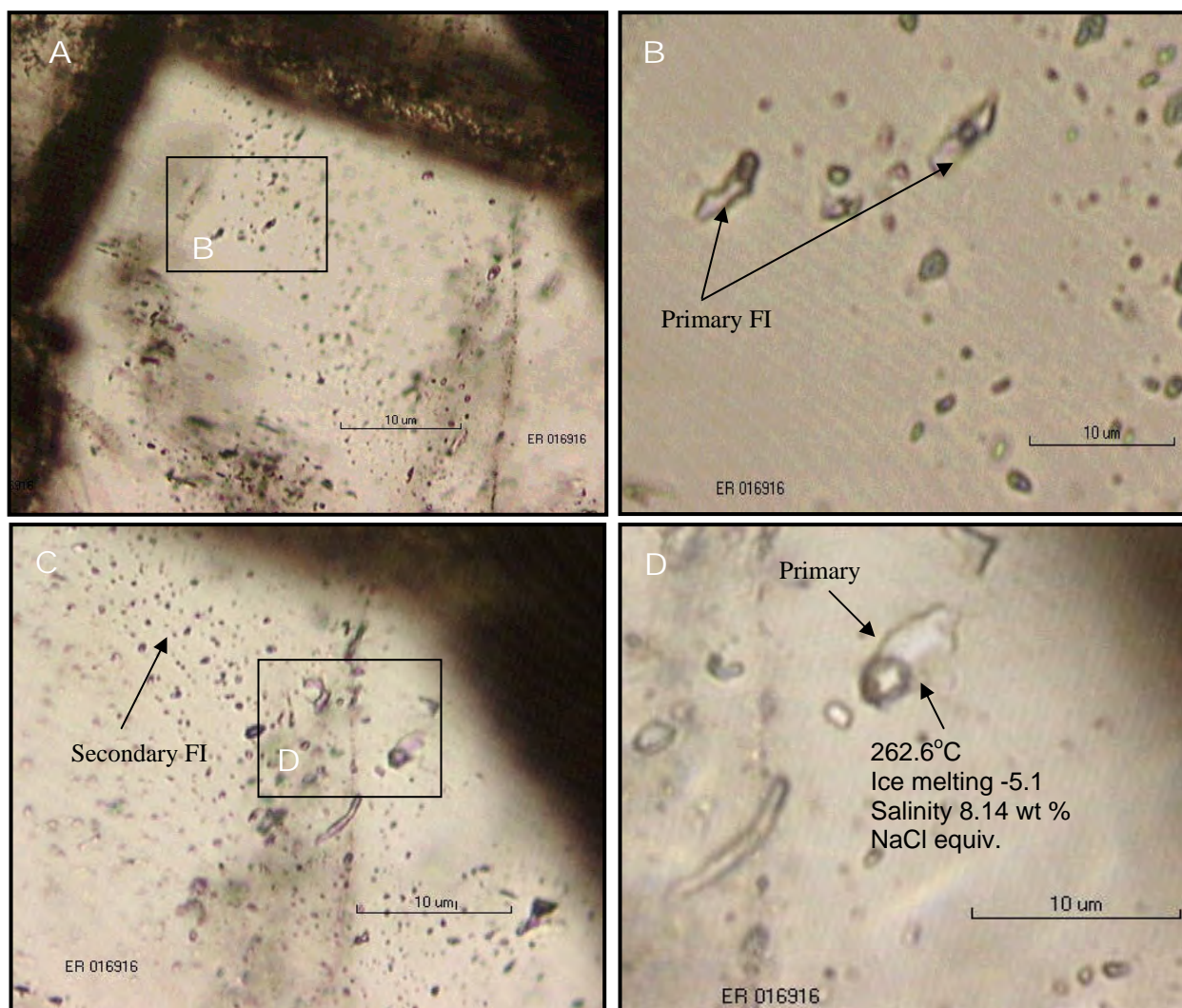


Figure 5.4 A) Photomicrographs showing Types I and II fluid inclusions in euhedral quartz (sample ER016916) B) Close-up of two primary inclusions (sample ER016916). C). Close up of two primary inclusions (sample ER016916). D) Close up of primary Type I inclusions.

5.3.1 Homogenisation temperatures

Homogenisation data for Type I inclusions from Wang Yai are shown in Table 5.4. A total of nineteen homogenisation temperatures were measured for three samples. Measured homogenisation temperatures display a range of 134 to 298.4°C. Primary fluid inclusions from sample ER016916 (0.85 g/t Au) show a range in temperature of 218 to 298.4°C, all but one occur between 240 and 290°C. The anomalous value of 218°C may be attributed to analyses of a secondary inclusion (consistent with other low temperatures

measured elsewhere). Fluid inclusions from this sample were analysed from euhedral quartz that infills open spaces in crystalline quartz. Primary fluid inclusions for sample ER016925 show lower (180 to 218°C) homogenisation temperatures than sample ER016916. Fluid inclusions from ER016925 were analysed from grey crystalline matrix quartz that is host to disseminated pyrite and electrum (0.86 g/t Au). $\delta^{18}\text{O}$ values for this sample are +12.4 per mil. Sample ER017499 is from Gift prospect vein system C (Figure 4.1) and yields homogenisation temperatures of 141 to 210°C. Fluid inclusions were analysed from a band of comb quartz with well developed euhedral crystals and growth zones. This sample yields the lowest temperatures for all three samples and the lowest gold grade (below detection). $\delta^{18}\text{O}$ values for this sample are +15.4 per mil. From this data set $\delta^{18}\text{O}$ values show a relationship with homogenisation temperature. $\delta^{18}\text{O}$ values show high values for low homogenisation temperatures and lower $\delta^{18}\text{O}$ values for high homogenisation temperatures. This implies that temperature is not solely controlling grade, other processes such as water rock interaction and boiling maybe responsible.

5.3.2 Salinity

The salinity values for the three samples range from 1.1 to 8.1 wt % NaCl equivalent. However most values are between 3 and 5 wt % NaCl equivalent. The salinity values do not show a spatial zonation or a correlation with gold grade. All samples lacked evidence of boiling textures. Salinity values for sample ER016916 (comb quartz) show a range of 2.1 to 8.1 wt % NaCl equivalent. Sample ER016925 (crystalline quartz) which is from the same prospect (T1 Hill) yields values of between 3.4 and 5.0 wt % NaCl equivalent and sample ER017499 from the C vein system at Gift yields values between 1.1 and 5.7 wt % NaCl equivalent.

Table 5.4. Summary of fluid inclusion data, Wang Yai, central Thailand

Location/Sample No./ Quartz texture/av. $\delta^{18}\text{O}$ value	Mineral studied	Inclusion type	Th (L- V)-L	Tm-ice	wt % NaCl equiv*
T1 Hill					
ER 016916	Quartz	I	253.0		
Euhedral well developed		I	264.0		
comb quartz		I	296.0	-2.8	4.7
		I	262.6	-5.1	8.1
		I	264.7	-4.5	7.2
		I	218.6	-2.0	3.4
		I	283.3	-2.5	4.2
		I	298.4	-1.2	2.1
		I	237.0	-2.8	4.7
T1 Hill					
ER 016925	Quartz	I	134.7	-3.1	5.0
Grey crystalline quartz		I	187.8	-2.0	3.4
+12.4 $\delta^{18}\text{O}$		I	213.4	-2.0	3.4
		I	218.8		
C vein system (Gift)					
ER 017499	Quartz	I	152.5		
Comb quartz		I	163.7		
+15.4 $\delta^{18}\text{O}$		I	203.0		
		I	215.7	-1.8	3.1
		I	141.2	-0.6	1.1
		I	185.4	-3.5	5.7

* Salinities were calculated using the last ice melting temperature (wt % NaCl equiv.) and equation of Bodnar (1993)

5.4 Discussion

5.4.1 Oxygen Isotopes

Quartz oxygen isotopic values show a clear correlation with vein textures and gold grade at Wang Yai (as outlined above). Well mineralised crystalline quartz dominated veins (i.e, Conical Hill, T1 Hill, T4 Hill, A and F Gift systems) show low $\delta^{18}\text{O}$ values (12 to 13 per mil). Unmineralised chalcedony dominated veins display high $\delta^{18}\text{O}$ values (14.5 – 17 per mil).

The histogram of calculated $\delta^{18}\text{O}$ SMOW values for fluid temperatures at 180°C, 250°C, and 300°C using quartz water fraction factor of Zheng (1993), shows that there is a shift to lower $\delta^{18}\text{O}$ isotopic compositions with decreasing temperature. For example, at Central Ridge and Gift the calculated fluid composition responsible for chalcedony (formed <200°C) can be a few per mil lighter than fluid responsible for the earlier high temperature (>200°C) quartz (see Table 5.2) There are four plausible processes that can be attributed to the shift to depleted oxygen isotope values. They include water rock interaction, fluid mixing, finite reservoir effects and boiling.

Water-Rock interaction: Water rock interaction is inherited during hydrothermal alteration. When hydrothermal fluids infiltrate a portion of rock there, is an inherent shift in isotopic composition of the fluid that will directly influence the composition of subsequent precipitating minerals (Taylor, 1974). For example if a hydrothermal fluid interacts with wall rock that has a higher isotopic composition than the fluid then mass-balance effects will result in the wall rock assuming heavier isotopic values and lighter fluid values. The degree at which the fluid composition shifts, is dependant on temperature (i.e; larger shift at low temps and smaller shift at high temps), and the water/rock ratio. The processes of isotopic exchange during fluid interaction can be explained using the model from Harris et al. (2005). This model is calculated for temperatures of 300°C (which are only slightly above the highest homogenisation temperatures at Wang Yai) and magmatic water with compositions between 5.7 and 9.8 per mil. Therefore assuming an average volcanic wallrock composition of +8 per mil and an unevolved magmatic fluid of +7 per mil water rock exchange will result in the enrichment of $\delta^{18}\text{O}$ in wall rock (up to 4 per mil) and depletion of $\delta^{18}\text{O}$ in fluids (Harris et al., 2005). This shift in $\delta^{18}\text{O}$ composition of fluid buffered against rock, becomes more pronounced at lower temperature (implicit in the fractionation factors used to model fluid compositions). Therefore the shift to depleted $\delta^{18}\text{O}$ values shown in Figure 5.2 may represent the presence of an evolved fluid that has interacted with wall rock.

Finite reservoirs effects: Finite reservoir effects can help explain isotopic variation in a hydrothermal system (Pollard et al., 1991). This process can be linked with water rock interaction. Finite reservoir processes is a consequence of hydrothermal fluids moving

through conduits to exchange heavy $\delta^{18}\text{O}$ values from the liquid to quartz as it is precipitated. This results in an imbalance of $\delta^{18}\text{O}$ values between precipitated substrate and fluids. Subsequently through simple mass balancing between quartz substrate and fluids the isotopic composition of fluids become lighter.

Boiling: Boiling is a process that may also be responsible for the shift in $\delta^{18}\text{O}$ values. At Wang Yai there is evidence of boiling in gold bearing veins (see Chapter 4 section 4.9). However it has been documented in many papers that boiling alone is unlikely to cause significant shifts in isotopic compositions. For example at Hishikari, Japan Hayashi et al. (2001) found that although bladed quartz (indicative of boiling) is associated with a large shift of $\delta^{18}\text{O}$ values (+6 per mil to 12 per mil) 92 % of the fluid must boil before this shift can occur. Hayashi et al. (2001) concluded that vein formation is unlikely during extreme boiling, therefore the shift in $\delta^{18}\text{O}$ values is attributed to fluid mixing occurring concomitant with boiling.

Fluid mixing: Fluid mixing of magmatic fluid and meteoric fluid may also be attributed to the shift in calculated $\delta^{18}\text{O}$ values although due to the limited data set and unknown δD fluid values constraining the evolution fluid mixing is quite problematic and beyond the scope of this project.

Of the four processes listed above it is likely that water rock interaction and finite reservoir effects are considered important the shift in $\delta^{18}\text{O}$ values. To help better constrain the degree of water rock interaction and fluid mixing $\delta^{18}\text{O}$ and δD values of host rock and associated hydrothermal alteration assemblages needs to be determined.

5.4.2 Sulphur Isotopes

δS^{34} isotopic values of pyrite from gold bearing veins and alteration assemblages at Wang Yai occur close to zero per mil. This suggests that a magmatic source of sulphur that may have come from at depth or from volcanic host rocks through which the fluid passed (Heald et al., 1987).

5.4.3 Fluid Inclusions

Primary fluid inclusion data from the samples analysed shows homogenisation temperatures are consistent with typical epithermal low sulphidation systems (Simmons et al., 2005). At Wang Yai homogenisation temperatures display a relationship with vein textures and gold grade. Mineralised crystalline quartz veins at T1 Hill show lower temperatures (180 to 218°C) than late stage unmineralised comb quartz (ER016916) (218 to 298.4°C). Based on the relationship between mineralisation and homogenisation temperatures of 180 to 218°C it is interpreted that ore bearing fluids were at temperatures from 200 to 250°C during the deposition phase. This temperature range is consistent with the 200 to 300°C range for 16 low sulphidation epithermal deposits in North and South America (Heald et al. 1987). Moreover, it is consistent with textural evidence and the preservation of chalcedony (implying temperatures <200°C) and boiling (e.g., adularia). The high and diverse range of temperatures for primary inclusions in sample ER016916 could indicate that during the ore depositional event boiling occurred (Bodnar et al., 1985).

The unmineralised chalcedony dominated veins at system C in the Gift prospect show low temperatures between 140 and 200°C. This temperature falls within the bracketed temperature of chalcedony formation (<180°C; Fournier, 1985). These veins maybe offshoots off the main vein system and appear to have formed at low temperatures. Heald et al. (1987) in their study of North and South American low sulphidation epithermal deposits highlights the presence of late stage, veins depositing gangue mineralogy at temperatures between 140°C and 200°C. These temperatures are consistent with the homogenisation temperatures of barren chalcedony dominated veins at system C in the Gift prospect.

Calculated salinity values show an average range of 3-6wt% NaCl equivalent. These values are slightly higher than values for typical gold dominated epithermal deposits hosted in andesitic rocks. Most gold dominated deposits have average weight percent NaCl values of around 1.6 to 2.0 wt % NaCl equivalent and up to 5 wt % equivalent for Au-Ag systems (Hedenquist and Henley, 1985; Sherlock et al., 1995; Simmons et al., 2005). Salinities up to 20wt % are found in some quartz carbonate veins in low

sulphidation systems (e.g 10 wt % NaCl equiv. at Creede, Barton et al., 1977) but these systems are Ag-Pb-Zn rich (not like Wang Yai). As the salinity values at Wang Yai are higher than that of other epithermal deposits it is possible that the presence of CO₂ vapor in fluid inclusions played a role in contributing to freezing point depression (i.e, increasing the salinity values; Hedenquist and Henley, 1985). If CO₂ vapour has contributed to the freezing point depression then it is possible that the salinity values are not representative of the original quartz precipitating fluids. Alternatively, the higher salinity of the fluids associated with mineralization may imply a small component of magmatic fluid introduced to the Wang Yai system. This requires further validation.

Chapter 6 Conclusions

6.1 Geological setting

Geological mapping at Wang Yai has revealed gold mineralisation is hosted in volcanogenic sandstone, breccia and conglomerate which are intruded by coherent feldspar phyric andesite. Minor lithological units include mudstone and thinly bedded fossiliferous limestone. The succession is cut by diorite dykes.

LA-ICP-MS U-Pb zircon studies of quartz phyric rhyodacite and quartz breccia/sandstone have yielded ages of 321 ± 5 Ma and 247 ± 4 Ma respectively. These ages suggest that basement felsic volcanics (rhyodacite) are overlain by Permian to Triassic volcanic stratigraphy.

The host rock geochemical characteristics at Wang Yai yield island arc and continental arc affinities. Older rocks including andesitic lithic breccia and andesitic sandstone have island arc affinities. This is consistent with palaeo reconstructions of the Permian which include island arc volcanism associated with subduction of the Shan-Thai and Indochina cratons (Dedenczuk, 1998). Younger intrusive rocks (andesite and diorite) yield continental arc affinities.

6.2 Nature of mineralisation

The volcanic succession at Wang Yai hosts eleven vein systems. The systems occur in the following prospects; Conical Hill, Central Ridge, T1 Hill, T4 Hill, S.V and Gift. Vein texture and mineralogy studies have identified zonation between gold-bearing vein systems and barren systems. Using current epithermal models this zonation has been explained through depth related zonation due to boiling. At shallow levels in the system Central Ridge, and Gift prospect vein systems B, C, D, and E show chalcedony and opaline quartz crustiform colloform veins which are indicative of fluid temperatures $<180^{\circ}\text{C}$. These barren systems do not show evidence of boiling related quartz textures and contain only trace amounts of pyrite \pm chalcopyrite and no electrum. The

characteristics of a deep level formation in gold bearing systems at Wang Yai are consistent with current epithermal models. At deeper levels gold bearing vein systems such as Conical Hill, T1 Hill, T4 Hill, S.V and A,F-(Gift) are characterized by the predominance of massive crystalline quartz, crustiform colloform banding, replacement textures and precious metals (argentite and electrum). The predominance of crystalline quartz in these systems suggests higher temperatures of formation than barren systems. A higher formation temperature for these systems can be explained by formation at deeper levels in the system. The quartz textures and mineralogy in these systems suggest a level of formation at or above the zone of boiling and precious metal deposition. Quartz replacement textures such as silica pseudomorphs after adularia and bladed quartz suggests ore deposition may have been in response to extensive boiling. The occurrence of precious metals and negligible base metals is consistent with the zone of extensive boiling.

6.3 Fluid characteristics

Oxygen isotope studies of vein quartz have revealed a correlation with respect to quartz textures and gold grade. Low O^{18} values are associated with high gold grade and crystalline quartz dominated vein textures. High O^{18} values are associated with low gold grade and chalcedony/opaline silica dominated vein textures.

Based on the relationship between homogenisation temperatures and mineralised veins fluids responsible for ore deposition are interpreted to be in the range of 200 – 250°C. The high variability in salinity values could indicate that extensive boiling occurred during mineralisation at Wang Yai.

Sulphur isotope values from gold bearing veins indicate the source of sulphur may have come from depth or from volcanic host rocks, through which hydrothermal fluids passed.

Significant findings and implications for exploration.

- Hand specimen analysis of quartz textures and gangue mineralogy in vein samples can be used to delineate vein systems that are favourable hosts of gold mineralisation.
- The relatively shallow formation depth for vein systems at Wang Yai suggests that there is great potential for mineralisation at depth.
- Vein systems that should be given the highest priority for further exploration include Conical Hill, Conical west, T4 Hill, S.V, and A and F system in the Gift prospect.
- Barren vein systems indicative of shallow formation should not be disregarded as potential for mineralisation may lie at depth.
- Oxygen isotopes values of vein quartz show a strong correlation with gold grade and gold 'kind' quartz textures which implicates their great potential for use as a vector to ore.

APPENDIX 1.

LITERATURE REVIEW

Characteristics of Low Sulphidation Epithermal Deposits

by

John de Little BSc.

Supervisor : Khin Zaw

Co-supervisors: Anthony Harris, Stuart Smith



A literature review submitted in partial fulfilment of the requirements for an Honours Degree at the School of Earth Science, University of Tasmania (July, 2005).

Declaration

This thesis contains no material which has been accepted for the award of any other degree or diploma in any tertiary institution, and to the best of my knowledge and belief, contains no material previously published or written by another person, except where due reference is made in the text of the thesis.

Signed

John de Little BSc.

Abstract

Low sulphidation epithermal deposits occur in subduction related island and continental arc settings. Deposits in island arc settings are generally exhibit characteristics indicative of greater depths of formation than deposits in continental arc settings. Five dominant types of alteration occur in epithermal low sulphidation deposits. They include silicic, argillic, phyllic, advanced argillic, and propylitic. The dominant ore minerals consist of pyrite, chalcopyrite, sphalerite, galena and electrum. They generally occur as free grains or in polyminerale sulphide aggregates. Electrum often occurs contemporaneous with chalcopyrite, galena, and sphalerite. The form of low sulphidation deposits is dictated by dynamic lithological, structural, and hydrothermal controls. Massive, stockwork, and breccia veins are the dominant hosts of mineralisation. In the vertical ore interval sulphides display a textural coarsening with depth. Base metals are more dominant in the base of the ore interval and precious metals are more abundant at higher levels in ore interval. Vein textures can be used as a vector to ore. Quartz textures inherited from a silica gel usually coincide with high gold grade. Mapping the distribution of temperature clays can help to determine to zones of up flow and sites of precious metal deposition.

Acknowledgments

I would like to thank Khin Zaw and Anthony Harris for their help with this review. I would also like to thank Laijing and my fellow honours students for their help and support.

Table of Contents

Declaration	ii
Abstract	iii
Acknowledgments	iv
Table of Contents	v
List of Tables and Figures	vii
Chapter 1 Introduction	1
Chapter 2 Tectonic and Volcanic Settings	5
Chapter 3 Alteration	7
3.1 Silicic Alteration	8
3.2	11
3.3 Argillic and Phyllic Alteration	11
3.4 Advanced Argillic Alteration	12
3.5 Propylitic Alteration	13
Chapter 4 Ore Mineralogy	14
4.1 Ore	14
4.1.1 Pyrite/Textures	15
4.1.2 Chalcopyrite/Textures	15
4.1.3 Sphalerite/Textures	15
4.1.4 Galena/Textures	16
4.1.5 Electrum/Textures	16
4.2 Temporal zonation	16
Chapter 5 Form, Deposit Zonation and Vein Textures	18

5.1	Form	18
5.2	Deposit Zonation	19
5.2.1	Ore Textural Zonation	19
5.2.2	Gangue Mineral Zonation	20
5.2.3	Sulphide Zonation	21
5.3	Vein Textures	22
Chapter 6	Minerals as Geothermometers	25
Chapter 7	Conclusion	27
Chapter 8	References	27

List of Tables and Figures

Figure 1 Map of Thailand showing the location of Chatree (modified from http://www.kingsgate.com.au	2
Figure 2 Map showing the location of Chatree and Wang Yai, central Thailand. (Kromhun 2005).....	3
Figure 3 The location of A, B, C, D, E, F, H, and J prospects at Chatree.....	1
Figure 4 Distribution of alteration in low sulphidation deposits (Hedenquist 2000)....	8
Figure 5. A- Crustiform colloform banding, Chatree (Kromkhun, 2005), B- Crustiform colloform banding, Wang Yai Prospect.....	9
Figure 6 Types of orebody forms, after Hedenquist (2000).....	18
Table 1 Types of alteration assemblages in low sulphidation deposits and Chatree (modified after Hedenquist, 2000)	7
Table 2 Characteristics of silicic alteration in low sulphidation deposits and Chatree (modified after Hedenquist, 2000).	10

Chapter 1 Introduction

Lindgren (1922) was first to propose the term 'epithermal', and he allocated this term for deposits which formed from aqueous fluids charged with igneous emanations at temperatures less than 200° C and consisting of a broad range of precious metals, base metals, mercury and antimony. Since Lindgren's first description of the term epithermal there has been extensive research on the characteristics of epithermal deposits which, has lead to subdivision of epithermal deposits into high and low sulphidation end members. This literature review will focus on low sulphidation and will aim to discuss in detail some of the main characteristics of low sulphidation deposits. The Chatree deposit and Wang Yai prospect (Thailand) will be used as a reference point to explain the characteristics. Chatree and Wang Yai are located within the Loei Fold Belt in central Thailand (see Fig. 1). Chatree is a working gold mine consisting of five gold rich vein systems (A, C, D, and H) (Fig 3.). Previous work undertaken by University of Tasmania students; David Dedenczuk, Shelley Greener, and Kamonporn Kromkhun on prospects A-D, C, and H respectively (Fig 3) will be used to review the characteristics of Chatree. The Wang Yai Prospect is located approximately 15km north east of Chatree on land that is currently used for farming rice and corn. Exploration to date has consisted of surface mapping, soil geochemistry, diamond drilling and RC drilling. Based on the current exploration data, proximity to Chatree, and float vein textures the Wang Yai Prospect has been classified as a low sulphidation epithermal deposit. Previous work undertaken by the author in February 2005 will be used when referring to Wang Yai.

Topics that will be discussed in this review include tectonic and volcanic settings, alteration, ore mineralogy, deposit form, zonation, vein textures and geothermometry.

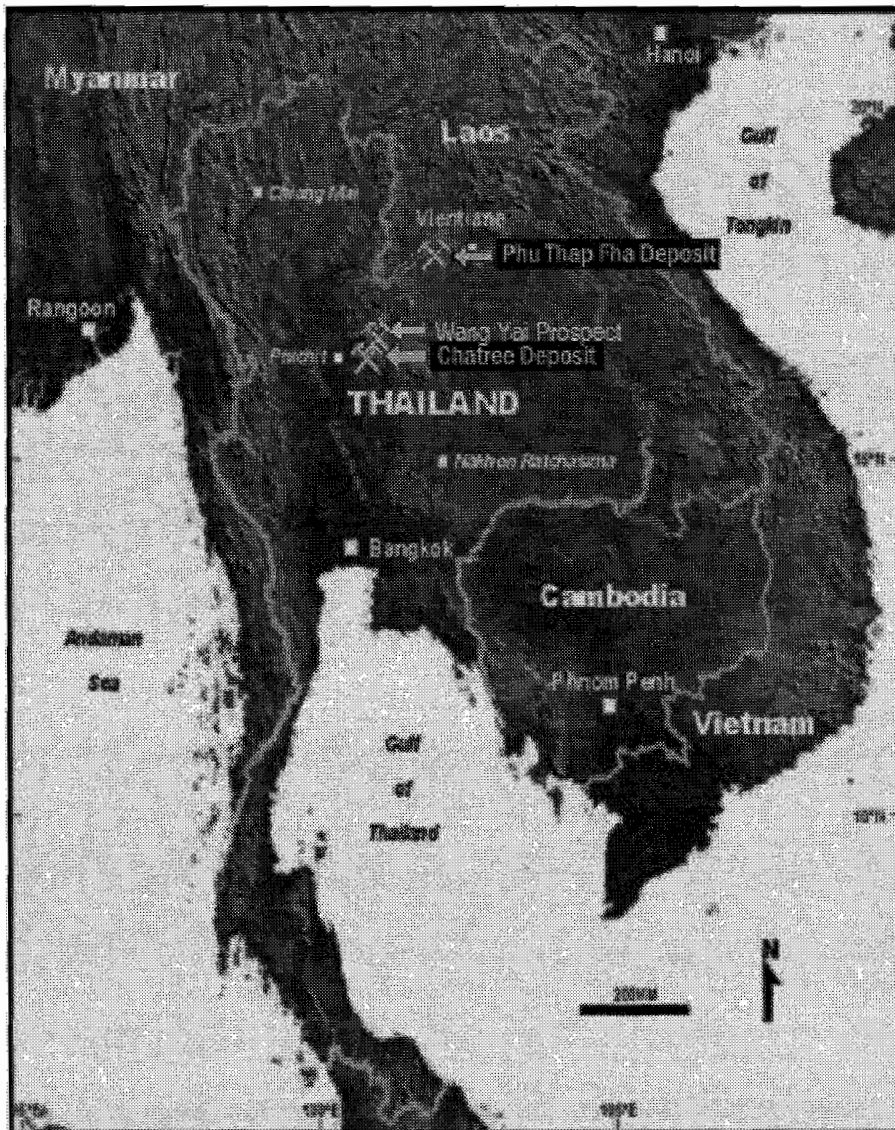


Figure 1 Map of Thailand showing the location of Chatree (modified from <http://www.kingsgate.com.au>)

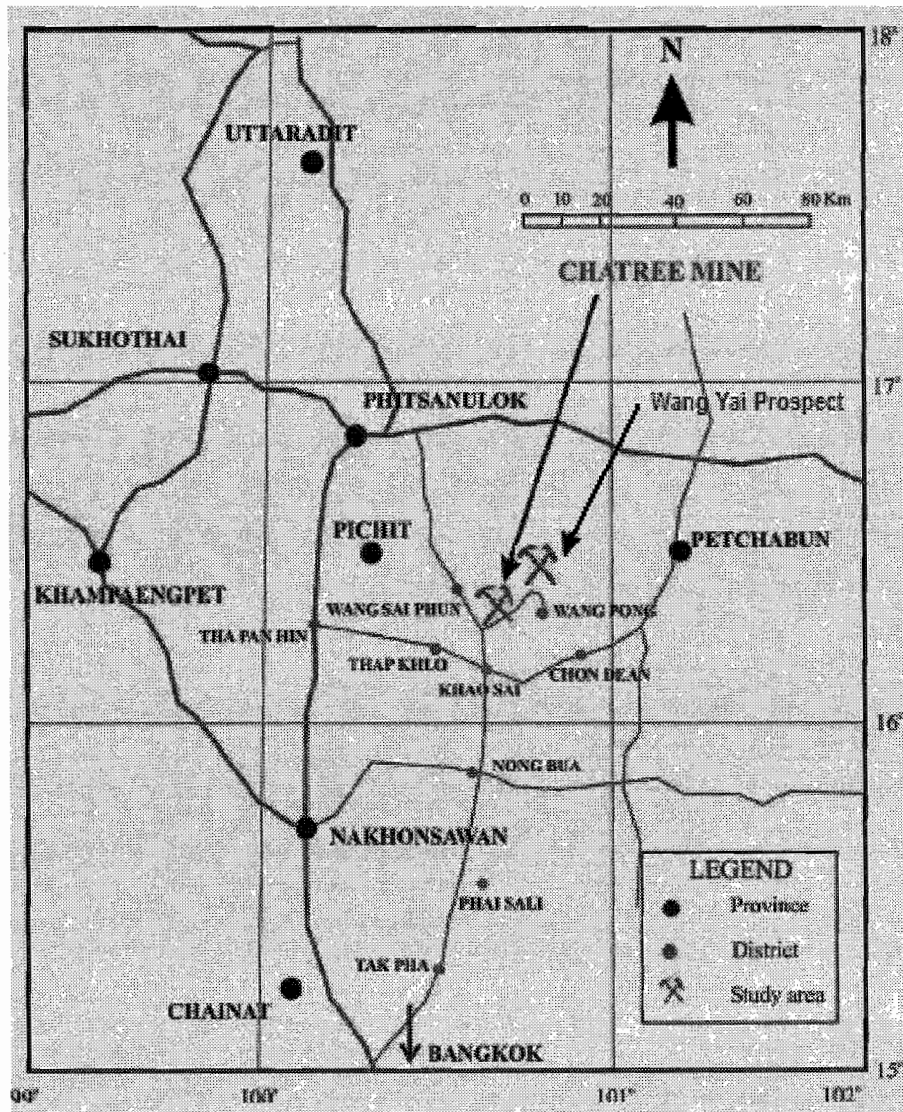


Figure 2 Map showing the location of Chatree and Wang Yai Prospect, central Thailand.
(Modified after Kromhun, 2005).

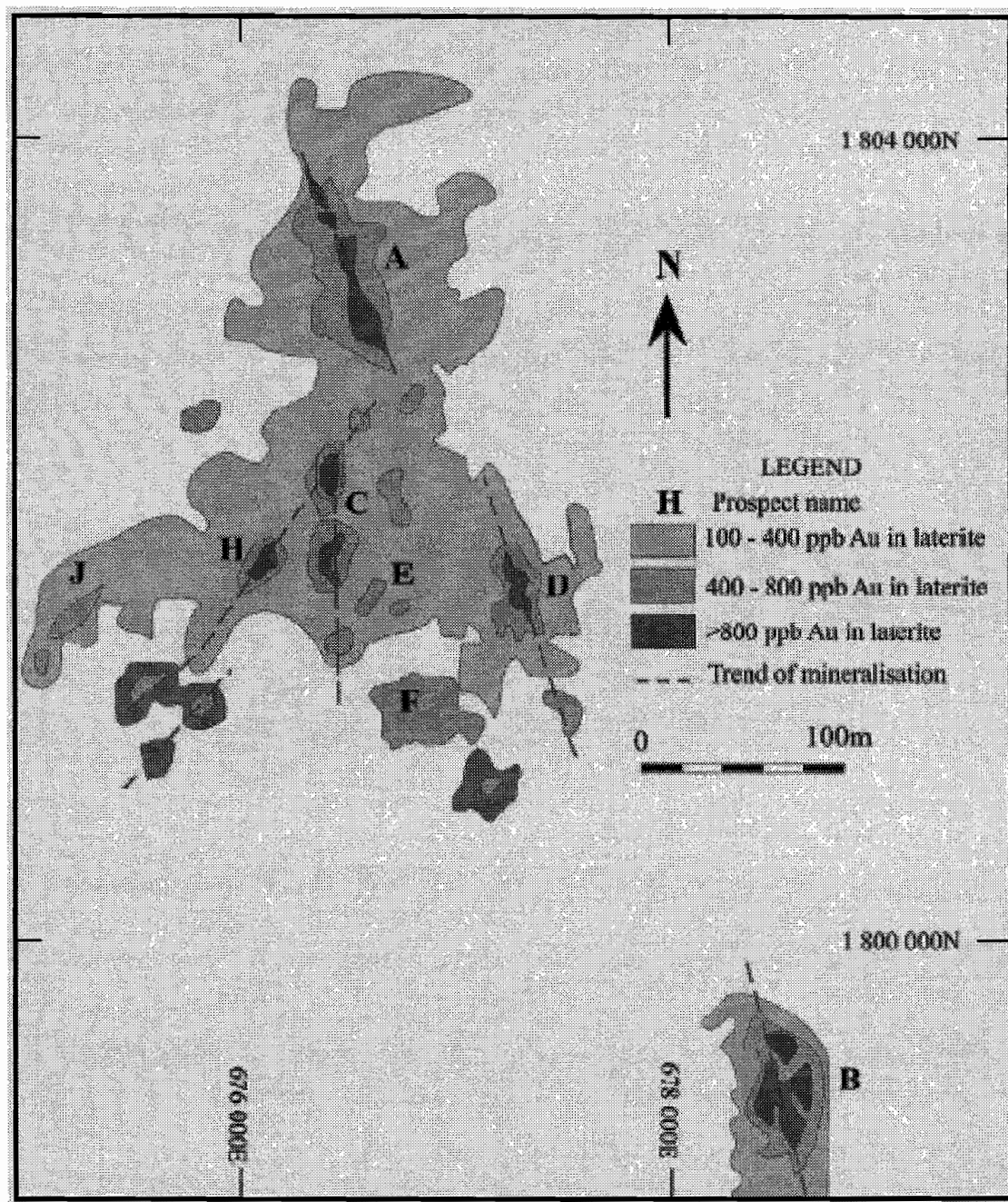


Figure 3 The location of A, B, C, D, E, F, H, and J prospects at Chatree

Chapter 2 Tectonic and Volcanic Settings

In the section below a comparison will be made between the two types of tectonic setting which epithermal environments occur. These two types of tectonic settings include subduction related island and continental arc settings (Cooke and Simmons 2000; White and Hedenquist 1995). The Chatree deposit, which was formed in an ancient island arc setting (Dedenczuk 1998) will be used as a reference point.

White et al., (1995) proposed that epithermal environments vary between island and continental arc settings, in terms of volcanic setting, depth, and type of deposits. The volcanic setting in island arcs is dominated by stratovolcanoes, as opposed to cordillera settings which dominate continental arc settings (White et al., 1995). An example of the former setting is the Chatree deposit, Thailand which is said to exhibit many of the characteristics of the stratovolcano/composite cone environment, namely thick, volcanic sequences, association with calderas, and intermediate-felsic rock compositions (Cumming 2004).

White et al., (1995) observed that epithermal deposits occurring in stratovolcanoes within island arc settings generally form at greater depths compared to deposits formed in continental arc settings. Chatree exhibits characteristics of the former. For example, although there is no record to date of the exact depth at which the Chatree deposit occurs, the presence of variable amounts of adularia, quartz rather than chalcedony, and base metals (Dedenczuk 1998) is consistent with Cainozoic, Philippine and Indonesian deposits thought to be formed at deeper depths than other epithermal deposits (White et al., 1995). At Chatree the surface exposure of vein float indicative of depths around 200-300m may suggest that if the deposit was formed at depth it is unlikely that it would be exposed at the surface. However it has been shown that the surface exposure of a deposit formed at depth is a common occurrence and is caused by the susceptibility of an overlying alteration cap to erosion (White et al., 1995). Further more, White and Hedenquist (1995) have reiterated the effect of erosion by demonstrating that rates in island arcs can be 10-20 times higher than in continental arcs.

In the study of south west Pacific epithermal deposits White et al., (1995) also found

that large epithermal deposits located in island arc settings exhibit distinct differences from smaller epithermal deposits formed in the same region. He found that large deposits displayed a transition to mesothermal conditions and a high sulphidation type alteration overprinting. In central Thailand, Chatree is the largest known epithermal deposit and is small in scale compared to the larger deposits in the Pacific. It does not display the characteristics of the larger deposits within the south west Pacific region.

Chapter 3 Alteration

Low sulphidation epithermal systems exhibit four main types of alteration including silicic, advanced argillic, argillic, propylitic and sericitic/phyllic. The types of alteration are summarised in terms of their characteristics and occurrence at Chatree Table 1. The generalised alteration distribution are shown in Fig 4.

In the section below, the types of alteration in low sulphidation deposits will be discussed. Themes that will be a focus include key minerals, spatial distribution, and significance. The Chatree deposit and other low sulphidation deposits will form a reference point. Vein stage alteration and geothermometry will be discussed in separate sections.

Alteration Type	Characteristics	Chatree	References
Silicic	Quartz veins and veinlets, silicified breccia and/or stockwork; shallow silicification, including chalcedony and/or opaline blankets; sinter	Quartz veins and veinlets, silicified breccia and stockwork, narrow silicification zones around veins	Hedenquist (2000), Kromkhun (2005)
Advanced Argillic	Kaolinite-alunite-(illite/smectite-native sulphur) \pm opaline blankets of steam-heated origin; commonly underlain by chalcedony blankets Kaolinite/halloysite-alunite-jarosite blankets or zones of supergene origin	Kaolinite \pm montmorillonite \pm pyrite \pm illite blanket of supergene origin	Hedenquist (2000), Kromkhun (2005)
Intermediate Argillic/	Illite/smectite halo to veins; illite \pm smectite halo to deeper sericitic zones		Hedenquist (2000), Kromkhun (2005)
Propylitic	Broad host to ore system, in some cases deuteric in origin and of questionable direct genetic relation to epithermal ore forming system; typically chloritic (not epidote), except at deeper levels	Epidote-chlorite-illite-quartz-carbonate-sericite-adularia	Hedenquist (2000), Kromkhun (2005)

Table 1 Types of alteration assemblages in low sulphidation deposits and Chatree (modified after Hedenquist, 2000)

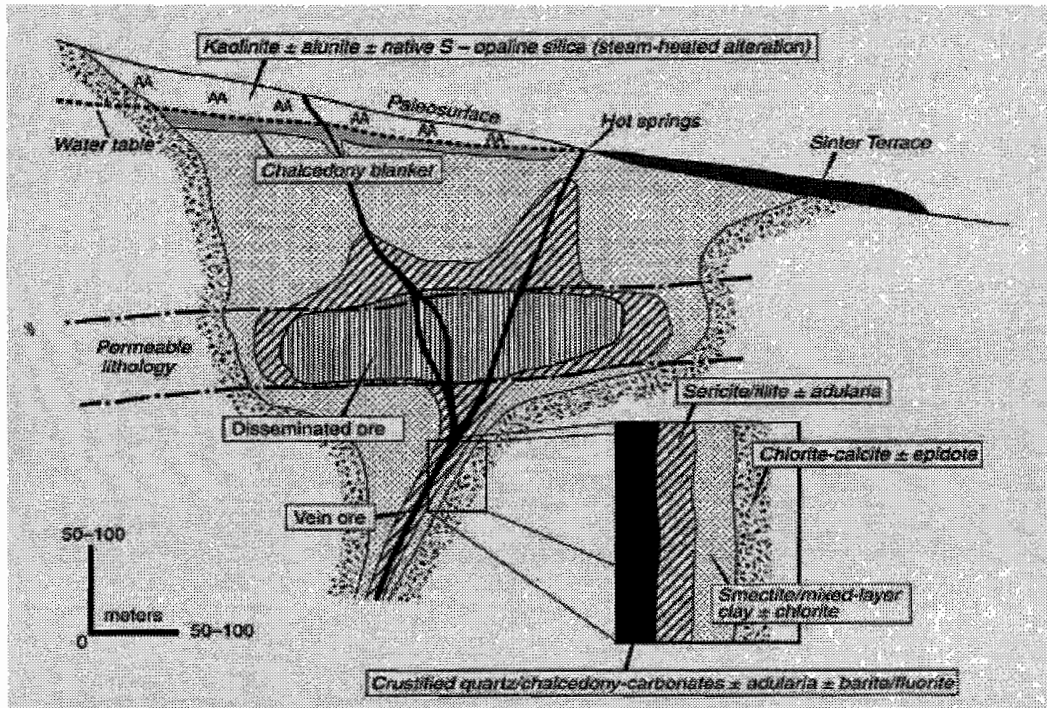


Figure 4 Distribution of alteration in low sulphidation deposits (Hedenquist 2000)

3.1 Silicic Alteration

Key minerals associated with silicic alteration include silica polymorphs (agate, chalcedony, quartz, opal), adularia, \pm albite (Buchanan 1981). At the Chatree deposit silicic alteration as defined by Kromkhun (2005) includes only the silica polymorphs (quartz and chalcedony), and for this reason only these two minerals will be considered in this section.

The formation, spatial occurrence, significance of silicic alteration together with the occurrence at Chatree is summarised in Table 2. The Chatree deposit and Wang Yai prospect share many similarities with the types of silicic alteration in Table 2. For example in zones A, D, C, and H chalcedony and quartz veins occur extensively. They generally contain fine bands of sulphides and assume textures such as cockade, colloform, and crustiform (Dedenczuk 1998; Greener 1999; Kromkhun 2005). The formation of these textures is likely to signify fluid conditions which are super

saturated in respect to amorphous silica and have undergone rapid cooling at temperatures $<180^{\circ}\text{C}$ (Simmons and Browne 2000). The factors said to be responsible for rapid cooling include decompressional boiling, mixing of different waters, pH changes, and the reaction of the solution with volcanic glass (Fournier 1985).

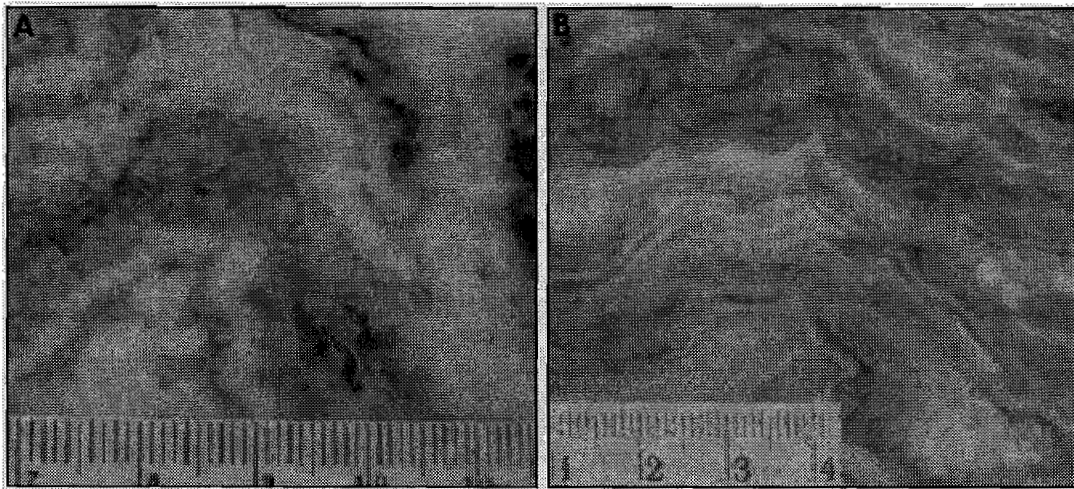


Figure 5. A- Crustiform colloform banding, Chatree (Kromkhun, 2005), B- Crustiform colloform banding, Wang Yai Prospect.

Silicification of wallrock is another type of silicic alteration observed at the Chatree deposit. Silicification at Chatree is generally vertically extensive and occurs as restricted silicified halos around major vein stages. The type of silicification observed at Chatree is common to many other epithermal districts. For example narrow, silicified, centimetre-scale halos around veins at prospect D (Dedenczuk 1998) are also a characteristic of the Victoria and Acupan deposits, Philippines (Claveria et al., 1999; Cooke and McPhail 2001). The abundance of silicification around the main ore zone in H zone at Chatree (Kromkhun 2005) is consistent with the thick silicified selvages forming around the ore horizons in North American deposits (Buchanan 1981). The degree of silicification at Chatree slightly varies between each zone. However, it is unlikely that the slight variation in the extent of silicification at zones A, D, C, and H, signifies anything of great importance and may just be a result of variation in reactivity of host rocks as well as changes in porosity and permeability (Cooke and Simmons 2000). Use of silicification as a vector to ore is negligible due the wide stability range of silica and the narrow zones of silicification.

Type	Formation	Where	Significance	Chatree	References
Sinter	Near-neutral pH hot springs	Only at surface	Paleosurface, topographic (hydrologic) depression, focus of upflow	Sinter is absent or has been eroded	Hedenquist (2000)
Residual silica (opaline)	Moderate leaching, pH 2-3, 80-90% SiO ₂	Vadose zone	Steam-heated origin, above paleowater table	Residual silica has not been observed	Hedenquist (2000)
Chalcedony horizon	Silica remobilized from steam-heated zone; deep fluid may contribute to outflow	At water table, up to 1-2+km from source	Paleowater table, maybe distal from source	Chalcedony horizon is absent in Chatree	Hedenquist (2000)
Chalcedony veins, colloform bands; crypto-crystalline veins	From low-T fluid, colloids; recrystallized from gel	Shallow depth, <150m	<200°C, rapidly cooling fluid, boiling at depth; cryptocrystalline at <200°C	Crustiform, colloform, cockade, breccia, comb	Dedenczuk (1998), Greener (1999), Hedenquist (2000), Kromkhun (2005)
Quartz veins, vugs	From cooling solution	>150m	>200°C	Vuggy textures in H zone, quartz veins in D and C zones	Dedenczuk (1998), Greener (1999), Hedenquist (2000), Kromkhun (2005)
Silicification	From cooling water	Surface to 500m, massive <150m	Shallow portion of system, pervasive flow	Developed around quartz veins, within, and below the ore zone.	Dedenczuk (1998), Greener (1999), Hedenquist (2000), Kromkhun (2005)

Table 2 Characteristics of silicic alteration in low sulphidation deposits and Chatree (modified after Hedenquist, 2000).

3.2 Argillic and Phyllic Alteration

The nature and mineralogy of argillic and phyllic alteration zones is highly variable between epithermal deposits and depends largely on the temperatures and fluid compositions (Silberman and Berger 1985). The key minerals making up the argillic alteration assemblage include, illite, interstratified illite/smectite, smectite, kaolinite and siderite (Hedenquist 2000). The key minerals at Chatree conform to this classification and include illite, smectite-(montmorillite), pyrite, and kaolinite (Dedenczuk 1998; Greener 1999; Kromkhun 2005). Phyllic alteration has been observed to occur at H zone and includes illite, illite-smectite and sericite.

Argillic alteration usually occurs as narrow halos between the silicic and propylitic alteration zones, the width of the zones relates to the degree of permeability within the host rocks (Hedenquist 2000). In the H zone, Kromkhun (2005) has recognised that argillic alteration is most dominant as replacement in permeable zones above ore, and illite, smectite-illite decrease with distance away from mineralization a feature which has also been observed at Broadlands Ohaaki, New Zealand and Cikidang, Indonesia (Simmons and Browne 2000; Rosana and Matsueda 2002). Zones D and C display a similar blanket of argillic alteration to H but do not display any clear zonation of clays around the vein margins. It has been noted that zone C does contain higher concentrations of illite than D (Dedenczuk 1998; Greener 1999).

According to Hedenquist (2000) argillic alteration assemblages are likely to have been generated by CO₂ rich steam water with a mild acidity (pH4-5) (Simmons and Browne (2000). At Chatree it has not been confirmed whether the key minerals which make up argillic alteration are in fact related to hydrothermal alteration or weathering. However, where adularia is present a hydrothermal origin is likely (Dedenczuk 1998). In the H zone a blanket of alteration overlying the ore zone is likely to be a product of weathering. Analysis using XRD may help to substantiate whether it is a product of steam heated waters.

3.3 Advanced Argillic Alteration

Advanced Argillic alteration is a stage which is not typically related to ore and generally occurs as a steam heated overprint in the vadose zone of epithermal environments (Fig 4). The key minerals occurring in advanced argillic alteration include, opal-cristobalite, kaolinite, smectite, and alunite (Hedenquist 2000). At Chatree a well developed advanced argillic alteration is not present, but it has been reported that in the shallow parts of H, C, A and D zones a overprinting from a low pH fluid has occurred (Dedenczuk 1998; Greener 1999; Kromkhun 2005)

In low sulphidation deposits advanced argillic alteration is commonly found in the hanging wall above the ore zones; it is also common for this alteration to overprint ore related assemblages at depth (Hedenquist 2000). The spatial distribution of intermediate argillic alteration at levels above the ore at Chatree is consistent with that seen from other deposits. For example, at Bulldog Mountain vein system in Creede, Colorado veins are capped by irregular zones of illite-smectite alteration with minor kaolinite (Plumlee and Whitehouseveaux 1994) and at Comstock, Nevada a blanket of advanced argillic alteration occurs peripheral to the ore zone (Hudson 2003), similarly at McLaughlin, an advanced argillic cap is also know to occur (Sherlock et al., 1995).

A key to understanding advanced argillic alteration in low sulphidation deposits is to first define the origin of acid waters, which can be from steam heated waters at or near the surface, or post mineral weathering of sulphide minerals (White and Hedenquist 1995). For the Chatree deposit it has not been confirmed whether the kaolinite dominated overprint is a result of steam heated waters or supergene weathering, although Greener (1999) has confirmed that in C zone the upper kaolinite is a result of weathering. If alteration was a result of steam heated waters then it is likely that blankets of intense silicification could form at the water table level (Hedenquist 2000), this however has not been observed at Chatree.

3.4 Propylitic Alteration

Propylitic alteration is considered by Buchanan (1981) to be a wide spread assemblage commonly forming halos of hundreds of meters around vein zones and usually it is considered to be post-ore. Key minerals making up the assemblage include chlorite, pyrite, carbonate, montmorillonite, illite, and epidote-(deeper levels), (Buchanan 1981). In zones A, C, D, and H at the Chatree deposit, propylitic alteration assemblages have been said to include chlorite, epidote, prehnite, sericite, quartz, albite, carbonates, pyrite, and hematite (Greener 1999; Kromkhun 2005).

In the model of alteration proposed by Buchanan (1981), the propylitic alteration forms an extensive halo surrounding the alteration phases associated with veins, and epidote increases with depth and alteration is typically pre-ore. The propylitic alteration at Chatree shares similarities with Buchanan model. For example Kromkhun (2005) has observed extensive propylitic alteration below the ore zone and an increase in abundance of epidote at depth, and Greener (1999) states that propylitic alteration overprints all other alteration assemblages.

Chapter 4 Ore Mineralogy

Variables such as pressure, hydrostatic conditions, differences in permeability make epithermal low sulphidation deposits extremely variable in their form, structure and mineralogy (Hedenquist et al., 1996). Despite highly variable mineral assemblages within and between deposits around the world, there is, however specific gangue and ore mineral assemblages that occur ubiquitously throughout most deposits. These mineral assemblages with the exception of steam heated overprints reflect the deposition from near neutral pH low-salinity water (Cooke and Simmons 2000).

In the section below the dominant sulphides that occur within deposit ore zones will be listed together with the textures they assume and also the associations they have with other sulphides. For the scope of this study only the sulphides occurring at the Chatree deposit, Thailand will be discussed. Examples of deposits sharing similar properties will also be given. The significance and zonation of sulphides with deposits will be discussed as a separate section below.

4.1 Ore

Ore assemblages in low sulphidation deposits around the world can generally be subdivided into silver rich ores and gold rich ores (Heald et al., 1987). Hedenquist (2000) describes sulphide assemblages occurring in end member low sulphidation deposits to comprise of pyrite-pyrrhotite-arsenopyrite and Fe-rich sphalerite. Intermediate sulphidation deposits contain higher quantities (>20% sulphides) including (Fe-rich) sphalerite, galena, tetrahedrite-tennantite, chalcopyrite and pyrite (Gemmell 2004). Generally intermediate deposits contain higher quantities of base metals. They display high Ag:Au ratios which reflect the abundance of native silver, silver sulphides and silver sulfosalts (Heald et al., 1987). Examples include; Creede, Kelian, Comstock, Fresnillo District, and Victoria. Typical low sulphidation deposits exhibit lower proportions of base metals, higher amounts of precious metals and high Au:Ag ratios. Examples include Hisikari, Round Mountain, and McLaughlin.

The dominant ore minerals at the Chatree deposit, Thailand consist, of pyrite,

chalcopyrite, sphalerite, galena, marcasite and electrum (Dedenczuk 1998; Greener 1999; Kromkhun 2005). This type of ore assemblage has been reported for a number of low sulphidation deposits such as Waihi, Kelian, Mt Muro, Creede, and Victoria. At these deposits minor amounts of acanthite-(Waihi), pyrrhotite, arsenopyrite, tetrahedrite-(Kelian), covellite-(Mt Muro), pyrargite-(Creede), have also been reported (Brathwaite and Faure 2002; Davies et al., 2004; Plumlee 1994; Sajona et al., 2002).

4.1.1 Pyrite/Textures

Pyrite is a ubiquitous mineral in low sulphidation deposits occurring during both alteration and mineralization stages. Pyrite in prospects A, D, C, and H at Chatree occurs in mineralized sections and disseminations within the wall rock. In mineralized sections it occurs as free grains and commonly contains inclusions of sphalerite, galena and electrum (Dedenczuk 1998; Greener 1999; Kromkhun 2005).

4.1.2 Chalcopyrite/Textures

Chalcopyrite is a mineral which occurs in low sulphidation deposits in a variety of forms. It is contemporaneous with, base metals and precious metals such sphalerite, galena and electrum at levels between 300-800m (Hedenquist 2000). In the vein stages at Chatree, chalcopyrite occurs as free grains or as sulphide polymineralic aggregates (Dedenczuk 1998). Dedenczuk notes the highest gold assay in 'A' is associated with a high concentration of chalcopyrite. Intimate relationships between chalcopyrite and electrum have also been observed in other deposits. At Waihi there is a correlation with the fine grain size of chalcopyrite and high concentrations of electrum (Brathwaite and Faure 2002), at Victoria, Philippines electrum preferentially occurs with chalcopyrite rather than with sphalerite and galena (Claveria 2001). Electrums association with the chalcopyrite phase seems to be restricted to the A and D zones, for it has not been observed in C and H.

4.1.3 Sphalerite/Textures

Sphalerite is the second most common sulphide observed at Chatree (Dedenczuk 1998). It occurs predominantly as free grains and polymineralic sulphide aggregates

in quartz gangue (Dedenczuk 1998). In all the zones at Chatree the Fe content of sphalerite is moderate to low. Hedenquist (2000) suggests that this is a common characteristic of intermediate sulphidation deposits. In all zones the sphalerite also exhibits chalcopyrite disease (Kromkhun 2005) and she has attributed this to the replacement of sphalerite by chalcopyrite at cool temperatures. At Creede the replacement of sphalerite by chalcopyrite has been attributed to the reaction with late stage Cu-Sb bearing fluids (Plumlee and Whitehouseveaux 1994).

4.1.4 Galena/Textures

In low sulphidation deposits the abundance of galena generally increases with depth (Hedenquist 2000). At Chatree galena is the rarest sulphide occurring as fine free grains, on the margins of pyrite, or within pyrite. It is also intimately associated with electrum (Dedenczuk 1998; Greener 1999; Kromkhun 2005). The abundance of galena does not increase with depth.

4.1.5 Electrum/Textures

At Chatree gold occurs as electrum. The electrum exhibits silver rich rims, and it often forms at the rims of pyrite or within pyrite or quartz (Diemar and Diemar 1999). Electrum in zones A, D, C and H tends to preferentially occur within microcrystalline quartz (Dedenczuk 1998). Greener (1999) noted that the silver content of electrum in C-zone is higher than A and D zones.

4.2 Temporal zonation

Constructing temporal relationships for pyrite, chalcopyrite, sphalerite, galena and electrum can be quite problematic owing to the large complexity and variability in the form, textures and vein stages of low sulphidation deposits. Dedenczuk (1998) has attempted to construct a paragenesis based on sulphide textural relationships at zones A and D at Chatree. Dedenczuk (1998) proposed that pyrite is the youngest and has precipitated through all stages; sphalerite is younger than galena and electrum, and chalcopyrite is the latest to form being later than pyrite and electrum and galena. He also notes that sphalerite, galena and electrum are said to be co-depositional with

quartz as they are restricted to quartz vein stages.

The above paragenesis is quite similar to the one constructed for the H zone. The differences are that in the H zone electrum is the last stage to form (Kromkhun 2005). Comparing the temporal relationships of key sulphides in Chatree to other deposits possesses extreme difficulty. There is no consistency of sulphides forming at specific times with specific minerals. Most of the key sulphides do however follow a general trend of occurring contemporaneous with electrum and in some cases electrum will occur adjacent or preferentially with certain sulphides. Claveria (2001) notes that at Victoria, Philippines electrum occurs contemporaneous with chalcopyrite, galena and sphalerite and that gold-rich electrum is associated with galena and sphalerite, and silver rich electrum is more associated with chalcopyrite. At Waihi, electrum also occurs contemporaneous with chalcopyrite, galena and sphalerite but occurs preferentially with chalcopyrite rather than sphalerite and galena (Brathwaite and Faure 2002).

Chapter 5 Form, Deposit Zonation and Vein Textures

Textures

5.1 Form

Ore deposition within epithermal deposits occurs in a variety of forms including disseminated, stockwork or vein style (Hedenquist 2000). Most epithermal deposits do not strictly conform to one particular style but comprise of a variety of forms ultimately reflecting the dynamic lithological, structural and hydrothermal controls (Fig. 6). For example at Comstock, Nevada sulphides occur within massive and stockwork veins and as disseminations within the wall rock (Hudson 2003), similarly at the Real de Angeles Deposit, Mexico one third of the mineralization occurs as disseminated zones between siltstone and sandstone horizons, whilst two thirds occur in veins (Pearson et al., 1988). Mineralisation at Chatree also occurs in a variety of forms, namely vein breccias and stock work veins.

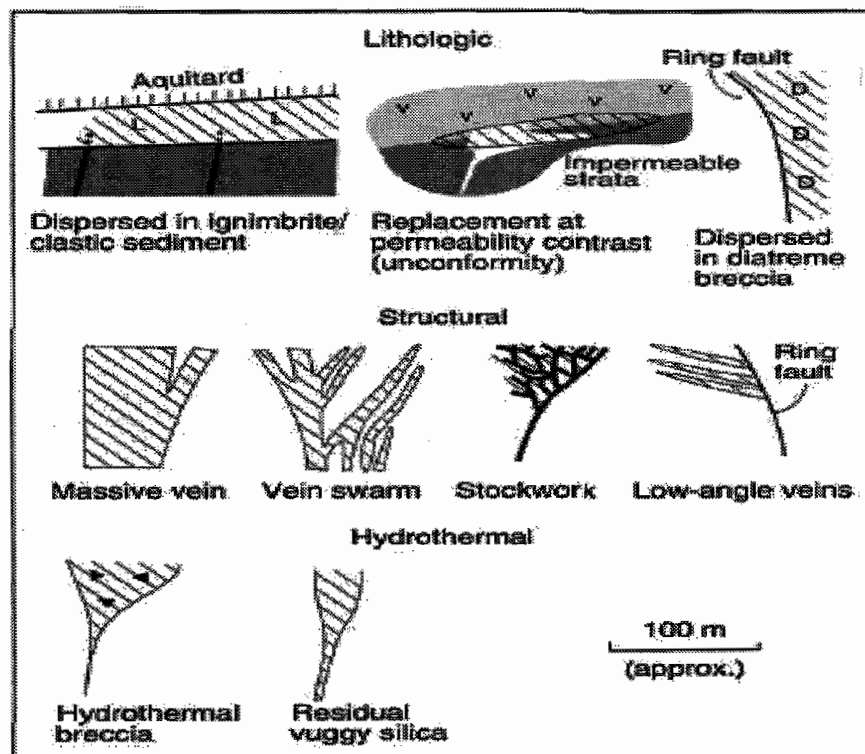


Figure 6 Types of orebody forms, after Hedenquist (2000)

5.2 Deposit Zonation

Most hydrothermal minerals are stable over a limited range of temperatures and/or pH ranges, therefore the distribution of alteration minerals allows the thermal and geochemical zonation within low sulphidation deposits to be reconstructed (Hedenquist et al., 1996). The ore associated with low-sulphidation deposits is produced by near-neutral pH thermal waters, with temperature decreasing both with decreasing depth and distance from fluid conduits (White and Hedenquist 1995). Depth related zonation patterns of mineralisation styles, alteration, gangue, and sulphide mineralogy are clearly evident in low-sulphidation deposits and these will form the major themes in this section. Recently, Hedenquist (2000) has outlined characteristics of low-sulphidation deposits as a function of depth, by drawing on the previous work of Lindgren, Buchanan, Heald, Sillitoe, White, and John. This will form the main reference point in this section. Specific examples from deposits such as Waihi, Golden Cross, Creede, Hishikari, Cracow, Pajingo, and Chatree will be used.

5.2.1 Ore Textural Zonation

Ore textures in and between epithermal deposits are highly variable in nature and form, ore textures in some deposits do however share a common trend of displaying a zonation from shallow levels to deeper levels. This variation has been described by Hedenquist (2000) to include textures typical at shallow depths (0-300m) and textures which are common at greater depths (300-800m). At shallow depths (0-300m) ore textures assume a combination of fine bands, combs and crustiform breccias. These textures are observed at shallow forming deposits including Hishikari, Waihi, Golden Cross, Pajingo and Cracow. One particular characteristic of the ore at these deposits is the formation of thin fine-grained dark sulphide bands known texturally as 'ginguro' ore, Fig 7. Ginguro ore is also known to occur at Chatree (Corbett 2002), and at the Wang Yai Prospect, Thailand. With increasing depths sulphide bands tend to become increasingly coarse grained (Hedenquist 2000). For example coarse-grained electrum-poor ore at Waihi, New Zealand has been observed to occur at depth and is found to grade to finer, more sulphide-electrum rich bands higher in the system

(Brathwaite and Faure 2002).

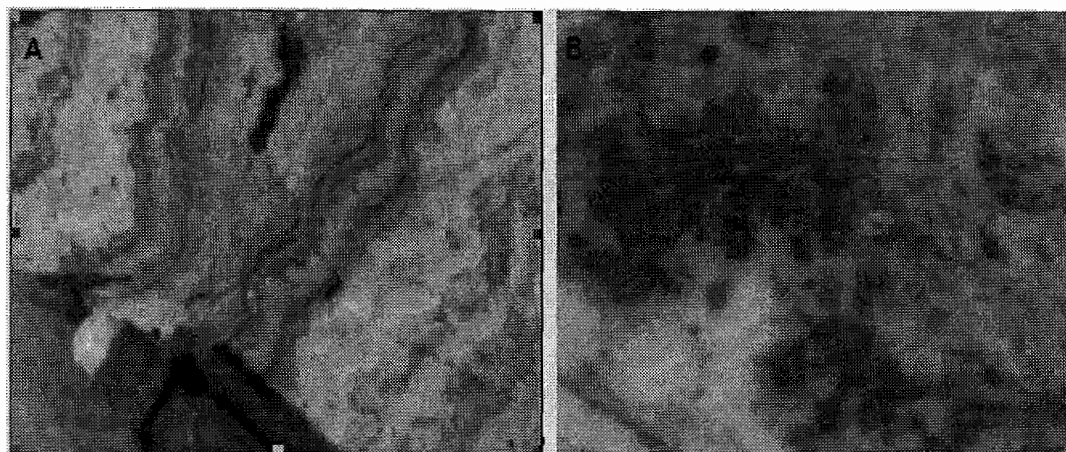


Figure 7. Photos of Ginguero ore. A. Ginguero bands in quartz crustiform colloform veins Hishikari, Japan (Corbett 2002). B. Ginguero bands within a chalcedonic vein Wang Yai Prospect, Thailand.

5.2.2 Gangue Mineral Zonation

This section will be made on gangue mineral zonation within the main vein stages of low sulphidation deposits. The gangue mineral zonation in the Chatree deposit will be a major focus, and a comparison between Chatree and other deposits will be made.

Common vein stage gangue minerals in low sulphidation deposits include quartz, chalcedony, calcite, adularia, illite and barite (White and Hedenquist 1995). They display a vertical zonation within the veins and therefore can be used to help determine the position in a epithermal system (Buchanan 1981). Chalcedony-adularia-illite-calcite assemblages are characteristic at shallow depths (0-300m) whilst quartz-carbonate-rhodonite-sericite-adularia \pm barite \pm anhydrite \pm hematite \pm chlorite are more common at depths of (300-800m) Hedenquist (2000).

Quartz is the most dominant gangue mineral in hydrothermal systems (Dong et al., 1995). The textures assumed by quartz display a vertical zonation, which can be used to give information on crystallization conditions, paleo-isotherms and proximity to ore. At high levels in a system the precipitation of opal or amorphous silica is a common occurrence and is indicative of temperatures of about 150° C. At deeper levels opal gives way to chalcedony indicating temperatures between 100-190° C.

Chalcedony gives way to crystalline quartz at the deeper levels indicating a temperature of 180°-190° C (Hedenquist 2000).

Adularia is a common gangue mineral in low sulphidation deposits often occurring in abundance throughout the vertical extent of a deposit. The morphology and textures assumed by adularia are proportional to temperature and pressure, therefore the zonation of textures can give information on the crystallization and thermal history (Dong and Morrison 1995). A study of the morphology of adularia in Queensland deposits has proposed that sub-rhombic crystals are indicative of formation at deep levels under slow crystallisation, very small rhombic crystals occur within crustiform, colloform banding, tabular crystals occur on the onset of rapid boiling, and pseudoacicular crystals are pseudomorphs of carbonate precursors (Dong and Morrison 1995).

Adularia is relatively widespread in deposits due to its relatively temperature insensitivity (White and Hedenquist 1995), however there are instances whereby adularia is found to be zoned within a deposit. For example Dong and Zhou (1996) have noted that adularia at Cracow, Queensland is widespread but is richest within the ore zone and Buchanan (1981) has noted that below the precious metal zone the abundance of adularia often decreases with increasing depth. The abundance of adularia within the ore zone is likely to indicate the presence of a boiling, low salinity, near neutral fluid (Cooke and Simmons 2000).

5.2.3 Sulphide Zonation

Buchanan (1981) showed that sulphides within the vertical interval of ore are zoned. He states that precious metal ore has an average restricted vertical interval of 350m, and below this level the base of precious metals values of galena, pyrite, sphalerite, and chalcopryrite increase. Base metals occurring below the level of precious metals have been reported in a variety of deposits. At Acupan Cooke and McPhail (2001) reported chalcopryrite, galena and sphalerite increasing in abundance at depth. Similarly at Coromandel Braithwaite and Christie (2000) noted high base metal assemblages occurring at depth. Also, at Creede gold and silver are more abundant at high elevations than base metals Heald et al., (1987), and at Pajingo precious metal

zones high in the vertical ore interval grade into base metal rich zones at depth (Bobis et al., 1995).

It is common in many districts to have levels where base metals and precious metals occur within a mixed layer. Buchanan (1981) proposes that this level marks the upper zone of base metals and lower zone of precious metals and is indicative of the zone of boiling. Examples of base metals and precious occurring together are common in the literature. At Kelian for example, gold is intimately associated with sphalerite, galena, pyrite and arsenopyrite (Davies et al., 2004). Similarly at Chatree base metal sulphides such as sphalerite, galena, and chalcopyrite occur intimately with electrum in polyminerale aggregates (Dedenczuk 1998). If this zone is indicative of boiling then there should be features related to boiling within this level. Evidence of boiling at Chatree is present in the form of abundant adularia and calcite, fluid inclusions and sulfur isotopes (Dedenczuk 1998).

Identification of distinct metal zonation within the Chatree deposit has been difficult due to the limited vertical extent of investigation. Greener (1999) investigated a interval of 110m and found no obvious vertical or horizontal zonation of base and precious metals. However this is not to say that the deposit does not contain a zonation typical of other low sulphidation districts. It is likely that an interval of 110m represents only a third of the average 350m vertical ore zone proposed by Buchanan (1981).

5.3 Vein Textures

In epithermal environments the morphology and textures of veins and minerals are highly variable in and between deposits. The occurrence of quartz is however consistent in all epithermal environments and commonly forms the major gangue mineral. For this reason, the study of vein quartz has been given much attention over recent years, especially by the work of Greg Morrison who has developed a classification scheme of epithermal textures and also a model comprising of seven different textural zones within the vertical extent of a typical low sulphidation deposit. The application of Morrison's work is widespread throughout the literature and we be drawn on heavily in this section.

At Chatree, Dedenczuk (1998) and Greener (1999) have reported crustiform, colloform, and cockade textures in quartz veins. Both authors have not observed a vertical zonation within the veins but do however note that precious and base metal ore preferentially occur as contemporaneous polymineralic sulphide aggregates within crustiform-colloform bands. Within the crustiform-colloform bands Dedenczuk (1998) found that the micro-crystalline quartz bands carry the highest ore concentrations. This feature has also been observed at the Golden Cross deposit, New Zealand (Simmons et al., 2000). Dedenczuk (1998) also noted that fine grained pyrite in prospect A assumes a colloform texture within micro-crystalline bands. Similarly this texture has also been observed in the bonanza ores at the Sleeper Deposit, Nevada (Saunders 1994).

The crustiform colloform textures assumed at the Chatree deposit can give information on the formation and fluid characteristics. Fournier (1985) states that colloform textures form from a silica gel precursor and therefore the fluid must be at low temperatures and high degrees of silica super saturation with respect to quartz. The crustiform textures can form from any process which causes a change in fluid conditions, namely cooling, mixing, boiling, and pressure release (Buchanan 1981). Further more Saunders (1994) highlights that micro-crystalline quartz generally represents an advanced stage of opal recrystallisation and sulphidic colloform textures may occur due to cooling from a subsequent pressure drop.

Using the quartz texture classification scheme proposed by Morrison, the level at which the Chatree ore zone is likely to occur is within the crustiform-colloform zone. According to the model proposed by Buchanan (1981) this zone also coincides with the level at which precious metal horizon occurs.

Certain types of quartz textures can be favourable to the precipitation of gold and therefore can be used as a vector to ore. Dong and Morrison (1995) showed a strong relationship between the silica textures indicative of boiling and high precious metal concentrations. They found that textures such as vein brecciation, moss and needle adularia, moss quartz, and pronounced crustiform-colloform banding usually correspond to high gold grades. Quartz textures inherited from a silica gel (ghost-sphere, flamboyant, and pseudoacicular) have also been found to correlate with high

gold concentrations (Dong et al., 1995).

Chapter 6 Minerals as Geothermometers

Many epithermal minerals are stable over a limited range of temperatures and pH's (Hedenquist et al., 1996). Determining the distribution of temperature sensitive minerals can give information on the geochemical zonation, paleo-isotherms and fluid flow direction in an epithermal system. For any deposit, the establishment of paleo-isotherms is of particular importance as they can give information on the direction of fluid flow, which in turn can be used to define fluid upflow zones and sites of metal precipitation. In deposits such as Round Mountain and Hishikari, clays have been used successfully to map paleo-isotherms to identify the centre and direction of fluid flow eg (Hedenquist et al., 1996).

Knowledge of the stability range of hydrothermal minerals in epithermal systems is of paramount importance when mapping paleo-isotherms. Reye (1990) used neutral pH Philippine geothermal systems to divide the alteration mineralogy into four zones and two sub zones. The four main zones consist of smectite, smectite-illite, illite and biotite, the two sub zones include calc silicates; epidote and amphibole (Fig 8).

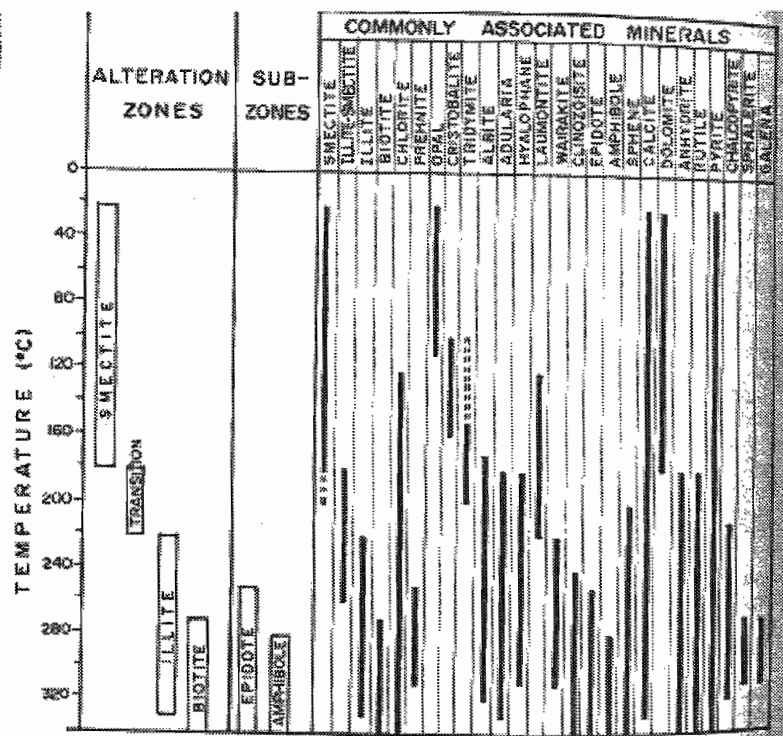


Figure 8 Stability Temperatures for minerals in Philippine geothermal systems (Reyes 1990)

At Chatree, PIMA and XRD was used in the identification of temperature sensitive clays. Dedenczuk (1998) and Greener (1999) showed that illite and smectite were the dominant clays in prospects A, D and C. According to Reyes (1990) this assemblage would place Chatree in the transition zone, thus indicating a temperature range of around 160-240° C. The crystallinity of illite has been used successfully as a vector to ore in some deposits. At Kelian, Indonesia the crystallinity of illite was found to increase with high gold grade (Davies et al., 2004). At Chatree, the crystallinity of illite did not show any relationship with gold grade so its use as a vector to ore is negligible. Greener (1999) did however note that the occurrence of illite is slightly more abundant in C-zone, than in A and D zones which may indicate lower formation temperatures for A and D zones. However, the accuracy of PIMA as a tool for determining paleo-isotherms is questionable. Dedenczuk (1998) reports of inconsistencies in the geothermometry data, and Greener (1999) describes the possibility of a masking effect imposed on clays by the younger intrusives. Further more changes in geometry, and or positioning of heat sources with time and sealing of permeable zones cause changes to alteration assemblages (Silberman and Berger 1985). If however, paleotemperatures are infact low, then it would be likely that some of the ore interval could potentially lie at depth, conversely if temperatures were found to be high it is likely that epithermal ore lies above and has been eroded.

Chapter 7 Conclusion

The Chatree deposit shares many of the characteristics of low sulphidation epithermal deposits found in stratovolcano settings within island arc tectonic environments. The alteration assemblages observed at Chatree are consistent with assemblages that occur in other low sulphidation deposits around the world. Ore mineralogy at Chatree is similar to the type of assemblages reported for a number of low sulphidation deposits including Waihi, Kelian, Mt Muro, Creede, and Victoria. The 'ginguro' ore textures are similar to those found in Japan, North America, and Australia. Crustiform, colloform, cockade vein textures indicate that the Chatree deposit lies within the precious metal zone of Buchanan's 1981 model. The use of temperature sensitive clays at Chatree has had mixed results. Illite, smectite, and inter-layered illite-smectite are known to occur. Their use as a vector to ore has not been successful due to the limited data sets and lack of analysis such as XRD to confirm PIMA results.

Many difficulties arise when trying to define a zonal variation within a small deposit such as Chatree. The vertical extent of the study area is commonly 100-200 metres and probably too narrow to display a consistent variation of sulphides, vein textures, and alteration between the different zones. There is however potential for further studies to be undertaken with regard to the lateral variation within the deposit. When further knowledge is gathered on the other peripheral zones B, J, and F (Fig 3) a greater lateral extent will be covered and will give a better representation of the deposit. On a broader scale, the current investigation into the Wang Yai prospect by the author is aimed at determining whether these two deposits are part of the same system, and if they are how do they differ

References

- Bobis, R. E., Jaireth, G., Morrison, G. (1995). "The Anatomy of a Carboniferous Epithermal Ore shoot at Pajingo, Queensland: Setting, Zoning, Alteration, and Fluid Conditions." Economic Geology **90**: 1776-1798.
- Brathwaite, R. L. and Christie A.B. (2000). "Deposit types and paleo-depth extents of Coromandel epithermal Au-Ag deposits." New Zealand Minerals and Mining Conference Proceedings **29-31**.
- Brathwaite, R. L. and Faure, K. (2002). "The Waihi epithermal gold-silver-base metal sulfide-quartz vein system, New Zealand: Temperature and salinity controls on electrum and sulfide deposition." Economic Geology **97**(2): 269-290.
- Buchanan, L. J., (1981). "Precious metal deposits associated with volcanic environments in the southwest." Arizona Geological Society Digest **14**(Relations of Tectonics to Ore Deposits in the Southern Cordillera): 237-262.
- Claveria, R. J. R., (2001). "Mineral paragenesis of the Lepanto copper and gold and the Victoria gold deposits, Mankayan Mineral District, Philippines." Resource Geology **51**(2): 97-106.
- Claveria, R. J. R., Cuisson, A.G., Andam, B.V., (1999). "The Victoria Gold Deposit in the Mankayan Mineral District, Luzon, Philippines." PacRim '99, Bali, Indonesia 10-13 October, Proceedings: 73-80.
- Cooke, D. R., and McPhail, D. C., (2001). "Epithermal Au-Ag-Te Mineralisation, Acupan, Baguio District, Philippines: Numerical Simulations of Mineral Deposition." Economic Geology **96**: 109-131.
- Cooke, D. R. and S. F. Simmons (2000). "Characteristics and Genesis of Epithermal Gold Deposits." Reviews in Economic Geology **13**(Gold in 2000): 221-244.
- Corbett, G. (2002). "Epithermal Gold for Explorationists." The Australian Institute of Geoscientists, 2002 (April 2002): 1-26.
- Cumming, G., Allen, A., McPhie, J., Zaw, K., 2004, Polymictic Andesitic Lithic

- Breccia from central Thailand: Evidence for the Collapse of a Volcanic Edifice, Progress Report 2 Geochronology, Metallogensis and Deposit Styles of the Loei Foldbelt in Thailand and Laos PDR, CODES ARC Linkage Project
- Davies, A. G. S., Van Leeuwen, T. M., Cooke, D.R., Gemmell., (2004). The Kelian gold deposit - exploration history, critical factors and deposit summary. 24 ct Au Workshop, CODES Special Publication 5. 5: 65-75.
- Dedenczuk, D. (1998). Epithermal gold mineralisation at Khao Sai, central Thailand. School of Earth Sciences. Hobart, University of Tasmania.
- Diemar, M. G., and Diemar, V.G., (1999). "Geology of the Chatree Epithermal Gold Deposit, Thailand." PacRim '99, Bali, Indonesia 10-13 October, Proceedings.: 227-231.
- Dong, G. and Morrison, G. (1995). "Adularia in epithermal veins, Queensland: morphology, structural state and origin." Mineral, Deposita **30**: 11-19.
- Dong, G., Morrison, G., Jaireth, S., (1995). "Quartz textures in epithermal veins, Queensland - Classification, Origin, and Implication." Economic Geology **90**: 1841-1856.
- Dong, G. and Zhou, T. (1996) "Zoning in the Carboniferous-Lower Permian Cracow epithermal vein system, central Queensland, Australia." Mineralium Deposita **31**: 210-224
- Fournier, R. O., (1985). "Silica minerals as indicators of conditions during gold deposition." U.S Geological Survey Bulletin **1646**: 15-26.
- Gemmell, J. B., (2004). Low- and intermediate-sulphidation epithermal deposits. 24 ct Au Workshop, CODES Special Publication 5. 5.
- Greener, S., (1999). Wall Rock Alteration and Vein Mineralogy of a Low Sulphidation Epithermal Deposit, Thailand. Unpub. B.Sc (Hons) thesis. Hobart, University of Tasmania.
- Heald, P., Foley, N. K., Hayba, D.O., (1987). "Comparative Anatomy of Volcanic-

Hosted Epithermal Deposits: Acid-Sulphate and Adularia-Sericite Types." Economic Geology **82**(Jan-Feb): 1-24.

Hedenquist, J. W. (2000). "Exploration for Epithermal Gold Deposits." Reviews in Economic Geology **Gold in 2000**: 245-277.

Hedenquist, J. W., Izawa, K., Arribas, A., White, N. C. (1996). "Epithermal gold deposits: Styles, characteristics, and exploration." Resource Geology Special Publication Number 1.

Hudson, D. M. (2003). "Epithermal alteration and mineralisation in the Comstock District, Nevada." Economic Geology **98**: 367-385.

Kromkhun, K. (2005). Geological setting, mineralogy, alteration, and nature of ore fluid of the H zone, the Chatree deposit, Thailand. Unpub. MSc thesis, Hobart, University of Tasmania.

Pearson, M. F., Clark, K.F., Porter, E.W, (1988). "Mineralogy, Fluid Characteristics, and Silver Distribution at Real De Angeles, Zacatecas, Mexico." Economic Geology. **83**(8): 1737-1759.

Plumlee, G. S. (1994). "Fluid Chemistry Evolution and Mineral Deposition in the Main-Stage Creede Epithermal System." Economic Geology. **89**(8): 1860-1882.

Plumlee, G. S. and Whitehouseveaux, P.H (1994). "Mineralogy, paragenesis, and mineral zoning of the Bulldog Mountain Vein System, Creede District, Colorado." Economic Geology **89**(8): 1883-1905.

Reyes, A. G. (1990). "Petrology of Philippine geothermal systems and the application of alteration mineralogy to their assessment." Journal of Volcanology and Geothermal Research **43**: 279-309.

Rosana, M. and Matsueda, H. (2002). "Cikidang hydrothermal gold deposit in Western Java, Indonesia." Resource Geology **52**: 341-352.

Sajona, F. G., Izawa, E., Motomura, Y., Imai, A., Sakakibara, H., Watanabe, K., (2002). "Victoria carbonate-base metal gold deposit and its significance in the

- Mankayan mineral district, Luzon, Philippines." Resource Geology **52**(4): 315-328.
- Saunders, J. A. (1994). "Silica and gold Textures in ores of the Sleeper Deposit, Humboldt-County, Nevada - Evidence for colloids and implications for epithermal ore-forming processes." Economic Geology **89**(3): 628-638.
- Sherlock, R. L., Tosdal, R.M., Lehrman, N.J., Graney, J.R., Losh, S., Jowett, E. C., Kesler, S.E., (1995). "Origin of the McLaughlin mine sheeted vein complex: Metal zoning, fluid inclusion, and isotopic evidence." Economic Geology **90**(8): 2156-2181.
- Silberman, M. L. and Berger, B.R. (1985). "Relationship of trace-element patterns to alteration and morphology in epithermal precious-metal deposits." Reviews in Economic Geology **2** (Geology and Geochemistry of Epithermal Systems): 203-232.
- Simmons, S. F. and P. R. L. Browne (2000). "Hydrothermal minerals and precious metals in the Broadlands-Ohaaki geothermal system: Implications for understanding low-sulfidation epithermal environments." Economic Geology **95**(5): 971-999.
- Simmons, S. F., Mauk, J.L., Simpson, M.P., (2000). The mineral products of boiling in the Golden Cross epithermal deposit. New Zealand Minerals & Mining Conference Proceedings, New Zealand.
- White, N. C. and J. W. Hedenquist (1995). "Epithermal Gold Deposits: Styles, Characteristics and Exploration." SEG Newsletter **23** (October): 9-12.
- White, N. C., Leake, M. J., McCaughey, S. N., Parris, B.W.et al. (1995). "Epithermal Gold Deposits of the Southwest Pacific." Journal of Geochemical Exploration **54**(2): 87-136.

APPENDIX 2

MICROPROBE DATA

SAMPLE	DataSet/PcS	Fe	Co	Ni	Cu	Zn	As	Se	Sb	Bi	
au	1 / 1.	0.0139	-0.0033	0.0166	-0.0047	0.0385	-0.0757	0.0386	0.0196	-0.1009	0.3372
	2 / 1.	0.0152	0.0003	0.0199	-0.0115	0.0036	0.0368	0.013	-0.0201	-0.0471	-0.0272
ag	3 / 1.	53.4422	46.6239	0.0414	0.0055	0.1201	0.0403	0.0369	-0.0097	0.0096	-0.1199
	4 / 1.	0.0293	-0.0072	0.0221	0.0383	0.046	-0.0463	0.0456	0.0053	0.0581	0.3569
au-fixed	5 / 1.	0.0374	-0.0071	0.0399	0.0311	0.0295	-0.0328	-0.0083	0.0219	0.0423	0.2522
	6 / 1.	0.0267	0.1194	-0.0286	-0.001	0.0019	-0.0589	0.0237	0.0231	-0.0112	0.1245
er179479 au1	7 / 1.	0.0307	0.0098	0.0214	-0.0123	0.0138	-0.0795	0.0238	0.0009	-0.0977	0.2655
er17957 1.1 AuAg	8 / 1.	14.0196	0.0202	0.0046	-0.022	-0.0144	0.0414	0.0262	1.8579	-0.0396	-0.1222
er17957 1.2 AgS	9 / 1.	4.2149	2.005	0.0302	-0.0059	0.0586	-0.0672	0.0234	0.0623	0.0171	0.0681
er17957 2.1 AuAg	10 / 1.	11.5987	0.016	0.0109	0.0067	0.0108	0.0168	0.0453	0.7487	-0.0308	-0.1119
er17957 2.2 AgS	11 / 1.	21.8723	16.8819	0.0243	0.0072	20.8067	-0.0067	0.04	0.0102	-0.0184	-0.0519
er17960 2.1 cuFeS	12 / 1.	13.1834	0.0138	0.0353	0.005	14.5304	0.0434	0.0238	0.0278	0.0085	-0.0123
er17960 2.2 AgS	13 / 1.	0.0465	-0.0106	0.0149	-0.0031	0.0084	-0.049	0.0211	0.0014	-0.0382	0.1208
er17960 1.1 AuAg	14 / 1.	0.0354	-0.0194	0.0016	0.0262	0.0228	-0.0731	0.0097	-0.0195	-0.0242	0.1225
er17960 1.2 AuAg	15 / 1.	17.0297	0.0106	0.0101	-0.0145	-0.001	-0.0261	0.0214	0.7036	-0.0619	-0.0125
er17960 1.3 AgS	16 / 1.	35.5208	29.1053	0.0335	0.0039	33.6966	0.0004	0.0456	0.0254	0.0223	-0.0668
er16933 1.1 CuFeS	17 / 1.	0.0357	0.0039	0.0166	-0.0131	-0.0223	-0.042	0.0185	0.0178	-0.0556	0.1072
er17426 AuAg	18 / 1.	0.0437	-0.0089	0.0195	-0.0021	0.013	-0.057	0.0123	0.0009	-0.0262	0.0844
er17426 AuAg2	19 / 1.	0.0306	0.0148	0.0053	0.0304	-0.018	-0.1028	0.028	0.0158	0.0291	0.124
er17426 1.1 AuAg middle	20 / 1.	0.0403	0.0347	0.0056	-0.0083	-0.0156	-0.0306	-0.0035	0.015	-0.0322	0.1247
er17426 1.2 AuAg edge	21 / 1.	11.7634	0.1138	0.013	-0.0015	0.0277	-0.0011	0.0028	3.2562	-0.042	-0.0587
er17426 1.3 AgS	22 / 1.	9.0045	2.5823	0.0251	0.0172	0.006	-0.0331	0.023	1.1265	-0.0429	-0.0463
er17426 2.1 AgS	23 / 1.	0.0258	-0.013	0.0003	0.0029	0.0038	-0.0741	0.0144	0.0127	-0.0015	0.2056
er17426 2.2 AuAg	24 / 1.	13.2855	-0.0046	0.0097	0.0018	0.0003	0.0122	0.0245	1.9863	-0.0844	-0.0485
er17426 2.3 AgS	25 / 1.	34.0882	28.2914	0.0218	-0.0039	33.1979	0.0062	0.0444	-0.0024	-0.0149	-0.013
er17426 2.4 CuFeS	26 / 1.	1.6566	-0.0039	0.0122	-0.0398	0.0187	-0.0339	0.0016	-0.0046	-0.0616	0.0175
er17426 2.5 AuAg											

Te	Ag	Pb	Au	Total	X	Y	Z	Comment	Point#
0.0114	0.5173	-1.8555	76.6965	77.6895	-19686	31293	148 au		1
0.1482	99.5704	-0.02	0.2532	100.0607	-9807	31416	138 ag		2
-0.0065	0.0332	0.0279	-0.0046	100.3811	-6667	2202	128 marcasite		3
0.0135	0.4156	-1.6321	76.8317	77.8625	-19697	31143	148 au		4
-0.0131	0.4068	-1.7047	99.5295	100.3907	-19706	31111	148 au-fixed		5
0.033	26.0735	-1.3287	72.3624	98.7881	9973	27947	593 er179479 au1		6
0.0908	40.017	-1.1574	60.7605	101.234	-20851	878	402 er17957 1.1 AuAg		7
0.1365	83.318	-0.0195	-0.138	99.4242	-21239	1116	402 er17957 1.2 AgS		8
0.062	42.0544	-0.4068	40.6364	89.2324	-19302	2900	413 er17957 2.1 AuAg		9
0.1352	82.82	-0.0097	-0.0249	95.4091	-19207	2731	413 er17957 2.2 AgS		10
0.0058	4.0588	-0.0499	0.101	63.8083	-14194	-31952	296 er17960 2.1 cuFeS		11
0.0621	70.1049	0.0051	1.0617	99.105	-14201	-31938	296 er17960 2.2 AgS		12
0.0631	40.3149	-1.0084	61.4944	102.0855	-17787	-32946	279 er17960 1.1 AuAg		13
0.1045	46.4639	-0.9834	53.6316	100.4183	-17260	-32938	279 er17960 1.2 AuAg		14
0.0994	84.3286	-0.0677	-0.1032	102.2034	-17820	-32904	279 er17960 1.3 AgS		15
-0.0186	-0.0194	0.0517	-0.0737	98.5056	-5482	3701	460 er16933 1.1 CuFeS		16
0.0508	31.051	-0.5367	33.5421	64.8436	-6684	-22191	361 er17426 AuAg		17
0.0355	40.6476	-1.4631	59.5406	100.3974	-6684	-22197	361 er17426 AuAg2		18
0.0633	41.8294	-1.1942	59.3512	101.522	-5660	-30512	347 er17426 1.1 AuAg mi		19
0.0662	42.0484	-0.7471	44.9912	87.3262	-5651	-30491	347 er17426 1.2 AuAg ed		20
0.126	82.3895	0.2017	0.2237	98.118	-5661	-30565	347 er17426 1.3 AgS		21
0.0903	61.2487	-0.4985	26.1379	100.2616	-4609	-22065	366 er17426 2.1 AgS		22
0.0194	40.5764	-1.4045	59.5099	100.3712	-4619	-22056	366 er17426 2.2 AuAg		23
0.1263	83.9196	0.035	-0.1782	99.4012	-4582	-22249	366 er17426 2.3 AgS		24
-0.0086	0.7993	-0.0517	-0.1033	96.4492	-4907	-21949	366 er17426 2.4 CuFeS		25
0.0582	29.6458	-0.5576	30.5567	61.9673	-4650	-21772	366 er17426 2.5 AuAg		26

APPENDIX 3

XRF DATA

XRF ANALYSES, SES-CODES, University of Tasmania

25/08/2005

Analyst: Phil Robinson

XRF sample preparation: Katie McGoldrick

Rock Crushing (WC mill) John De Little

ORE2 Program (ScMo X-ray tube)

Fusion Discs

Sample No.	SiO2	TiO2	Al2O3	Fe2O3	MnO	MgO	CaO	Na2O	K2O	P2O5	BaO	(Ba from pills)	
												LOI	Total S
ER017154	50.09	1.69	17.93	10.27	0.15	3.93	8.88	3.17	1.31	0.56	0.029	2.45	100.46
WYRD30-66.8	51.06	1.42	16.23	11.39	0.16	5.01	8.59	2.69	0.89	0.29	0.019	2.36	100.11
LDRD009-113.5	52.49	0.49	20.66	8.03	0.22	3.31	6.49	2.6	2.19	0.12	0.085	3.31	100.00
WYRD16-102.2	52.77	0.58	17.73	8.84	0.16	6.54	1.6	5.93	0.79	0.16	0.016	4.78	99.90
ER017645	71.1	0.45	13.57	4.75	0.05	1.67	0.25	4.96	0.86	0.08	0.006	2.14	99.89
ER016838	52.96	1.22	17.72	9.22	0.14	3.26	7.8	4.07	1.15	0.27	0.021	2.51	100.34
WYRD16-116.5	54.76	1.41	14.52	10.64	0.18	3.46	6.79	3.74	0.73	0.34	0.012	3.3	99.88
WYRD16-154.4	61.63	0.6	14.28	8.21	0.09	3.92	0.95	4.21	0.82	0.22	0.011	4.77	99.71
ER017159	60.72	1.33	15.25	8.63	0.11	2.25	1.64	5.52	1.64	0.29	0.027	2.85	100.26
WYRD16-83.6	56.63	0.57	16.89	7.72	0.14	4.78	1.6	1.91	4.25	0.17	0.030	5.24	99.93
ER017162	77.93	0.17	11.81	1.75	0.01	0.62	0.11	5.56	0.26	0.02	0.012	1.79	100.04
WYRD16-135	51.25	1.26	16.59	10.32	0.16	4.89	6.25	4.58	1.37	0.25	0.021	3.48	100.42

Results quantitative - MOCOMP (Archive: MOCOMP

(ppm)

Sample No.	Y	U	Rb	Th	Pb	As	Bi	Zn	Cu	Ni
ER017154	39	<1.5		39	4	3 <3		<2	91	195
WYRD30-66.8	29	<1.5		20	<1.5	4	3	<2	102	113
LDRD009-113.5	10	<1.5		44	<1.5	2 <3		<2	55	110
WYRD16-102.2	11	<1.5		17	2	2 <3		<2	246	12
ER017645	26	<1.5		19	3	2 <3		<2	53	23
ER016838	29	<1.5		22	2	3	6	<2	95	105
WYRD16-116.5	33	<1.5		11	2	4	7	<2	115	96
WYRD16-154.4	18	<1.5		23	<1.5	6	4	<2	59	87
ER017159	32	<1.5		27	2	3	5	<2	97	49
WYRD16-83.6	14	<1.5		122	<1.5	2 <3		<2	81	38
ER017162	23	<1.5		7	2	3 <3		<2	134	32
WYRD16-135	26	<1.5		24	2	3	8	<2	104	94

Pressed Powder Pills XRF ANALYSES, SES-CODES, University o John de Little(Hons 1.65.305.37800.
GOLD1 program Traces run with Au X-ray (ppm)

Sample No.	Nb	Zr	Sr	Cr	Ba	Sc	V	La	Ce	Nd
ER017154	8.2	220	552	62	259	25	288	18	46	28
WYRD30-66.8	3.4	127	387	63	172	34	307	10	25	18
LDRD009-113.5	0.7	20	404	6	763	27	234	3	9	5
WYRD16-102.2	<1	34	139	50	146	32	263	4	10	4
ERO17645	3.6	104	69	8	51	19	28	9	25	16
ERO16838	3.1	127	581	17	192	25	277	12	27	19
WYRD16-116.5	4.4	152	318	13	105	28	313	11	28	18
WYRD16-154.4	1.5	53	110	11	98	28	165	3	13	11
ERO17159	5.4	169	281	1	240	24	240	15	31	22
WYRD16-83.6	1.8	43	121	35	265	31	232	7	7	7
ERO17162	3.6	120	61	1	109	8	13	10	21	15
WYRD16-135	3.1	114	539	81	188	32	312	6	22	16

APPENDIX 4

STABLE ISOTOPE DATA

UTAS silicate oxygen isotope analyses
Stable Isotope Geochemistry laboratory
Oct-05

Sample	$\delta^{18}\text{O}_{\text{SMOW}}$	g/t Au	Easting	Northing	Location
ER017966	13.5	6.3	688472	1809579	Conical Hill
ER017427	13.0	36.5	688610	1809582	Conical Hill
ER017244	16.5	0.00	688830	1809795	Central Ridge
ER017244	16.2	0.00	688830	1809795	Central Ridge
ER016951	14.0	0.00	688729	1810100	Central Ridge
ER016934	14.5	0.4	688710	1810214	Central Ridge
ER017439	17.5	0.0	688724	1810140	Central Ridge
ER016905	12.2	2.0	688675	1810815	T1 Hill
ER016925	12.4	0.7	688755	1810678	T1 Hill
ER016926	13.3	3.8	688733	1810691	T1 Hill
ER017453	13.3	0.1	689355	1811093	T4 Hill
ER017511	11.1	0.1	690508	1811487	S.V
ER017507	14.6	0.0	688268	1813097	Gift
ER017509	14.8	0.0	688206	1813207	Gift
ER017499	15.5	0.0	688458	1813343	Gift
ER017464	12.5	2.8	687610	1811933	Gift